AN INTEGRATIVE INVESTIGATION OF SOURCES, FATE, AND TRANSPORT OF BACTERIA IN MILWAUKEE COASTAL BEACHES

by

Marcia R. Silva

A Dissertation Submitted in

Partial Fulfillment of the

Requirements for the Degree of

Doctor of Philosophy

in Engineering

at

The University of Wisconsin-Milwaukee

May 2013

ABSTRACT

AN INTEGRATIVE INVESTIGATION OF SOURCES, FATE, AND TRANSPORT OF BACTERIA IN MILWAUKEE COASTAL BEACHES

by

Marcia R. Silva

The University of Wisconsin-Milwaukee, 2013

Under the supervision of Hector R. Bravo and Sandra L. McLellan

Beach water quality criteria are determined by the Environmental Protection Agency (EPA) and water quality advisories or closings are issued based on fecal indicator bacteria (FIB) at the beaches. Understanding of sources, fate and transport of FIB at a beach environment is of economic and social interest for public users, beach managers, policy makers and scientists. This is a complex problem and it is a multidisciplinary issue by nature. Scientists have generally taken a reductionist approach to tackle complex environmental issues. However, as alluded by Gallagher and Appenzeller (1999) and adopted by Boehm (2000), many complex systems are best interpreted using an "integrative agenda". Sources and transport of bacteria at a beach environment has been studied by Boehm (2012) in this context. Results from such study indicate that large scale feature is best interpreted with information about small–scale interactions.

In this dissertation, I examined the sources of fecal indicator bacteria (FIB) in ten Lake Michigan beaches. In depth studies were performed at one study site (Bradford Beach) to investigate possible sources of FIB, including groundwater-lake water interactions and runoff infiltrating through the sand. The impact of hydrological and geophysical factors that are associated with

formation of standing water were also investigated, including the potential of FIB reservoirs in the sand matrix to serve as a sink and source of bacteria at the beach environment. In order to better understand bacterial association with particles at a large scale, I examined the small scale interactions between bacteria and particles by developing a new non-invasive optical technique and applying the technique to assess attachment of bacteria to sand particles in a sheared fluid simulating condition found in the surf zone. Finally, I used knowledge obtained from the understanding of small scale interactions to interpret results acquired from a statistical model and time series applied to large scale features at Bradford Beach and Atwater Beach.

This work is relevant to the study of sources and transport of bacteria not only in large lakes, but in rivers and oceans. The results also extend to the investigation of other microbial pollutants and their association with particles in a water body and the potential to track the transport of these pollutants in sediments, air and water.

References:

Boehm, A. (2000). "An integrative investigation of particle distributions in natural waters." Department of Chemical and Biochemical Engineering and Materials Science. Irvine, University of California, Irvine: 194.

Gallagher, R and T. Appenzeller (1999). "Beyond reductionism." Science 284:79.

Russell, T. L., K. M. Yamahara and A. B. Boehm (2012). "Mobilization and transport of naturally occurring enterococci in beach sands subject to transient infiltration of seawater." Environmental Science and Technology 46:5988-5996.

To my husband Aderiano,

my daughter Nicole and my son Vitor,

and my parents Adão and Teodora (*in memoriam*).

LIST OF FIGURES

Figure 1. 1 Multidisciplinary analysis of sources, fate and transport of FIB..... 3
Figure 1. 2.Research approach..... 3
Figure 2. 1Milwaukee beaches sampled from March 2006 until September 2008 in southern Lake Michigan. 11
Figure 2. 2 Rainfall data for Milwaukee from 2006 to 2008. Data was obtained from the National Weather Service Milwaukee station at General Mitchell Airport (42°57°N, 87°54°W)..... 15
Figure 2.3 Hydrograph of river discharge into Lake Michigan. Flow was measured at the channel downstream from the confluence of three major rivers that in the Milwaukee River basin. Another CSO event occurred on 3/13/06, not shown in the graph. The presence of SSO and CSO events are indicated. The primary discharge points from sewage overflows are rivers prior to confluence and the harbor. 16
Figure 2. 4*E. coli*, enterococcus, and turbidity levels at Doctors Park from 2007 to 2008. No data available from 2006. 25
Figure 2. 5 *E. coli*, enterococcus, and turbidity levels at Klode Park from 2007 to 2008. No data available from 2006. 26
Figure 2. 6 *E. coli*, enterococcus, and turbidity levels at Atwater Beach from 2006 to 2008. 26
Figure 2. 7 *E. coli*, enterococcus, and turbidity levels at North Beach from 2006 to 2008..... 27
Figure 2. 8 *E. coli*, enterococcus, and turbidity levels at Bradford Beach from 2006 to 2008..... 27
Figure 2. 9 *E. coli*, enterococcus, and turbidity levels at South Shore Beach - Old from 2006 to 2008..... 28
Figure 2. 10 *E. coli*, enterococcus, and turbidity levels at South Shore Beach - New from 2006 to 2008..... 28
Figure 3. 1 (A) Water sampling sites. Green dots show the lake water sites, black circles show piezometers and are labeled from 1 to 15, and red crosses show pan lysimeters that are adjacent to piezometers. Stormwater outfalls at the beach (O2 to O7) and north of the beach (O8 to O12) are indicated. (B) Sand sampling sites. The yellow circles show the sites where sand cores were collected with core liner tubes, the blue stars show the transects of sand cores collected with a vibracore, red dots show the sampling sites of surface sand sites 1-10 (S1–S10). On the insert: sketch of the beach profile showing the main features; drawing is not to scale. 36
Figure 3. 2 (A) Geometric mean of *E. coli* densities was higher in sand sites along the backshore where the geometric mean of moisture content was higher. Sand sites S4, S7 and S8 had chronically high moisture and also the highest *E. coli* levels. (B) Densities of *E. coli* had a positive non-linear correlation with moisture content. 45
Figure 3. 3 “Differential” topographic map: (A) April 2010 and Post 7/22/10 storm. (B) November 2009 and April 2010. Red lines show erosion and blue lines show accretion.... 47
Figure 3. 4 Elevation of ground surface and groundwater table. Sample locations indicated by piezometer number. Topographical profiles are average of three surveys, except for PZ-2 (elevation estimated from contour maps) and groundwater elevations refer to the 2009-2010 measurements..... 50
Figure 3. 5 Elevation contours for groundwater table on 7/15/10 show higher elevation on the SW corner of the contour (as expected) and on the NW corner probably due to infiltration from rain gardens on a rain event (6.96 cm). Higher concentration of bacteria was more

predominant in the middle of the beach, where groundwater table was closer to the ground. 53
Figure 3. 6 Relationship of formation of standing water and wave height and rainfall. There is a stronger correlation between standing water and rainfall than standing water and wave height..... 54
Figure 3. 7 Relationship between presence of sewage indicator in standing water and rainfall and wave height. *Bacteroides* human in standing water was frequently related to heavy rainfall events and/or wavy days, except on 5/9/2009. 56
Figure 3. 8 Schematic illustration of transport of FIB at the beach environment. Vertical transport of bacteria infiltrating through the sand (sample collected at the pan lysimeter) and eventually reaching ground water (piezometer) was prevalent. No evidence of horizontal transport of bacteria through the groundwater was observed, suggesting this mechanism is not responsible for FIB movement through the beach. 60
Figure S3. 1 Topographical survey performed on November 2009. Larger and deeper depressions are mostly located on the northern part of the beach around sand site S7 and S8 (581.25 ft = 177.17 m), but also on the southern part of the beach around sand site S4 (581.50 ft = 177.24 m). 72
Figure S3. 2 Geophysical surveys characterized the material below the beach. Resistivity profile (pseudosection) with 5 meter spacing. It shows higher resistivity to the south (left-hand side of the figure) and lower resistivity at depth, indicating coarser sand to the south. 72
Figure S3. 3 Visualization of groundwater elevation contours on the northern part of the beach: (A) average level from October 2009 to December 2010 and (B) on July 16, 2010, after a rainfall event. It is possible to observe flow away from the lake in PZ-7 possibly due to wave wash at that location, which coincides with one of the breaches on Fig. 3.3A. Direction of water movement is indicated by arrows and their sizes indicate the relative magnitude of flow. 73
Figure 4. 1A schematic illustration of the experimental set up of the bench scale optical system; drawing not to scale. 82
Figure 4. 2 Steps of image processing to count fluorescent particles: (A) Acquisition of raw images with image system; (B) Characterization of background level; (C) Subtraction of the background; (D) Separation of FP pixels from background pixels; (E) Computation of watershed transform; (F) Separation of clustered cells from each other by marker controlled watershed segmentation; (G) Removal of artifacts (particles < 2 pixels and > 50 pixels); (H) Quantification of fluorescent particles. 85
Figure 4. 3 Calibration curve for seven different dilutions of GFPuv-labeled *E. coli* in Milli-Q water comprised of at least six trials per dilution. R^2= 91%. 90
Figure 4. 4 Effects of (a) exposure time and (b) lens aperture on the mean cell image brightness and the measurements of cell concentration 91
Figure S4. 1 Experimental set up of the optical system for laboratory flume experiment 99
Figure S4. 2 Normalized quantum efficiency of the CCD sensor (SONY ICX204AL) and the emission spectra of GFPuv with excitation wavelength of 399 nm (peak absorption) and 473 nm (laser used in current study). Note: emission spectra are measured with scanning fluorescence with the emission wavelength between 485 and 540 nm. Dashed lines on the emission spectra are not real data but extrapolations from measurements. 100
Figure S4. 3 Simplified optical configuration of the cell imaging system 101

Figure S4. 4 Fluorophore photobleach assessment. Five hundred images were acquired at every time interval (t = 0, 0.5, 1, 2, and 3 hours) and concentration of FP was assessed. A t-test ($p<0.001$) showed that concentration of FP did not present statistically significant change over time, suggesting that fluorophore photobleach was below level detection for the extent of 3 hours. The source of water is Lake Michigan. Each data point corresponds to 500 measurements. 104
Figure 5. 1 Cumulative particle size distribution of environmental sand particles in the water column. Distribution of particles ≤ 231µm was measured by LISST (indicated by O). Number concentration was estimated for particles >231µm (indicated by +). 120
Figure 5. 2 Measurement of percent attachment of bacteria to sand particles: (A) shear rate (17, 23, 31, 42, and 51 s^{-1}); (B) concentration of sand particles (1.5, 15 and 150 mg/ml); (C) diameter of sand particles (248 µm and 366 µm); (D) mixing time (1, 2, and 3 hours); (E) ionic strength (0, 1.1 and 11 M $CaCO_3$); (F) absolute value of Δ zeta potential between bacteria and sand particles (3.47, 9.02, 10.37 mV). All experiments were submitted to shear rate of $31s^{-1}$ for 3hr and 150 mg/ml sand (d_{50} =366 µm), when not informed otherwise. Error bars in grey in (A) refer to control experiments (no addition of sand) performed at 17, 31, and 51 s^{-1}. Although results of standard method and optical method pertain to the same experimental conditions, there is a lag between respective error bars to facilitate reading. 122
Figure 5. 3Measurements of the term $\boldsymbol{\alpha\beta nj}$ by determining the slope between ln (n_0/n_t) *vs* t. . 124
Figure 5. 4 Sand grains collected from the bottom of the beaker after transport experiments observed with the microscope with GPF filter (A) and BF (B). 127
Figure 5. 5 Particle size distribution (PSD) of particles suspended in the water column after 3 hours mixing bacteria and sand particles (d_{50}=366 µm) at $G=31s^{-1}$ just before stopping the mixer and 10-30 min just after. Particles larger than >6.14 µm settle at least one order of magnitude in terms of number concentration. 128
Figure A. 1 Sampling sites at Bradford Beach (A) and Atwater Beach (B) 140
Figure A. 2 Scatter plot of observed versus predicted values for top four statistical models. On the plots, false positives (Type I error) represent data points in the upper left quadrant of the graph and false negatives (Type II error) represent points in the lower right quadrant. The blue and green lines represent EPA threshold for *E. coli*: log of 235 CFU/100 ml. 147
Figure A. 3 Cumulative number concentration of suspended sediments during 08/04/09 and 08/05/09. 151
Figure A. 4 Cumulative number concentration of suspended sediment obtained from LISST. The date and time indicated with arrows show the only two data points in which suspended sediment increased coinciding with increased TKE dissipation. 152
Figure A. 5 Time series of FIB and TKE dissipation (ϵ) during 08/04/09. 153

LIST OF TABLES

Table 2. 1 Characterization of Lake Michigan beaches from 2006 to 2008 19
Table 2. 2 Human *Bacteroides* marker detection in stormwater outfalls in Milwaukee beaches from 2006 to 2008. 20
Table 2. 3 Comparison of mean levels of *E. coli* (CFU/100ml) within Lake Michigan beaches in Milwaukee from spatial surveys conducted during and after CSO and SSO events. CFU (Colony Forming Unit), CSO (Combined Sewer Overflow), SSO (Sanitary Sewer Overflow) (n=3 to 4 for all samples; exceptions on footnote) 24

Table 3. 1 Groundwater levels at piezometers (PZ) from October 2009 to December 2010. 39
Table 3. 2 Impact of rainfall in FIB concentration in groundwater (GW) and groundwater level. 51
Table 3. 3 Statistics of FIB in backshore sand and water at Bradford Beach during wet and dry days. 57
Table 3. 4 Variability of FIB in groundwater (GW) beneath the beach at different locations. 64
Table S3. 1. Statistics of mean grain diameter (d_{50}) (mm) of sand on the northern and southern part of Bradford Beach. 71
Table S3. 2 Spearman's rank correlation (rho) of groundwater levels and environmental variables. Significant correlations at $p \leq 0.05$ are flagged. PZ-5 is not listed because it was dry most of the time. 71
Table 4. 1 Sensitivity data of the GFPuv *E. coli* used in this research. FP denotes fluorescent particles and BCK denotes background particles. 94
Table 5. 1 Equations used to calculate collision efficiency (α) and collision frequency (β) 118
Table 5. 2Characterization of sand particles used in this study 119
Table 5. 3 Comparison of parameters obtained experimentally and by coagulation models for the same experimental conditions 125
Table 5. 4Measurements of collision efficiencies (α) in transport experiments or in the field .. 126

Table A. 1 Variables used in statistical analysis performed in Virtual Beach. 143
Table A. 2 Determination of Type I, Type II, specificity, sensitivity, accuracy, and R^2 of the best four models 148
Table A. 3 Multiple linear regressions predictions of the top four models 148
Table A. 4 FIB concentration and mass of sediments collected at two-week periods of deployment of sediment traps at different hydrologic scenarios at Bradford Beach and Atwater Beach. Results represent average (AVE) and standard deviation (STD) of FIB concentration and mass of sediment collected at six-replicate horizontal array. 150
Table SA. 1 Raw data collected in 2008, 2009 and 2010 and utilized in MLR models 155

LIST OF VIDEOS

Video S4. 1 Video recording the fluorescent cells travelling in the flume due to the background flow (85 μm s^{-1}) 99

TABLE OF CONTENTS

CHAPTER 1 - INTRODUCTION 1

CHAPTER 2 - ENVIRONMENTAL AND SOCIAL IMPACT OF STORMWATER OUTFALLS AT LAKE MICHIGAN BEACHES 6

2.1 ABSTRACT 6

2.2 INTRODUCTION 8

2.3 MATERIALS AND METHODS 10

2.4 RESULTS AND DISCUSSION 18

2.5 CONCLUSIONS 29

2.6 ACKNOWLEDGMENTS 29

2.7 REFERENCES 29

CHAPTER 3 - EFFECT OF HYDROLOGICAL AND GEOPHYSICAL FACTORS ON FORMATION OF STANDING WATER AND FECAL INDICATOR BACTERIA RESERVOIRS AT A LAKE MICHIGAN BEACH 31

3.1 ABSTRACT 31

3.2 INTRODUCTION 33

3.3 MATERIALS AND METHODS 35

3.4 RESULTS 43

3.5 DISCUSSION 60

3.6 CONCLUSIONS 65

3.7 ACKNOWLEDGEMENTS 66

3.8 REFERENCES 67

CHAPTER 4 - DIRECT OPTICAL METHOD FOR ASSESSMENT OF GREEN OF GREEN FLUORESCENT PROTEIN (GFPUV)-LABELED *ESCHERICHIA COLI* IN BENCH-SCALE MODELED AQUEOUS SYSTEMS 74

4.1 ABSTRACT 74

4.2 INTRODUCTION 75

4.3 EXPERIMENTAL CONFIGURATION 79

4.4 RESULTS AND DISCUSSION 89

4.5 CONCLUSIONS 95

4.6 ACKNOWLEDGMENTS 96

4.7 REFERENCES 96

CHAPTER 5 - QUANTITATIVE ANALYSIS OF THE ATTACHMENT OF FECAL INDICATOR BACTERIA TO SEDIMENT PARTICLES IN A SHEARED FLUID 105

5.1 ABSTRACT 105

5.2 INTRODUCTION 106

5.3 EXPERIMENTAL SECTION 109

5.4 RESULTS AND DISCUSSION 118

5.5 ACKNOWLEDGMENTS 129

5.6 REFERENCES 130

CHAPTER 6 - CONCLUSIONS AND FUTURE WORK 132

APPENDIX: COASTAL LOADING AND TRANSPORT OF FECAL INDICATOR BACTERIA AT TWO LAKE 137

ACKNOWLEDGMENTS

I would like to acknowledge and thank my advisors Hector R. Bravo and Sandra L. McLellan for their guidance and support and for their investment and trust in me throughout this research. They were compassionate mentors and will always be my role models. I would like also to acknowledge J. Val Klump, David Schwab, and Qian Liao for their contribution to my career and for serving on my committee. The work in this dissertation could not have been completed without Douglas Cherkauer whose groundwater expertise was invaluable for the groundwater-lake water interaction study at Bradford Beach and Zhongfu Ge for his invaluable contribution on estimation of hydrodynamic variables at Atwater Beach. Special thanks to William Kean who shared his expertise in geophysical surveys. I would like to thank Alexandria Boehm for kindly reviewing the abstract of this thesis.

I would also like to thank researchers and students from the Bacterial Genetics Laboratory and from the Environmental Hydraulics Laboratory, in which my research was performed, for their support and friendship. Special thanks to Patricia Bower who has accompanying me during my Masters and Ph.D. work. I am deeply thankful to Donald Szmania, Kim Weckerly, Thomas Hansen and Harvey Bootsma for assistance in research and friendship. I am also thankful to Carmen Aguilar, Betty Warras, Thomas Consi, Joan Flores, and Jennifer L. Klumpp for believing in me and for providing endless

encouragement throughout these years and for David Yu, David Garman and Rudi Strickler for trusting my work.

I would not have been able to complete this work had it not been for my family unconditional support, trust and love. Lastly, I would like to thank God for giving me resilience and strength.

CHAPTER 1

INTRODUCTION

1.1 Introduction and Motivation

One of the Ocean and Human Health concerns is fecal pollution at beaches, which is a major problem around the globe. In October 2000, a Federal Beach ACT was approved in the U.S. This Act declared that each State having coastal recreational waters would have to adopt water quality criteria and standards for the coastal recreational waters of the State for all pathogens and pathogen indicators to which the new or revised water quality criteria were applicable (Public Law 106-284). Since then, there was an increasing public awareness about the impact of fecal pollution to public beaches, since water quality advisories or closures occur when levels of fecal indicator bacteria exceed standards set by individual State authorities (EPA 2003a).

According to the National Resources Defense Council's (NRDC) annual survey in 2008 (NRDC, 2008), the number of beach closings and advisories were their fourth-highest level in the 19-year history of the report. This may be due to increased testing at beaches, highlighting that

previously, fecal pollution at beaches went unrecognized. The U.S. Environmental Protection Agency (EPA) requires that for freshwater, beaches be posted with an advisory sign informing the public of increased health risk when a water sample exceeds 235 colony-forming units (CFU) of *E. coli* per 100 milliliters of water and a closed sign when a water sample exceeds 1000 CFU/100 ml.

Wisconsin became the first state in the U.S. to implement a beach monitoring program in accordance with federal program criteria, where counties test beaches up to four times a week for *E. coli* and inform swimmers about water quality conditions. Wisconsin has been praised by EPA as a model for other states (EPA 2003b).

In order to guarantee the safety of swimmers and at the same time keep the beaches open whenever possible, it is mandatory to understand the sources, fate and transport of bacteria at the beach environment. This is a multidisciplinary topic by nature and sciences involved in this study are presented in Figure 1.1. Several studies have noted that there are a variety of point and non-point sources of bacteria that vary from beach to beach and even at the same beach within a short distance. An integrative approach of this topic helps to define the dynamics of the transport of bacteria. Investigating small scale interactions assist on interpretation of large scale features. Details of the research approach are shown in Figure 1.2.

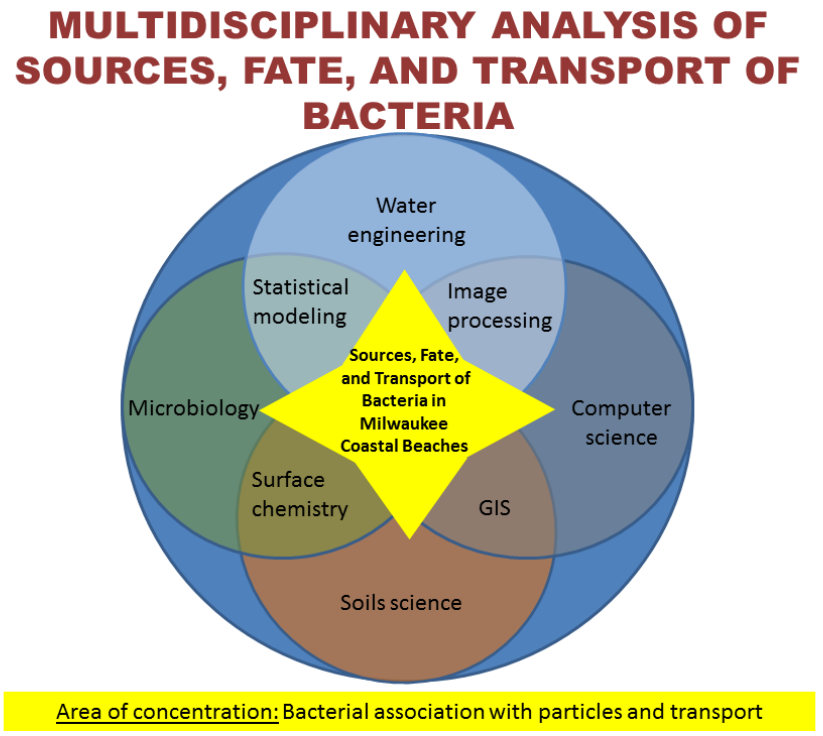

Figure 1. 1 Multidisciplinary analysis of sources, fate and transport of FIB

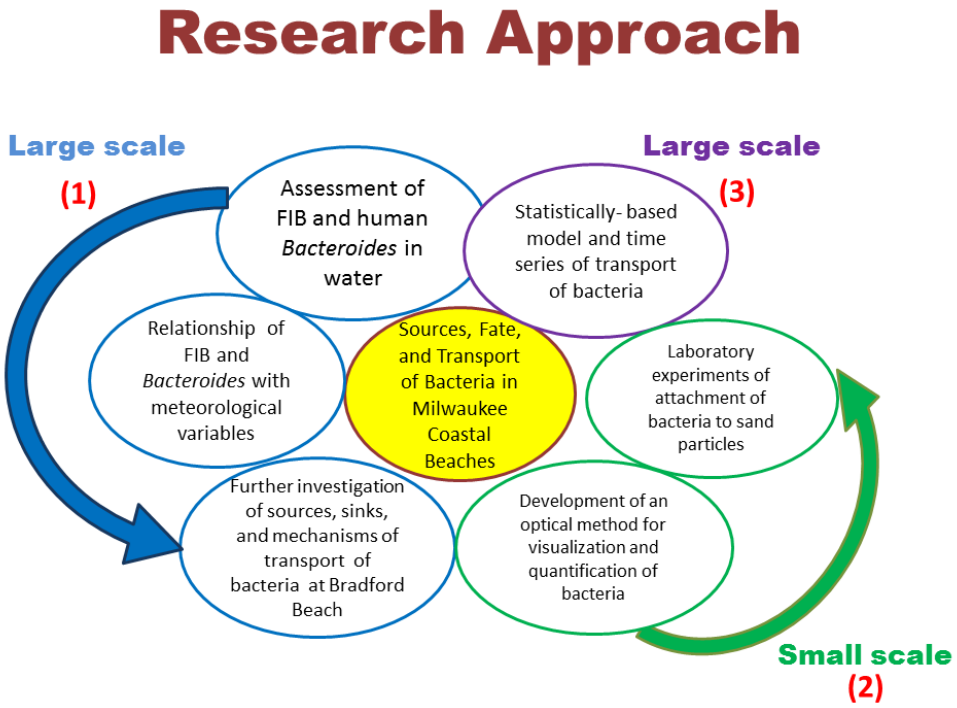

Figure 1. 2.Research approach

1.2 Scope and objectives

In particular, the objectives are:

(i) Determine the major sources of bacteria at nine Milwaukee beaches (Chapter 2);

(ii) Select one study site for an in depth investigation of the sources, fate and distribution of bacteria in water and sand and interaction between these two matrices at a beach environment. This is a complex problem since it is impacted by numerous variables such as meteorological aspects, physical properties of the beach (grain size, topography), wave action, lake level, groundwater-lake water interaction and interactions between particles and bacteria. Understand the hydrological and geophysical factors that impact formation of standing water at Bradford Beach, therefore creating conditions that promote prolonged survival and a potential source of bacteria at the beach environment (Chapter 3);

(iii) Develop an optical laboratory technique for the noon-invasive visualization and quantification of model organisms (GFPuv labeled *E. coli*) in water (Chapter 4);

(iv) Characterize the factors that drive the attachment of bacteria to particles and assess quantitatively this attachment utilizing the novel optical technique (Chapter 5);

(v) Develop a statistical model to determine variables with higher correlation with FIB concentrations at the surf zone at two Milwaukee beaches: Bradford Beach and Atwater Beach. Further investigate other possible hydrodynamic variables that would be impacting on FIB concentrations at the swash zone, including: turbulent kinetic energy (TKE), TKE dissipation (ϵ), and grain size distribution of suspended sediment. Verify in the field, findings obtained from laboratory experiments about linear relationship

between shear rate (up to $31s^{-1}$) and mixing time and % attachment of bacteria to particles (Appendix).

1.3 Organization of thesis

This thesis includes a compilation of published and in preparation manuscripts. Each Chapter represents a complete work and may be read alone without reference to other Chapters. A summary of the results of all the Chapters is discussed along with future work in Chapter 6.

References:

1. PUBLIC LAW 106–284. OCT. 10, 2000. Beaches Environmental Assessment and Coastal Health Act of 2000.

2. U.S. Environmental Protection Agency. 2003a. Bacterial water quality standards for recreational waters. EPA/823/R-03/008. U.S. Environmental Protection Agency, Washington, D.C.

3. NRDC. 2008. Testing the Waters 2008: A Guide to Water Quality at Vacation Beaches. National Resources Defense Council, Washington, DC.

4. U.S. Environmental Protection Agency. 2003b. Beach Currents Newsletter-Fall 2003. EPA/823/N-03/001. U.S. Environmental Protection Agency, Washington, D.C.

CHAPTER 2

ENVIRONMENTAL AND SOCIAL IMPACT OF STORMWATER OUTFALLS AT LAKE MICHIGAN BEACHES

2.1 ABSTRACT

Milwaukee is the largest city in Wisconsin and is home for approximately one million people. Lake Michigan waters in Milwaukee's coastal area are mainly used for recreational purposes and drinking water. Coastal waters are impacted by many sources of pollution. The presence of sewage is a major concern.

Milwaukee Metropolitan Sewerage District's service area consists of 95% of separated sewers and 5% combined sewers. Separated sewer service areas have stormwater systems that collect surface runoff and discharge the stormwater directly to waterways untreated. Leaking or failing sanitary sewer infrastructure may allow human sewage to enter the stormwater system. Under heavy rain events, there may also be sanitary sewage overflows (SSOs) and combined sewer overflows (CSOs) which discharge sewage into Lake Michigan.

Beach water and outfall samples from nine beaches in Milwaukee were monitored for *Escherichia coli* (*E. coli*), enterococci and the human *Bacteroides* marker from 2006 to 2008. Almost all of the outfalls are from separated sewer systems, except one at South Shore Beach and one at Bay View Beach that discharge untreated sewage during heavy rain events when there are CSOs. McKinley is the only beach at which outfalls could not be sampled.

The geometric mean of fecal indicator bacteria in beach water samples ranged from 59 to 268 CFU/100 ml for *E. coli* and from 11 to 154 CFU/100 ml for enterococci. Outfalls at all beaches were found to be positive for the human *Bacteroides* marker at least once during the study period, except McKinley, where outfalls were not sampled. McKinley Beach also presented the lowest *E. coli* and enterococci levels compared to the other beaches. Presence of outfalls at the beaches represents an environmental and societal concern since they may be source of human sewage contamination, posing a human health risk.

2.2 INTRODUCTION

In October 2000, a Federal Beach ACT was approved in the U.S. This Act declared that each State having coastal recreational waters would have to adopt water quality criteria and standards for the coastal recreational waters of the State for all pathogens and pathogen indicators to which the new or revised water quality criteria was applicable (Public Law 186-284). Since then, there was an increasing public awareness about the impact of fecal pollution to public beaches, since water quality advisories or closures occur when levels of fecal indicator bacteria exceeded standards set by individual State authorities (EPA 2003a)

According to the National Resources Defense Council's (NRDC) annual survey in 2008 (NRDC, 2008), the number of beach closings and advisories were their fourth-highest level in the 19-year history of the report. This may be due to increased testing at beaches, highlighting that previously, fecal pollution at beaches went unrecognized. The U.S. Environmental Protection Agency (EPA) requires that beaches be posted with an advisory sign informing the public of increased health risk when a water sample exceeds 235 colony-forming units (CFU) of *E. coli* per 100 milliliters of water and a closed sign when a water sample exceeds 1000 CFU/100 ml.

Wisconsin became the first state in the U.S. to implement a beach monitoring program in accordance with federal program criteria, where counties test beaches up to four times a week for *E. coli* and inform swimmers about water quality conditions. Wisconsin has been praised by EPA as a model for other states (EPA 2003b).

Wisconsin had 578 closing/advisory events in 2008. Nationwide, total closing/ advisory days for events lasting six consecutive weeks or less increased 18% (from 747 days in 2007 to 883 days in 2008). For events lasting six consecutive weeks or less, 66% of closing/advisory days in 2008

were due to detection of high bacteria levels through laboratory tests. In response to NRDC report, the Environmental Protection Agency (EPA) has agreed to update its 20–year-old beach water quality standards by 2012, through conducting new health studies and swimmer surveys, approving a water-testing method that will produce same-day results (the current EPA approved method requires 24 hr to release final results), and protecting the public from a broader range of waterborne illnesses.

Fecal indicator bacteria, such as *E. coli* and enterococci are abundant in the gastrointestinal tracts of most warm-blooded animals; therefore they are used to indicate fecal contamination (Bower *et al*, 2005). The presence of *E. coli* is not always related to presence of pathogens, but pathogens are rarely detected without detection of fecal pollution. Presence of human fecal pollution is of health concern since humans are reservoirs for human enteroviruses, noroviruses, Coxsakie A and B, Hepatitis A, *Cryptosporidium parvum*, *Giardia lambia* and pathogenic enteric bacteria such as *Salmonella* and *Shigella* spp. (McLellan and Salmore, 2003; McLellan et al, 2007). New alternative fecal indicators have been investigated by studying the composition of low-abundance and dominant populations in microbial communities released into the environment as a result of sewage overflows (McLellan *et al*, 2010). Potential sources of *E. coli* contamination at Wisconsin beaches include urban storm water, leaky sanitary pipes, sewage overflows, and agricultural runoff. In addition, wildlife and waterfowl feces contribute to high levels of *E. coli* in both beach sand and water (WDNR, 2009).

In this study, characterization of nine beaches in Milwaukee, Wisconsin, is performed in terms of *E. coli*, enterococci, and turbidity levels, presenting data from 2006 to 2008. In addition, beach water and outfalls at or near the beaches were also tested for the human *Bacteroides* marker throughout the study period. The percentage of exceedance of the EPA limit for recreational

water is presented for each beach. Environmental and social impact of stormwater outfalls at Lake Michigan beaches is discussed.

2.3 MATERIALS AND METHODS

Study area

Beach water samples were collected from March 2006 until September 2008 in southern Lake Michigan, corresponding to latitude-longitude coordinates of 43.10°N, 87.52°W (Doctors Park) to 42.590°N, 87.51°W (Bay View Beach), as shown in Fig.2.1.

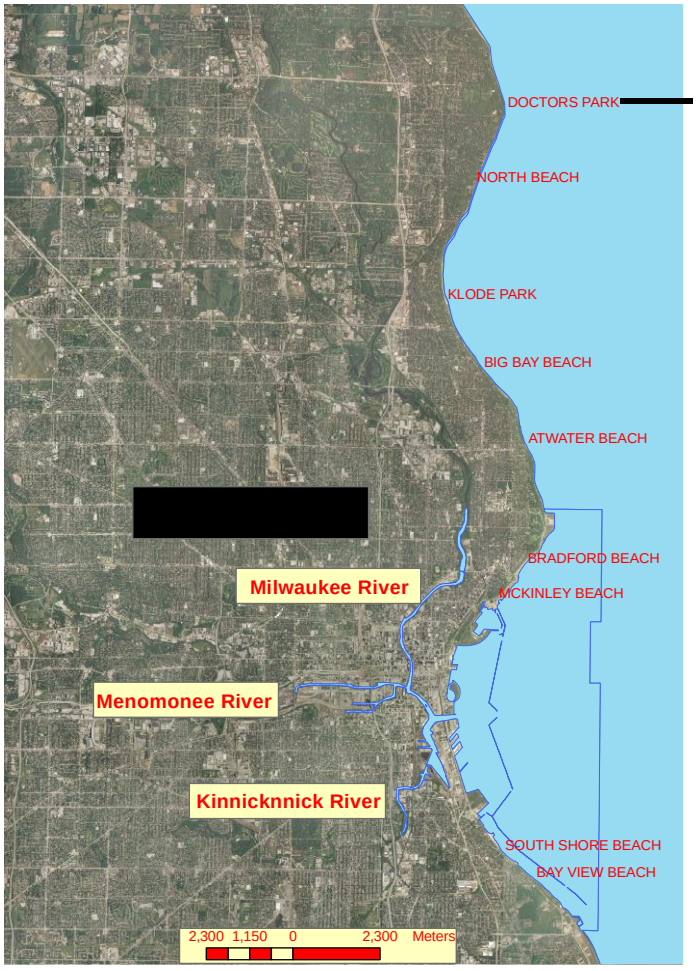

Figure 2. 1Milwaukee beaches sampled from March 2006 until September 2008 in southern Lake Michigan.

Two beaches are located south of Milwaukee harbor and inside of the marina break wall (South Shore Beach and Bay View Beach). The other beaches are located north of Milwaukee Harbor; the furthest beach sampled is Doctors Park located at approximately 16 km of Milwaukee harbor. The harbor is the primary discharge point for an 850-square-mile basin that includes agricultural, suburban, and urban land use. Only two CSO outfalls discharge on Lake Michigan itself: one is

located at Russell Avenue, just north of South Shore Beach and the other outfall is located at Bay View Beach.

Doctors Park and North Beach are located in the Village of Fox Point, which is a suburban residential community of 2.8 square miles and approximately 6,818 residents. Doctors Park is located in the Fox Point area, and it is surrounded by the wooded acres of the park. There is a long steep walk down a path lined with trees to the bottom of the bluff where the sandy beach is situated. All the other beaches studied are urban beaches: Bay View Beach, South Shore Beach (New and Old), McKinley Beach, Bradford Beach, Atwater Beach, Big Bay Beach, Klode Park, and North Beach.

Bay View is one of the neighborhoods of Milwaukee and it is located on the southeast shore of the city overlooking Lake Michigan. South Shore Park is a relatively small, narrow park along the Lake Michigan shoreline south of downtown Milwaukee in the Bay View neighborhood. A stone breakwater protects the shoreline in South Shore Park. The South Shore Yacht Club is located on the north end of the park. McKinley Beach is located at the 119-acre McKinley Marina Park, just outside of the marina breakwall. Bradford is one of Milwaukee's most popular beaches for swimming and sunbathing, and it is located just north of downtown. Atwater Beach is located approximately 5 km north of Bradford Beach, in the Village of Shorewood. Big Bay and Klode Park are located north of Atwater Beach, in the Village of Whitefish Bay. Atwater Beach has three groins built in early 1900’s to retain sand. Because they are a physical obstacle, they interfere with lake water circulation at the beach. Big Bay Park consists of a stone walkway, following natural ravine from street-level down the bluff to the short of Lake Michigan. Near the foot of this walkway, a groin extends out into the Lake for shoreline protection. The groin has led to the buildup of a sandy beach area used for public swimming. Klode Park is located in

the northeastern portion of the village of Whitefish Bay. It is located in a bay; therefore in a more protected area and similarly to McKinley Beach it has a circular shape.

Lake Michigan beach water samples and outfall samples

Nine coastal beaches spanning the Western shore of Lake Michigan (Fig. 2.1) were sampled from March 2006 to September 2008. Beach samples were collected in knee deep (~0.5 m) water approximately 2 m from shore.

Outfalls located at or near the beaches were also sampled; except at McKinley Beach because access is difficult (one outfall located to the north and the other located to the south of the beach). There is one outfall on the northern part of Doctors Park; three outfalls at or near Klode Park, one to the south, one to the north and one at the beach; one outfall just south of North Beach and thirteen along the beach; one outfall on the southern part of Big Bay Beach; one submerged outfall just north of Atwater Beach and one outfall 1 km to the north of the beach (results not shown in this study); eight outfalls along Bradford Beach, and four to the north of the beach; one outfall 0.5 km to the north of South Shore Beach – Old an one outfall on the southern part of Bay View Beach. Not all outfalls were sampled during the study period.

These sites are potentially influenced by localized sources, primarily stormwater and shorebirds, as well as regional contamination, including urban stormwater, agricultural runoff, and sewage overflows when they occur. Three or four evenly spaced samples were taken. In all, 946 beach water samples and 343 outfall samples were collected at the nine beach sites.

Rainfall and Streamflow Data

Rainfall data for 2006–2008 were obtained from the National Weather Service Milwaukee station at General Mitchell Airport (42°57°N, 87°54°W). Data from selected dates were plotted in Fig.2.2. Two CSO/SSO events occurred in 2006. The first event happened on March 13, when it rained 2.79 cm on March 12, followed by 1.35 cm on March 13. The second event happened on July 10 due to 7.0 cm of rain on the previous day. In 2007, two CSO/SSO events occurred due to heavy rains. The first one occurred on April 3 and 4 due to 3.84 cm of rain on April 3. The second event occurred on August 20 due to a total of 9.0 cm of rain falling for three days, starting on August 18. In 2008, record rainfalls occurred in southeastern Wisconsin during the month of June, accounting for a total of 27.79 cm within 11 days. The Milwaukee River drainage basin received the majority of its rainfall during four days, June 5, 7, 8 and June 12, and the CSO lasted from June 7 to June 15. Wind directions were prevalent southwest with average wind speeds of 16.1 km/h with wind gust of 51.5 km/h.

River discharge rates to Lake Michigan were obtained for the Milwaukee river mouth, using United States Geological Survey (USGS) gauge station 4087000 (http://waterdata.usgs.gov/wi/nwis/rt). Data from selected dates were plotted in Fig. 2.3. Volumes of CSO and SSO discharges entering Lake Michigan were provided by MMSD.

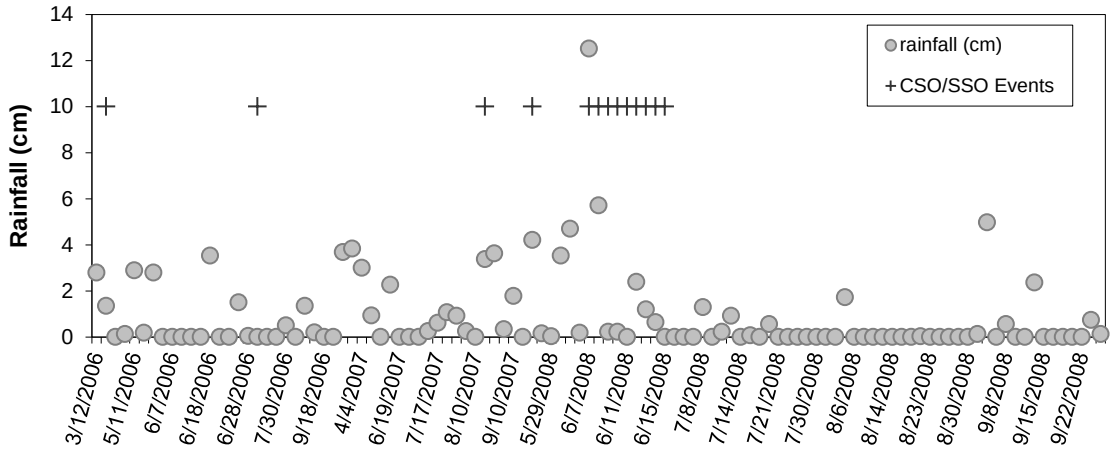

Figure 2. 2 Rainfall data for Milwaukee from 2006 to 2008. Data was obtained from the National Weather Service Milwaukee station at General Mitchell Airport (42°57°N, 87°54°W).

E. coli and Enterococcus Enumeration

Each water sample was filtered through a 0.45-µm-pore-size 47 mm nitrocellulose filter and placed on modified m-TEC (Difco, Sparkes, MD) agar according to the EPA method for *E. coli* enumeration (EPA 2002a) and on mEI agar (Difco, Sparkes, MD) for enterococcus enumeration (EPA 2002b). The volumes filtered varied according to expected contamination, where 10 ml and 100 ml volumes were analyzed for water beach samples, and 1 ml and 10 ml volumes were analyzed for outfalls at the beaches, and the remaining beach samples. The plates were incubated at 44.5°C for 24 h for *E. coli* enumeration and at 41°C for 24 h for enterococcus enumeration.

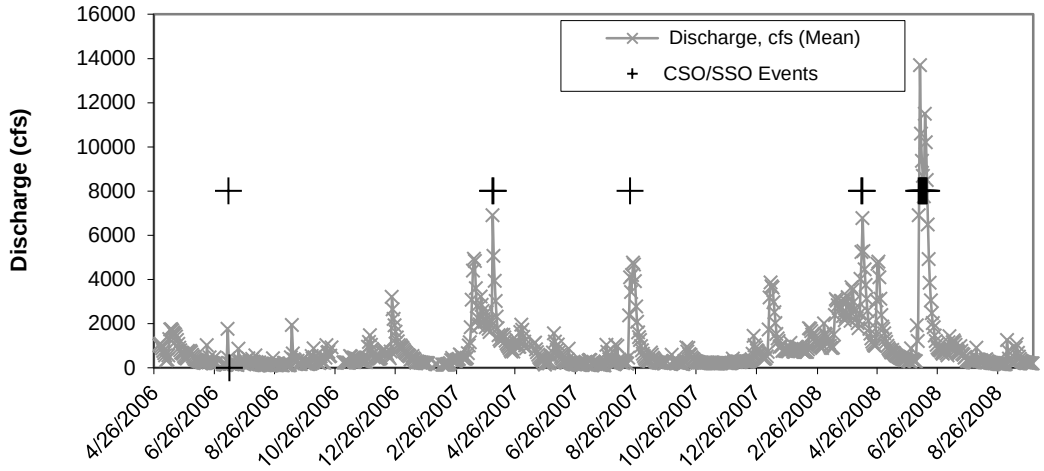

Figure 2.3 Hydrograph of river discharge into Lake Michigan. Flow was measured at the channel downstream from the confluence of three major rivers that in the Milwaukee River basin. Another CSO event occurred on 3/13/06, not shown in the graph. The presence of SSO and CSO events are indicated. The primary discharge points from sewage overflows are rivers prior to confluence and the harbor.

DNA Extraction

Water sample volumes filtered for DNA extraction ranged from 100 to 200 ml for beach samples and outfall samples. All samples were filtered onto a 0.45 µm nitrocellulose filter and frozen at -80°C for DNA extractions. The frozen filters were broken into small fragments with a metal spatula. The DNA was extracted using the Qbiogene FastDNA Spin Kit for Soil (Qbiogene, Inc., Irvine, CA) as specified in the manual, except that the cells were mechanically lysed using the MiniBead- Beater-8 Cell Disruptor (BioSpec Products, Bartlesville, OK) on the homogenization setting for 1.0 min at room temperature. The DNA was eluted in 100 µl of sterile distilled water. The number of culturable *E. coli* cells per filter was calculated from the cell counts on modified m-TEC medium. The DNA concentration was determined using the NanoDrop ND-1000 Spectrophotometer (NanoDrop Technologies, Wilmington, DE).

Human *Bacteroides* Marker Assessment

Human *Bacteroides* marker (HF183F/708R) was based on the 16S rRNA gene (Bower *et al*, 2005). Primers were synthesized by Sigma Genosys (The Woodlands, TX).

PCR analysis was conducted with either 1 or 2 µl of undiluted DNA samples or samples diluted to a range of 10 to 40 ng/PCR. All samples were amplified with human *Bacteroides* primers. The 25µl PCR mixtures consisted of the QIAGEN Taq PCR Master Mix Kit (2x-concentrated 5-U/µl Taq, 3 mM $MgCl_2$, and 400 µM of each deoxynucleoside triphosphate), and each primer was present at a final concentration of 0.35 µM. All PCRs were run in the MJ Research PTC-Quad thermal cycler (Watertown, MA). The PCR conditions were 1 cycle at 94°C for 4 minutes; 35 cycles at 94°C for 30 s; annealing temperature for 30 s; 72°C for 30 s; 1 cycle at 72°C for 6 min; and a 10°C hold. The annealing temperature was 59°C. The PCR products were visualized on 2% agarose gels following staining with ethidium bromide and were compared with a 100-bp DNA size standard (Fisher Scientific, Pittsburgh, PA).

Statistical Analysis

The geometric mean of each sampling region for 2006 to 2008 surveys was calculated to account for the variability in bacterial counts over different days within a given region. Values for *E. coli*, enterococcus, and turbidity from samples collected at the same beach, but in different sites, were averaged. Differences in *E. coli* levels between CSO conditions and post CSO were evaluated using a Students t-test in Sigma plot, v.8.02 (SPSS, Inc.).

2.4 RESULTS AND DISCUSSION

Contaminant Loads Entering Lake Michigan

The hydrograph of river discharge into Lake Michigan (Fig. 2.3) shows that there is an immediate response at the river mouth to rainfall (Fig. 2.2) in Milwaukee watersheds, increasing the discharge at the junction within the same day. The CSO/SSO events occurred with a minimum of 2.8 cm of rainfall in March 2006.

Although *E. coli* levels reached very high counts at all beaches during the study period (up to 66,880 CFU/100 ml), the geometric mean of *E. coli* at Klode Park, McKinley Beach, Big Bay Beach, Atwater Beach, Bradford Beach, South Shore Beach – New, and Bay View Beach were under the EPA limit for issuing an advisory sign, ranging from 59 CFU/100 ml to 225 CFU/100 ml (Table 1). From these beaches, McKinley Beach and South Shore Beach - New had the lowest % exceedance compared to the other beaches (23.7% and 36.0%, respectively), which ranged from 38.9% to 58.9%. Only two beaches: Doctors Park and South Shore Beach - Old had high geometric mean for *E. coli* (268 CFU/100 ml and 304 CFU/100 ml, respectively) throughout the three years, exceeding the EPA limit for *E. coli* in 47.0% and 57.1% of the cases, respectively.

Geometric mean of enterococci ranged from 11 CFU/100 ml to 154 CFU/100 ml for all beaches. South Shore Beach – Old had the highest level of bacteria counts, ranging from 0 to 13,900 CFU/100 ml and McKinley had the lowest level of bacteria counts, ranging from 0 to 557 CFU/100 ml).

Table 2. 1 Characterization of Lake Michigan beaches from 2006 to 2008

Beach	*E. coli* (CFU/100 geometric mean	% exceedance 235 CFU/100	Enterococci geometric mean	Turbidity (NTU) geometric mean	% positive Human *Bac.*
Doctors Park	268 (14 - 3,445) (n=17)	47.0	68 (3 - 1,213) (n=16)	44 (7 - 546) (n=17)	0/20 (0%)
Klode Park	103 (9 - 2,840) (n=18)	38.9	125 (4-4,015) (n=17)	13 (2 - 46)	1/32 (3 %)
North Beach	225 (7 - 6,833) (n=17)	58.8	154 (3 - 7,100) (n=17)	86 (7 - 426) (n=17)	1/21 (5%)
Big Bay	127 (0-4,239) (n=19)	57.9	101 (0 - 2,890) (n=18)	11 (3 - 42) (n=15)	5/19 (26%)
Atwater	143 (6 - 7,433) (n=29)	41.9	43 (0 - 4, 627) (n=27)	25 (3 - 1,100) (n=26)	1/81 (1%)
Bradford	174 (0 - 6,827) (n=58)	53.4	38 (0 - 3,369) (n=52)	22 (3 - 215) (n=35)	19/143 (13
McKinley	59 (0 - 4,343) (n=38)	23.7	11 (0 - 557) (n=36)	19 (3 - 280) (n=22)	0/46 (0%)
South Shore	304 (0 - 8,967) (n=39)	66.7	100 (0 - 13,900) (n=40)	12 (2 -52) (n=26)	0/51 (0%)
South Shore	60 (0 - 66,880) (n=35)	35.9	18 (0- 1,210) (n=40)	8 (2-62) (n=27)	1/48 (2%)
Bay View	217 (4 - 5,313) (n=26)	57.7	88 (0 - 3,873) (n=27)	10 (3 -62) (n=27)	0/30 (0%)

Although a very limited number of water samples had been found positive for human *Bacteroides* marker. (Table 2.1), beach outfalls were found positive for this sewage indicator at least once at all beaches (Table 2.2). Human sewage is flowing out of municipal storm sewers

and into Lake Michigan beaches on rainy days without CSO and/or SSO events, and even during periods of dry weather.

Table 2. 2 Human *Bacteroides* marker detection in stormwater outfalls in Milwaukee beaches from 2006 to 2008.

Beach	Number of Outfalls sampled	Number of Samples	% Positive for Human *Bacteroides* marker
Bradford Beach	14	136	21%
Klode Park	3	42	31%
North Beach	8	30	50%
Atwater Beach	1	8	63%
Doctors Park	1	10	30%
Bay View	1	17	71%
South Shore	1	26	73%
Big Bay Beach	1	16	75%

CSO outfalls located near South Shore Beach and at Bay View Beach were found 73% and 75% positive for human *Bacteroides* marker, respectively. These two beaches are located within a breakwall near the harbor. Theses beaches exceeded the EPA limit for recreational water quality on 66.7% (South Shore - Old), 35.9 % (South Shore - New), and 57.7% (Bay View Beach) of samples sampled in this study. Previous studies of South Shore Beach conducted in our lab have demonstrated that the chronic beach closures can be attributed in part to poor circulation and local stormwater runoff (Scopel et al, 2006).

The outfall at Big Bay Beach and the outfall submerged just north of Atwater Beach were found 71% and 63%, respectively, positive for human *Bacteroides* marker. This beach exceeded the EPA limit for recreational water quality on 57. 9% and 41.4 %, respectively, of samples tested for *E. coli*. This high frequency of positive for this sewage indicator might be due to sewage leaks caused by breaks or improper connections in the city's storm sewer system.

Similar conditions were observed at outfalls at North Beach, Klode Park, Doctors Park, and Bradford Beach, where 50 %, 31%, 30%, and 21% of the samples were found positive for the human – specific marker.

Water circulation is very complex in Lake Michigan and researchers have been successful in modeling it (Bravo *et al*, 2009), showing that flow direction can change rapidly in a very short time, although more work is needed especially in the nearshore region. Little is known about swash zone and surf zone regions in Lake Michigan, but some parameters could explain why outfalls have been found positive for sewage indicator, when water samples were not, such as flow rate and discharge of stormwater outfalls (parameters that are not measured), lake water circulation, patterns of longshore currents versus cross-shore, and currents & wave condition. Another possible explanation is the method for detection of human *Bacteroides* marker. This method has been improved in our lab recently, increasing the volume of water to be filtered for DNA (400 ml, instead of 200 ml, when possible) and smaller pore size to filter samples for DNA (0.22 µm, instead of 0.45 µm).

Detailed Assessment of CSO/SSO Events

CSO/SSO events are not the main source of sewage contamination in Milwaukee costal area. The construction of an inline storage system in Milwaukee reduced the number of combined

sewer overflows from 40 – 60 per year to 0 – 4 per year with the average approximating 1.5 per year over the past 10 years (Patz *et al*, 2008). However, it is important to understand the impact of sewage overflows at the beaches, in order to be able to protect the public from waterborne illnesses.

E. coli levels exceeded 235 CFU/100 ml at most of the beaches during CSO/SSO events, mainly at the beaches in southern of Milwaukee harbor (South Shore Beach and Bay View Beach) from 2006 to 2008. Both beaches have a CSO outfall near or at the beach, which obviously facilitate sewage presence at these beaches during these events. However, bacterial densities were not always high during these events at all beaches, and the human *Bacteroides* marker was not found positive all the time during these events. This might be due to different patterns of water circulation, wave, current & wind patterns, not discussed in this paper.

The June 2008 CSO/SSO event was very well documented for three beaches: Bradford Beach, South Shore Beach - New and South Shore Beach – Old, and Bay View Beach. These beaches were sampled daily from June 9 until June 15. Average of *E. coli* levels were compared between *E. coli* levels one-day post CSO/SSO event (June 16) and nine- days post CSO/SSO event (June 24). Overall, bacterial levels were slightly different between average of CSO/SSO event and one-day post CSO/SSO event ($p=0.366$), showing that the environment was still severely impacted by the 9-day overflow event.

South Shore Beach - New presented lower counts of *E. coli* compared to South Shore Beach - Old, and had not exceeded EPA limits for *E. coli* in one CSO/SSO event (6/12/08). The differences between the two beaches have been shown in a previous study, although the two sites are only ~ 170 meters apart.

The old beach is adjacent to a two square city block parking lot that is sloped to drain to Lake Michigan, and runoff from this impervious surface appears greatly contribute to *E. coli* levels at the beach. In addition, the old beach is a sandy beach and the new one is a rocky beach. The beach sand itself may serve as a reservoir for *E. coli* and the presence of birds dropping at that beach just enhance the problem.

All the other beaches, all located north of Milwaukee harbor and not enclosed by a breakwall, do not have CSO outfalls, although at least one stormwater outfall near or at the beach was found positive for Human *Bacteroides* marker, according to Table 2.2, indicating presence of sewage. This might be due to leaky pipes, cross-contamination between stormwater and sanitary pipes, misconnections, and water aging infrastructure in Milwaukee.

Bacteria levels usually increased after rainfall events at all beaches, and usually decreased afterwards (Fig. 2.4 to Fig. 2.10). Turbidity was found not to be proportional to bacterial densities at all beaches, evidence that there are other parameters impacting turbidity, such as resuspension events and presence of cladophora.

Table 2. 3 Comparison of mean levels of *E. coli* (CFU/100ml) within Lake Michigan beaches in Milwaukee from spatial surveys conducted during and after CSO and SSO events. CFU (Colony Forming Unit), CSO (Combined Sewer Overflow), SSO (Sanitary Sewer Overflow) (n=3 to 4 for all samples; exceptions on footnote)

Date	Doctors Park	North Beach	Klode Park	Big Bay Beach	Atwater Beach	Bradford Beach	McKinley Beach	South Shore Beach - Old	South Shore Beach - New	Bay View Beach
7/10/2006*	-	-	-	-	-	-	-	1,740 +	1,320 +	-
4/3/2007*	-	-	-	-	-	0	0 º	-	-	50
8/20/2007*	168	577	141	253	122	828	126	2,187 +	497 +	1,107
8/22/2007	-	-	-	-	27	-	37	283	18 º	43
8/23/2007	-	-	256	343	17	-	62	-	-	-
6/9/2008*	2,090	1,137 +	368	823+	477	1,487 +	507	6,500+	340+	1,500+
6/10/2008*	53+	327 +	15+	12 +	18	510	410	1,550 +	1,640 +	1,077 +
6/11/2008*	-	-	-	-	-	281	-	940+	325+	720 +
6/12/2008*	-	-	--	-	-	127+	-	800+	150+	310 +
6/13/2008*	1,443 +	1,297 +	180 +	2,493 +	233	257+	264	1,900 +	1,070 +	653 +
6/14/2008*	-	-	-	-	-	333	-	903 +	757+	507 +
6/15/2008*	-	-	-	-	-	92	-	1,550+	990+	223+
6/16/2008	-	-	-	-	-	316	-	707+	540 + º	853 +
6/24/2008	14	15	10	14	26	78	34	500+	108+	275

- No data collected for this beach during specific spatial survey
\+ At least one outfall at or near the beach was found positive for *Human Bacteroides marker* Human
* CSO/SSO events occurred
º McKinley Beach (n=1), South Shore Beach - New (8/22/07: n=2; 6/16/08: n=1)
Gray squares show that *E. coli* levels exceeded 235 CFU/100 ml

There were some cases in which samples were collected during baseline conditions or light rainfall events, and presented high levels of bacteria. For instance, beaches were surveyed on

7/17/2007 (rainfall = 0.60 cm) and *E. coli* levels exceeded 3,000 CFU/100 ml at Doctors Park (Fig. 2.4) and reached 358 CFU/100 ml at Klode Park (Fig. 2.5). Although outfalls have been tested for human *Bacteroides* marker that day and were found negative, the source of contamination could still be sewage flowing out the storm water system, discharged at a specific time during the day (and not at the time that the outfall was sampled). Similar results were identified at Atwater Beach (Fig. 2.6), where the submerged outfall just north of the beach was found positive for human *Bacteroides* marker randomly, and independent of rainfall events. Geometric mean of turbidity at Atwater Beach was 25 NTU, but it exceeded 1000 NTU twice during the study period, probably due to frequent presence of cladophora in that region. There were some spikes in turbidity during the June 2008 CSO/SSO event.

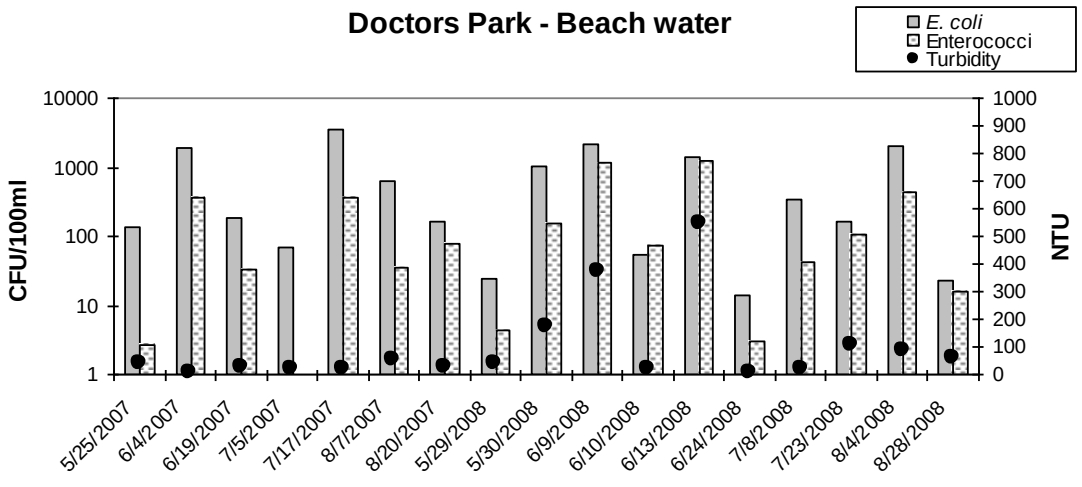

Figure 2. 4*E. coli*, enterococcus, and turbidity levels at Doctors Park from 2007 to 2008. No data available from 2006.

Geometric mean of turbidity at Doctors Park and Klode Park was 44 NTU and 13 NTU, respectively, but there were some spikes during rainfall events and/or CSO/SSO events, reaching 546 NTU at Doctors Park and only 46 NTU at Klode Park. Similarly, Big Bay Beach had low

level of turbidity during the time of the study, with low geometric mean of 11 NTU, and it reached its maximum of 42 NTU in a baseline survey. This can be explained for the frequent discharge of sewage at that beach, since 75% of the outfalls samples were positive for the human-specific marker during the study.

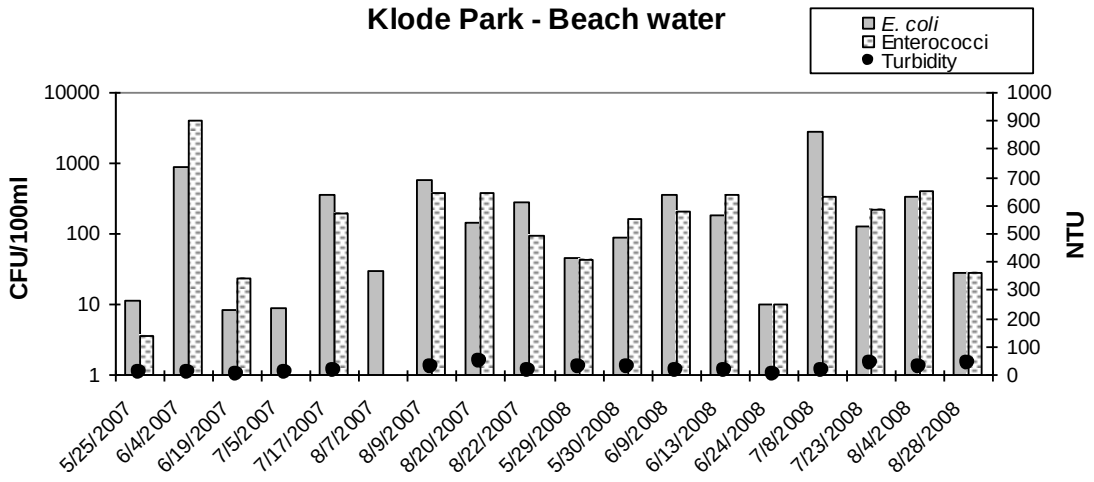

Figure 2. 5 *E. coli*, enterococcus, and turbidity levels at Klode Park from 2007 to 2008. No data available from 2006.

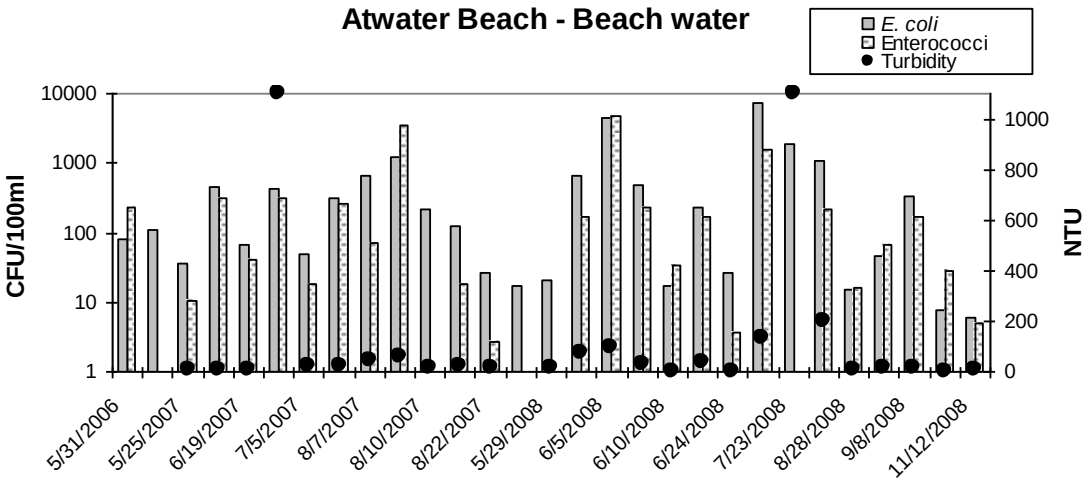

Figure 2. 6 *E. coli*, enterococcus, and turbidity levels at Atwater Beach from 2006 to 2008.

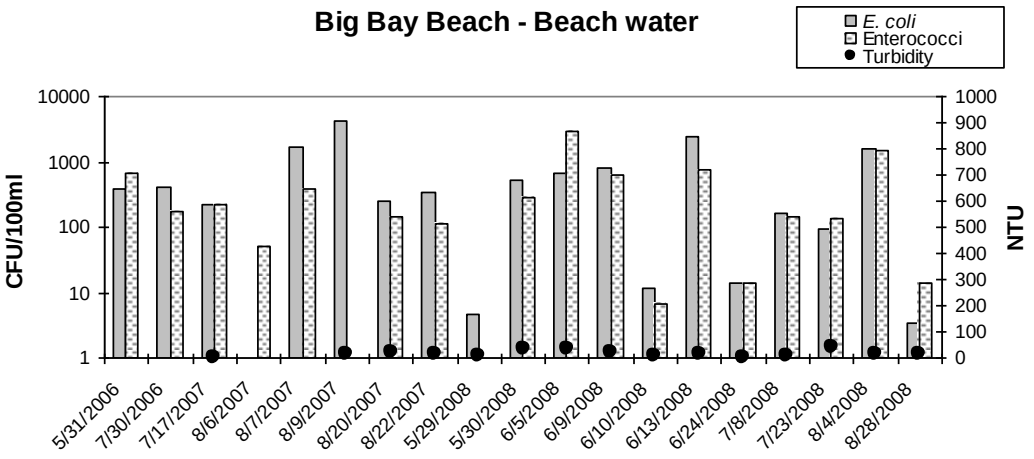

Figure 2. 7 *E. coli*, enterococcus, and turbidity levels at North Beach from 2006 to 2008.

On the other hand, turbidity levels were high at North Beach (graph not shown), with geometric mean of 86 NTU, and it reached 426 NTU in a baseline survey. High levels of turbidity might be related to frequent presence of cladophora in that region.

Bradford Beach (Fig. 2.8) and McKinley Beach (graph not shown) had similar trends of turbidity, where the geometric mean was 22 NTU and 19 NTU, respectively, but it exceeded 200 NTU and 160 NTU, respectively during heavy rainfall and CSO/SSO events.

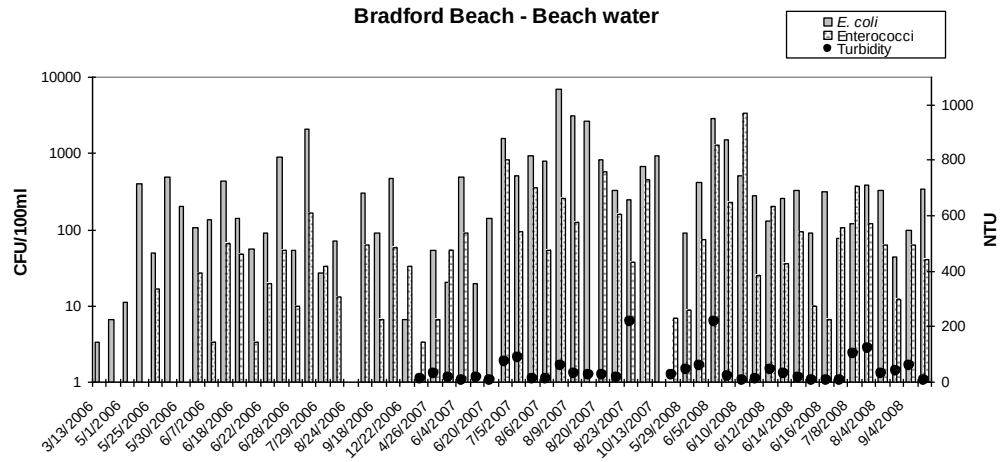

Figure 2. 8 *E. coli*, enterococcus, and turbidity levels at Bradford Beach from 2006 to 2008.

The two beaches located within the breakwall had also similar trends of turbidity. Geometric mean of turbidity at that beach was 12 NTU (South Shore Beach – Old) and 8 NTU (South Shore Beach – New), but it reached a maximum of 52 NTU and 62 NTU, respectively during the June 2008 CSO/SSO events (Fig. 2.9 and Fig. 2.10). The geometric mean of turbidity at Bay View Beach (graph not shown) was 10 NTU, but it reached a maximum of 62 NTU during the April 2008 CSO/SSO event.

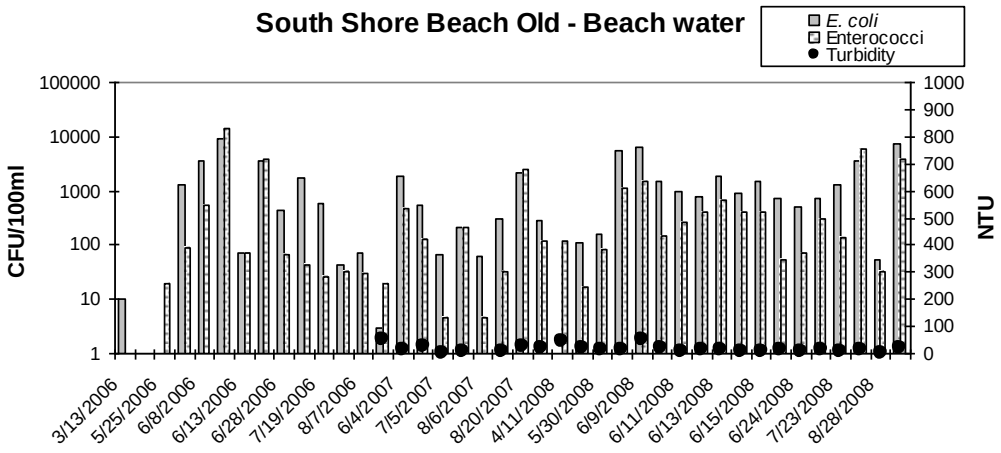

Figure 2. 9 *E. coli,* enterococcus, and turbidity levels at South Shore Beach - Old from 2006 to 2008.

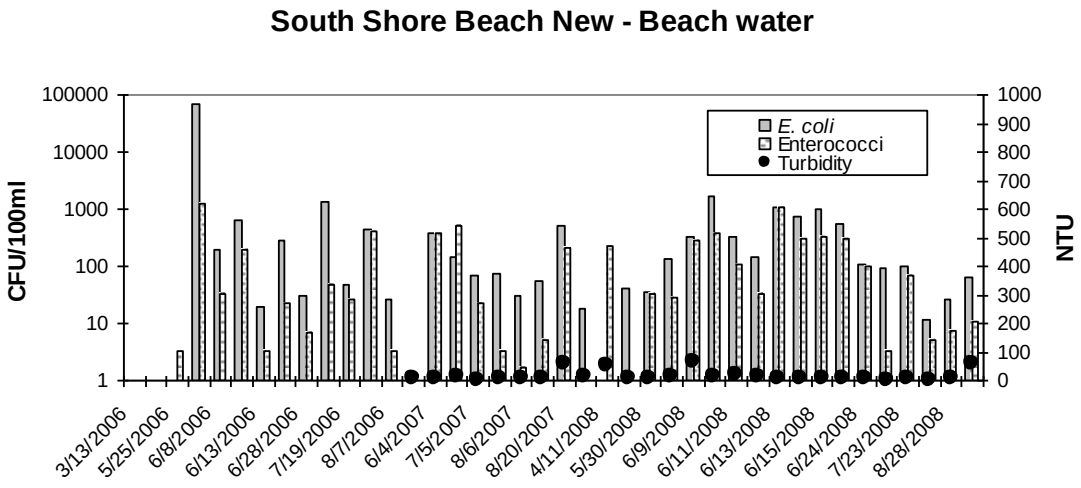

Figure 2. 10 *E. coli,* enterococcus, and turbidity levels at South Shore Beach - New from 2006 to 2008.

2.5 CONCLUSIONS

From this study, we conclude that (1) the urban environment presents several risks of water contamination, and most of the beaches in Milwaukee are located in urban areas. Stormwater runoff contains several pollutants, including fecal indicator bacteria, which may indicate presence of pathogens, posing health risks. Most of the time, urban stormwater is conveyed in separate sewers systems and discharged directly into receiving waters, (2) Aging water infrastructure may cause sanitary sewage to infiltrate into stormwater pipes, which may discharge directly at the beaches, and (3) CSOs or SSOs are not the main sources of sewage contamination in Milwaukee coastal area.

2.6 ACKNOWLEDGMENTS

This work was funded by the University of Wisconsin Sea Grant Institute under a grant from the National Sea Grant College Program, National Oceanic and Atmospheric Administration, U.S. Department of Commerce. Federal grant number A06OAR4170011, Project Number R/UC-2. Authors thank to Patricia Bower, Elizabeth Sauer, Jessica VandeWalle, Melinda Bootsma, Colin Peake, Lisa Stewart, Sabrina Mueller-Spitz, Jeff Ecklund, Jessica Chepp, Caitlin Carlson, Erika Jensen, Morgan Depas, Meredith Van Dyke, Ryan Jenner, Sarah Edquist, Andrea Zimmerman, and Alisa Lilly for helping with lab arrangements, sampling and analysis.

2.7 REFERENCES

PUBLIC LAW 106–284. OCT. 10, 2000. Beaches Environmental Assessment and Coastal Health Act of 2000.

U.S. Environmental Protection Agency. 2003a. Bacterial water quality standards for recreational waters. EPA/823/R-03/008. U.S. Environmental Protection Agency, Washington, D.C.

NRDC. 2008. Testing the Waters 2008: A Guide to Water Quality at Vacation Beaches. National Resources Defense Council, Washington, DC.

U.S. Environmental Protection Agency. 2003b. Beach Currents Newsletter-Fall 2003. EPA/823/N-03/001. U.S. Environmental Protection Agency, Washington, D.C.

Wisconsin Department of Natural Resources. 2009. Beaches monitoring season begins at Great Lakes beaches. Retrieved from http://dnr.wi.gov/news/DNRNews_Article_Lookup.asp?id=1111

McLellan, S.L. & Salmore, A.K. 2003. Evidence for localized bacterial loading as the cause of chronic beach closings in a freshwater marina. Water Research 37:2700-8.

Bower, P.A., Scopel, C.O., Jensen, E.T., Depas, M.M. & McLellan, S.L. 2005. Detection of genetic markers of fecal indicator bacteria in Lake Michigan and determination of their relationship to *Escherichia coli* densities using standard microbiological methods. Appl. Environ. Microbiol. 71(12): 8305-8313.

McLellan SL, ET Hollis, MM Depas, M Van Dyke, J Harris, and CO Scopel. 2007. Distribution and fate of *Escherichia coli* in Lake Michigan following contamination with urban stormwater and combined sewer overflows. J Great Lakes Res. 33:566-580.

S.L. McLellan, S.M. Huse, S.R. Mueller-Spitz, E.N. Andreishcheva, and M.L. Sogin. 2010. Diversity and Population Structure of Sewage Derived Microorganisms in Wastewater Treatment Plant Influent. Appl. Environ. Microbiol. 12 (2):378-392.

U. S. Environmental Protection Agency. 2002. Method 1603: *Escherichia coli (E. coli)* in water by membrane filtration using modified membrane-thermotolerant *Escherichia coli* agar (modified mTEC). Office of Water, U.S. Environmental Protection Agency, Washington, D.C.

U. S. Environmental Protection Agency. 2002. Method 1600: Enterococci in water by membrane filtration using membrane-Enterococcus Indoxil-β-D-Glucoside Agar (mEI). Office of Water, U.S. Environmental Protection Agency, Washington, D.C.

Scopel, C.O., J. Harris, and S. L. McLellan. 2006. Influence of Nearshore Water Dynamics and Pollution Sources on Beach Monitoring Outcomes at Two Adjacent Lake Michigan Beaches. J Great Lakes Res. 32:543-552.

Bravo, H. H., P. N. Shedivy, and D. J. Schwab. Submitted. Hydrodynamic and transport model for the Lake Michigan coast around Milwaukee. Journal of Hydraulic Engineering.

Patz, J.A., Vavrus, S.J., Uejio, C.K. & McLellan,S.L. 2008. Climate Change and Waterborne Disease risk in the Great Lakes region of the U.S. Am J Prev Med. 35(5):451-8.

CHAPTER 3

EFFECT OF HYDROLOGICAL AND GEOPHYSICAL FACTORS ON FORMATION OF STANDING WATER AND FECAL INDICATOR BACTERIA RESERVOIRS AT A LAKE MICHIGAN BEACH

3.1 ABSTRACT

Water quality impairment of Great Lakes beaches is caused by fecal pollution from point and nonpoint sources, and further exasperated by the condition of the beach environment. Erosion due to wind or wave action, invasive vegetation and chronically wet, flooded or standing water

are conditions that can magnify water quality problems at beaches. We investigated the hydrological and geophysical characteristics of the Bradford Beach on Lake Michigan (Milwaukee, WI) and the linkage between standing water and persistent contamination by fecal indicator bacteria (FIB). Our study showed that there is a significant positive correlation between high concentrations of *Escherichia coli* (*E. coli*) in sand and chronic high moisture content caused by standing water. Overall, the main factor influencing the formation of standing water was rainfall, with notable differences in standing water and/or wet sand conditions in the northern and southern parts of the beach that could be accounted for by differences in ground water elevations and beach erosion and accretion patterns. Mean grain diameter (d_{50}) was smaller (0.253 mm) on the northern end versus the southern end (0.326 mm); however, hydraulic conductivity was essentially the same for the two regions. Rain gardens that capture runoff contributed to transient increases in the water table following rainfall. Standing water was a health concern, especially following heavy rainfall events when stormwater discharged to rain gardens overflowed and wave run-up delivered contaminated water to the backshore of the beach. During these events, the groundwater table rose and was closer to the ground surface, and FIB levels measured in piezometers reached up to 10^4 CFU/100 mL, whereas during dry conditions, levels averaged < 6 CFU/100 mL. On these same days standing water samples were positive for the *Bacteroides* genetic markers of human fecal pollution, and coincided with positive samples at stormwater outfalls that discharge to the rain gardens and directly to Lake Michigan immediately north of the beach.

3.2 INTRODUCTION

A variety of non-native bacteria, fungi, parasites, and viruses have been found in beach sand (Kishimoto et al. 1969; Bolton et al. 1999; Alm et al. 2003; Boehm et al. 2003; Watanabe et al. 2003; Whitman et al. 2003; WHO 2003; Kinzelman et al. 2004a; Beversdorf et al. 2007; Figueira et al. 2007; Silva et al. 2009; Abdelzaher et al. 2010; Halliday et al. 2011). Among these, *Escherichia coli* (*E. coli*) and enterococci, two commonly used fecal indicator bacteria (FIB) have been found at high levels in sand (Whitman et al. 2003; Yamahara et al. 2007). FIB such as *E. coli* and enterococci are correlated with disease in swimmers (usually gastrointestinal) (U.S.EPA 1983; U.S.EPA 1984). These FIB are generally nonpathogenic organisms used as proxies for the presence of fecal pathogens because they are more easily isolated and enumerated than pathogens (WHO 2003). There is a concern whether or not sand may serve as a reservoir for pathogens, thereby becoming a route of disease transmission (Heaney et al. 2009; Halliday et al. 2011; Heaney et al. 2012).

Although association of higher FIB counts in surface sand with higher moisture content has been reported in a number of studies (Bolton et al. 1999; Alm et al. 2003; Beversdorf et al. 2007; Yamahara et al. 2012), a mathematical relationship between the two variables has not been proposed yet. Studies have also shown that sand can serve as both a sink and a source of FIB to lake water (Whitman et al. 2003; Boehm et al. 2005; Beversdorf et al. 2007; Edge et al. 2007; Ishii et al. 2007; Skalbeck et al. 2010; Phillips et al. 2011). Furthermore, microcosm experiments have shown that *E. coli* survived longer in lake water with sand than in lake water without sand (Sampson et al. 2006). It has been suggested that organic material content of soil can prolong

survival of fecal organisms (Mallman et al. 1951; Tate 1978); therefore sand could enhance survival of FIB.

Some beaches in the Great Lakes region have reported the presence of backshore wet sand and standing water, which could facilitate reservoirs of FIB in sand. Beach slope is an important characteristic and low elevation beach areas have been associated with standing water through the capillary draw of the shallow water table resulting in wet sand surfaces (Pittner et al. 2009; Skalbeck et al. 2010). Coarser sands are associated with drier sand beach by increasing infiltration and decreasing capillary action (Pittner et al. 2009; Skalbeck et al. 2010; Spina 2011). Steeper slope and coarser sand can produce a drier sand surface and minimize the potential for wave runup. Knowledge of depth to the water table aids in determination of the moisture conditions at a beach and potential consequences for persistence of FIB. Only a few studies have examined the groundwater conditions beneath the beaches of the Great Lakes (Visocky 1977; Crowe et al. 2009; IJC 2010; Skalbeck et al. 2010; Spina 2011) or examined the link between groundwater and densities of surface water FIB (Weiskel et al. 1996; Haack et al. 2003; Boehm et al. 2004; Whitman et al. 2006; Skalbeck et al. 2010; Russell et al. 2012). Nonetheless these studies were based in either limited measurements of concentration of FIB in groundwater or limited groundwater level measurements per sampling season.

The objectives of this investigation were to: a) to assess relevant hydrological, geophysical, and water quality characteristics of Bradford Beach associated with formation and retention of standing water, b) explore linkage between standing water and sand FIB reservoirs, c) examine if standing water was a health concern, d) assess groundwater conditions beneath the beach.

3.3 MATERIALS AND METHODS

Study Site

Bradford Beach is a man-made urban beach in Milwaukee County on the shore of Lake Michigan (43º03'41.30" N, 87º52'20.41" W) which was constructed in the late 1930s via filling the nearshore lakebed (Fig. 3.1). The beach spans a total distance of approximately 700 m along shore and the cross shore extends 125 m from the water's edge to Lincoln Memorial Drive. Dolostone boulders and concrete riprap bound the beaches north and south ends (erosion protection). Across the road from the beach, a 25 m glacial bluff rises up from the original natural shore line. The beach consists of a flat region of medium to fine-grained, imported sand that overlies glacial till.

The beach profile of Bradford Beach from waterline to bluff consists of the beach face, the berm, the backshore where the swales are located and the top of the beach (Fig. 3.1). A strip of darker sand along the beach located in the backshore region corresponds to sand that is constantly wet and those are the locations where standing water was observed throughout this study. The 0.12 km^2 drainage area of Bradford Beach has seven subwatersheds that discharge in stormwater outfalls designated as O0 and O2 to O7, with the largest watershed discharging to the northernmost outfall (O7), which corresponds to 47% of the full drainage area, of which 8% is impervious surface. The second largest is the outfall discharging just south of the beach house (O2), which corresponds to 15% of the full drainage area, of which 31% is impervious surface. These outfalls previously discharged directly onto the sand and since June 2008, discharge to rain gardens. After construction of the rain gardens, anecdotal evidence suggests that standing water was more frequently observed, especially on the northern part of the beach, however beach

flooding and standing water were documented prior to 2008. The beach is also impacted by outfalls located north of the beach (O8 to O12), which discharge stormwater often contaminated with sewage (Silva and McLellan, 2010), directly to the lake that can reach the beach through longshore currents. Even though all the outfalls at or north of Bradford Beach are stormwater outfalls it is possible that the sewage intrusion comes from a cross connection between a sanitary pipe and the stormwater system. There were no reports of faulty plumbing at restrooms at or nearby the beach. In addition, under heavy rainfall events, sanitary sewer overflows (SSO) and combined sewer overflows (CSO) occurred 2-3 times per year during the extent of this study, discharging sewage into Lake Michigan.

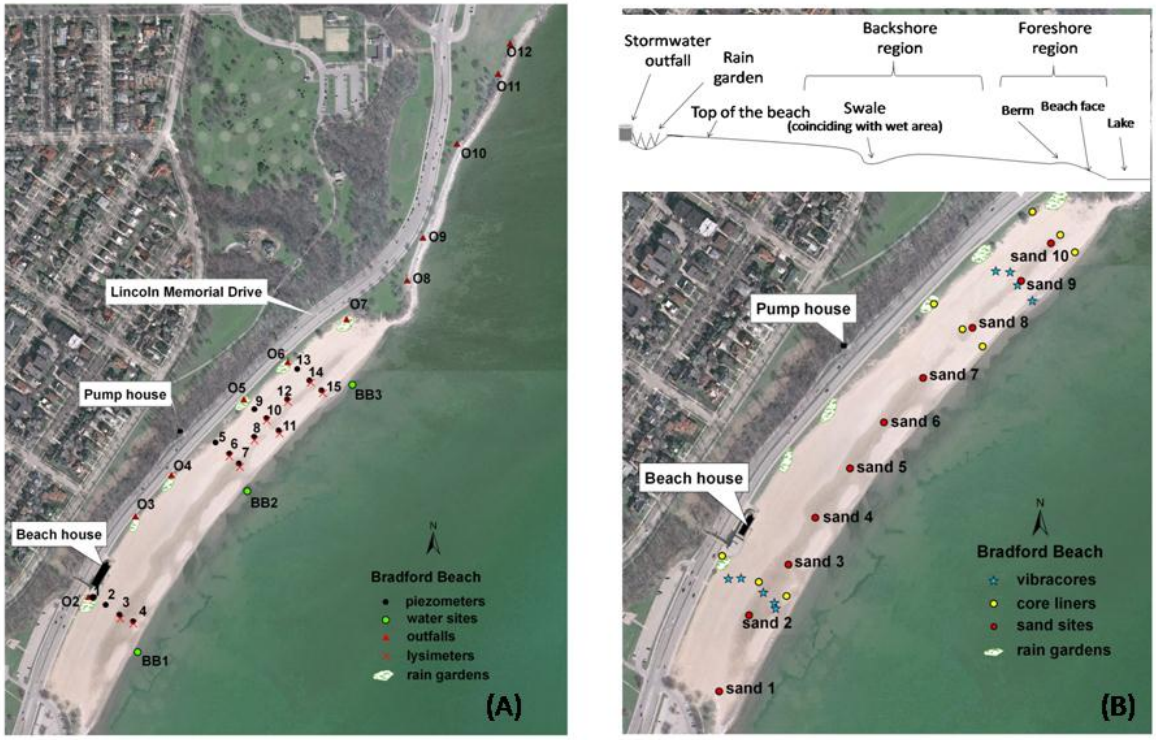

Figure 3. 1 (A) Water sampling sites. Green dots show the lake water sites, black circles show piezometers and are labeled from 1 to 15, and red crosses show pan lysimeters that are adjacent to piezometers. Stormwater outfalls at the beach (O2 to O7) and north of the beach (O8 to O12) are indicated. (B) Sand sampling sites. The yellow circles show the sites where sand cores were collected with core liner tubes, the blue stars show the transects of sand cores collected with a vibracore, red dots show the sampling sites of surface sand sites 1-10 (S1–S10). On the insert: sketch of the beach profile showing the main features; drawing is not to scale.

Hydrologic data collection and calculation

Daily lake water levels were obtained from station ID 9087057 operated by NOAA (http://tidesandcurrents.noaa.gov/data), located just south of Milwaukee Harbor. Daily precipitation data were obtained from the weather station operated by NOAA at the Milwaukee Mitchell Airport, located 16.7 km south of Bradford Beach. Although not as conveniently located, the station was sufficiently close to provide useful precipitation data for the study. Daily average wave height obtained through hydrodynamic modeling was provided by NOAA Great Lakes Environmental Research Laboratory (GLERL). Hourly images of the presence of standing water on Bradford Beach were obtained by a network camera installed on the top of the beach house on the study site.

Piezometers were used for two purposes: for measurement of ground water levels and for sampling groundwater for FIB analysis. Four piezometers were deployed on the southern part of the beach and eleven on the northern part of the beach, as shown in Fig. 3.1A. The piezometers consisted of a 1.2 m long, 5.1 cm diameter (ID) polyvinyl chloride pipe. They were perforated with 1.3 cm holes throughout a 76 cm segment of the pipe and wrapped with 100 μm polyester filter felt. Pan lysimeters (SoilmoistureModel 1960) were installed adjacent to piezometers with the crown 8 cm below the ground. The pan lysimeters are designed to capture surface runoff infiltrating through the sand and were installed shallow enough to not capture ground water. By excluding groundwater, these measurements helped distinguish when the piezometers were impacted by wave runup or surface runoff. Depth to water was measured in piezometers to the nearest 1 mm using an electronic water level sounder (Solinst Model 101). The groundwater elevation was calculated by subtracting the depth to water measurement from the top-of-casing

(TOC) elevation. Groundwater level measured from October 2009 to December 2010 at the 15 piezometers is summarized in Table 3. 1. Variability was measured according to Eq. 3.1.

$$\mathrm{MV} = \frac{\sum_{i=1}^{N}(x_i - \bar{x})^2}{N \times R} \qquad \textbf{Equation 3. 1}$$

where:

MV- Measure of Variability (m)

xi- groundwater level measurement (m)

N- number of observations at a given piezometer

R- full range of groundwater levels for all the 15 piezometers

Groundwater velocity (V) from the rain gardens toward the lake was estimated by Eq. 3.2.

$$V = \frac{K_h \, x \, \frac{\Delta h}{\Delta l}}{n} \qquad \textbf{Equation 3. 2}$$

where:

K_h – horizontal hydraulic conductivity

$\frac{\Delta h}{\Delta l}$ – hydraulic gradient

n- porosity

Table 3. 1 Groundwater levels at piezometers (PZ) from October 2009 to December 2010.[1]

		N	Mean (m)	Median (m)	Δ (m) = Max-Min	Variability (m)	Depth to groundwater (m)
Next to rain gardens	PZ-1	115	177.38	177.32	1.06	0.02	0.885
	PZ-9	91	176.655	176.641	0.824	0.008	1.268
	PZ-13	117	176.636	176.602	0.816	0.007	1.078
Middle of the beach	PZ-2	79	177.174	177.153	0.557	0.007	NA
	PZ-3*	121	177.121	177.069	0.698	0.021	0.242
	PZ-6	122	176.8	176.782	0.674	0.008	0.365
	PZ-8*	120	176.68	176.629	0.887	0.017	0.550
	PZ-10*	122	176.609	176.59	0.854	0.005	0.583
	PZ-12*	122	176.59	176.574	0.794	0.007	0.651
	PZ-14*	121	176.567	176.558	0.753	0.008	0.644
Next to the lake	PZ-4*	122	176.814	176.78	0.782	0.021	0.335
	PZ-7*	97	176.767	176.712	0.592	0.015	0.233
	PZ-11	120	176.574	176.561	0.744	0.007	0.796
	PZ-15	47	176.538	176.543	0.476	0.006	0.784

Collection and analysis of water samples

Lake water samples were collected 1-2 m from shore in knee-deep water into Nalgene® polypropylene bottles. Bottles were full-volume flushed three times with water from the sample site. Lake water sampling sites are shown in Fig.3. 1A. Samples from stormwater outfalls (O2 to O12) were collected directly into Nalgene® bottles. Standing water was sampled with sterile Whirl-Pak™ bags and transferred to clean bottles. Samples of groundwater and runoff infiltrating through the sand were collected at piezometer and pan lysimeter locations, respectively, using a battery-powered portable sampling system (Barnant Company Model number 7577-00) or a hand pump. Deionized water was first pumped to clean the tubing line

[1] Statistics for PZ-5 was not presented because it was dry most of the time. Piezometers in standing water zones are marked with an asterisk.

before pumping the subsurface water samples into clean bottles. To make certain that the water being collected was groundwater, piezometers were purged with a bailer after rainfall or as needed until clear water and no sand was observed before sampling. All water samples were placed on ice and in darkness until filtering in the lab the same day for culture of FIB. Samples were filtered for DNA analysis within 18 h. Sampling sites are shown in Fig.3.1A.

Each water sample was filtered through a 0.45-µm-pore-size 47 mm nitrocellulose filter and placed on modified m-TEC (Difco, Sparkes, MD) agar according to the EPA method for *E. coli* enumeration (U.S.EPA 2002a), on mEI agar (Difco, Sparkes, MD) for enterococci enumeration (U.S.EPA 2002b), and on MI agar (Difco, Sparkes, MD) for total coliforms enumeration (EPA 2002; U.S.EPA 2002c). *E. coli* concentration and moisture content were not normally distributed in its original scale and had to be log transformed to be tested for difference of means.

Collection and analysis of sand samples

Surface sand samples were collected with a spatula at a depth < 5 cm and placed in individual 50 mL polypropylene tubes for each sample location (sand sites S1 to S10). Sediment core samples were collected by core liner tubes on 10/13/07. The 0.91 m long and 6.8 cm (I.D.) core liner tubes were inserted into the sand using a rubber mallet. A second sediment core collection was performed by vibracore on 07/02/09. Three transects with a total of nine sites were established. Vibracores (Wacker Model H55) were acquired by mechanically vibrating a 1 m or shorter section of 7.4 cm (I.D.) aluminum irrigation pipe down to the depth of the water table. Sand (20 g) collected separately from top, middle and bottom of each core was vortexed with 30 mL of sterile water and *E. coli* was determined according to previous published method (Beversdorf et al. 2007). Sampling sites are shown in Fig.3.1B.

DNA Extraction, PCR detection, and qPCR quantification of human Bacteroides genetic marker.

For beach water, standing water or outfall samples, a volume of 100 to 200 mL of sample was filtered onto a 0.22 μm pore size 47 mm nitrocellulose filters and stored at -80°C. For samples of groundwater and runoff infiltrating through the sand, usually 500 mL was filtered. Extraction of DNA for stormwater outfall samples was performed using MPBIO FastDNA Spin Kit for soil (MP Biomedicals, Santa Anna, CA) as previously described (Sauer et al. 2011). Extraction of DNA of groundwater, rainfall infiltrating through the sand, and lake water samples were performed in crude cell lysates after bead beating alone (Lavender et al. 2009). PCR and qPCR analysis for human *Bacteroides* genetic marker using HF183 primer (Bernhard et al. 2000) were performed according to previous published methods (Sauer et al. 2011).

Geophysical surveying

Electromagnetic studies were conducted with a Geonics EM31-MK2 Ground Conductivity Meter that detects subsurface ground conductivity changes to a depth of about 6 m. Conductivity changes can be due to lithologic changes, changes in water saturation and/or changes in pore fluid conductivity. Soundings were conducted at two points approximately 100 m apart along a line centered in the middle of the beach parallel to the shore. The sounding used an ABEM Terrameter SAS 1,000/VES resistivity meter in a Wenner configuration with “a” spacings ranging from 0.47 m to 67 m. Resistivity profiles were performed using a 16 electrode GF Instruments ARES-Automatic Resistivity System. Ground Penetrating Radar (GPR) data were collected with a Geophysical Survey Systems Inc. SIR 3000 GPR unit. Survey lines were marked every 1 m to use for tie points for the GPR distance data.

Beach topographical surveys

Three comprehensive topographical surveys were conducted at the Bradford Beach in November 2009, April 2010, and July 2010. The accuracy parameters were predetermined with the intention of capturing the topographic relief of the site within 3 cm. Two types of technology were utilized in these surveys. Real Time Kinematic Global Positioning System (GPS) technology with a Virtual Reference Station network base correction was used to establish primary control and to capture XYZ data on the ground. The second type of technology consisted of a Trimble S6 Robotic Total Station. The TOC of the piezometers were measured during these surveys.

Saturated hydraulic conductivity (K), grain size, and moisture content

Determination of hydraulic conductivity (K) was performed on surface sand core samples using the American Society for Testing and Materials (ASTM) constant head method (ASTM 2006a). This laboratory procedure measures vertical K. Grain size analyses were conducted using ASTM method (ASTM 2006b). Samples were placed in aluminum bowls and oven dried for 24 h at 110 °C, the oven dried samples were place in a stack of sieves (75-µm, 106-µm, 150-µm, 250-µm, 425-µm, 850-µm, 2-mm, and 4.75-mm), and then the stack was placed in a mechanical shaker for 10 min and the fraction of sample retained on each sieve was weighed on an electronic scale to nearest 0.01 g. The percent moisture of surface sand samples was determined by wet and dry weight measurements of approximately 1 g of sand removed from the sample, according to a previously published method (Beversdorf et al. 2007).

Statistical Analysis

Difference between means of log *E. coli* concentration during wet and dry days, K and sand mean diameter (d_{50}) from northern and southern part of the beach were evaluated using a Student's t-test (two-tailed) with equal variance (Matlab, Mathworks, Natick, MA). The correlation between concentration of *E. coli* in sand and moisture content and the correlation between groundwater elevation and hydrologic variables were tested using Spearman's rank correlation coefficient (rho). Tests were considered significant at $p \leq 0.05$ and were performed in SPSS v11.0 software. Binary logistic regression between variables was performed in Minitab 15 1.0.0 software. Groundwater flow direction was obtained by curvilinear interpolation using Matlab to the piezometric gradient determined from a triangular interpolation of 11 piezometers on the northern part of the beach.

3.4 RESULTS

***E. coli* and moisture content in the backshore sand**

The beach environment can be very complex and sand contamination is highly variable over short distances (Yamahara et al. 2007), making it difficult to determine the sources of FIB and establish a relationship between sources of FIB and environmental variables. We applied filters for the selection and treatment of the dataset in order to determine a relation between FIB concentration and moisture content. The two filters applied were: (1) selection of 10 sand sites located in only one region of the beach: the backshore region and (2) geometric mean of FIB and moisture content was used to minimize the influence of extreme data points and to determine the general trend of the relation between the two parameters.

Sand sites along the backshore are shown in Fig. 3.1B. *E. coli* densities and relationship to moisture content at the different sand sites are shown in Fig. 3.2A. Sand sites S4, S7 and S8 had chronically high moisture and also the highest *E. coli* levels. Fig. 3.2B shows that the geometric mean concentration of *E. coli* per sand site was proportional to the geometric mean of the moisture content of the respective sand sites (R^2=0.80). However, the prediction bounds were one order of magnitude only for moisture content greater than 8%. The function that described the relationship between the two variables was non-linear, with a sharp increase in *E. coli* density with increasing moisture, reaching a plateau of about 10^3 colony forming units (CFU)/100 g after 8% of moisture content. The non-linear relationship indicates the great dependence that FIB concentration has on moisture content of the sand, especially over 8%.

We also compared overall levels of *E. coli* for wet and dry days, where dry days (baseline) were defined as no precipitation in the previous 24 h and a maximum of 0.15 cm in the previous 48 h. The mean *E. coli* concentration in sand for wet days was 4,900 CFU/100 g (n=33, STDEV=8,400 CFU/100 g), which was nearly four-fold higher the mean concentration for dry days (mean =1,300 CFU/100 g, n=44, STDEV=4,200 CFU/100 g). The mean moisture content in sand for wet days was 10.5%, which was nearly twice the mean moisture content for dry days (6.1%). There was a significant difference between wet and dry days for both the mean log *E. coli* concentrations ($p<0.05$) and mean log moisture content ($p<0.05$) in sand collected at the backshore.

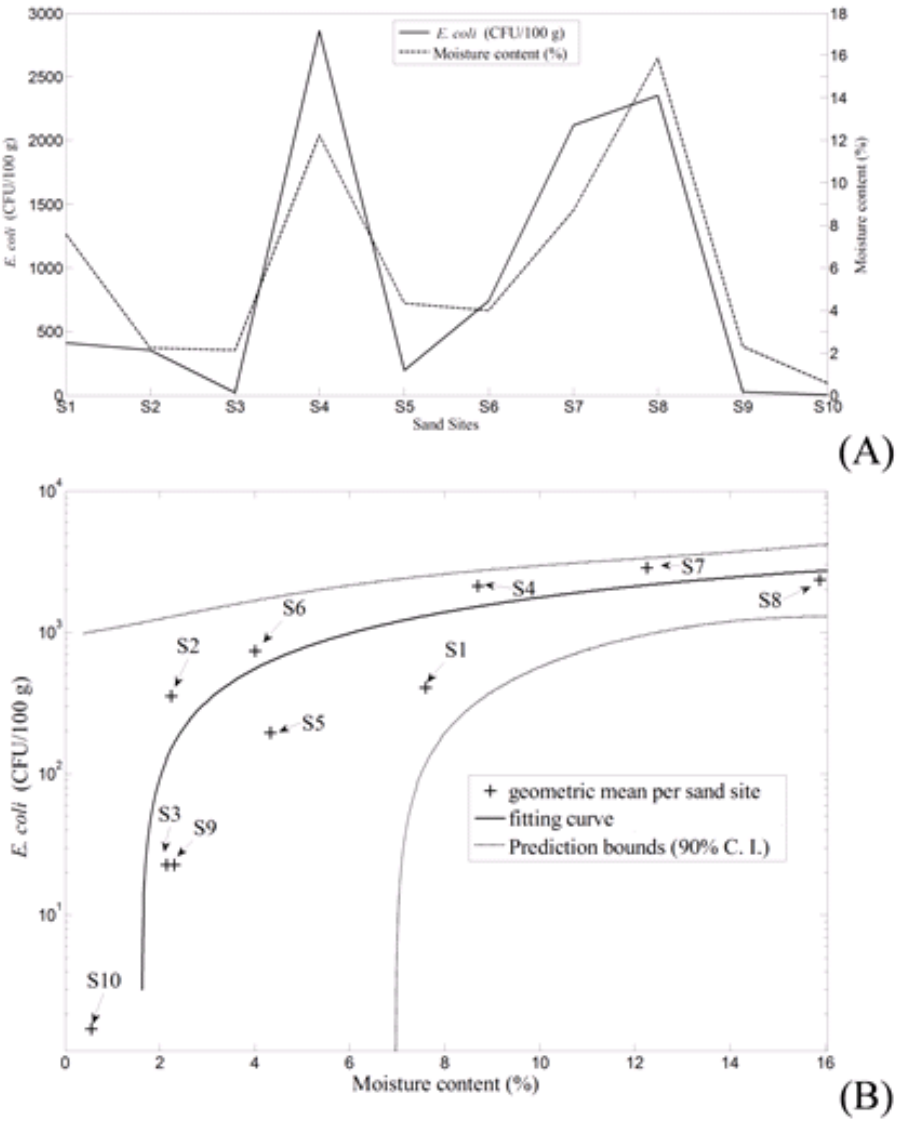

Figure 3. 2 (A) Geometric mean of *E. coli* densities was higher in sand sites along the backshore where the geometric mean of moisture content was higher. Sand sites S4, S7 and S8 had chronically high moisture and also the highest *E. coli* levels. (B) Densities of *E. coli* had a positive non-linear correlation with moisture content.

Topographic surveys

Topographical profiles have been performed at other Great Lakes beaches and they have shown the dynamics of sand at the shoreline (Skalbeck et al. 2010). We performed comprehensive topographical surveys at Bradford Beach to be able to characterize in details (every 3 cm) the

ground surface of the beach (not only profiles). The topographical surveys revealed a swale in the middle of the beach running parallel to shore. The width of the swale ranged from about 12 m to 26 m, depending on the location and the length corresponded to the darker sand strip (Fig.3.1) and it covered almost all extent of the beach. In this study standing water pools are defined as body of stagnant water. The length of the standing water pools ranged from about 3 m reaching up to 150 m (heavy rainfall events) and the depth reached up to 0.15 m (that is the difference in elevations between wet regions and their surrounding dry area obtained by topographical maps). We examined the topography of the beach in relation to sand samples sites that had consistently wet sand. Surveys also indicated that deeper and larger depressions are mostly located on the northern part of the beach, but also on the southern end around sand site S4 (Fig. S3.1 in the supplemental material). Piezometers sites PZ-3, PZ-4, PZ-7, PZ-8, and PZ-10 are located in wet areas in which the depth to groundwater from the surface is shallow (ranging from 0.233 m to 0.651 m) and are present in the swales (Table 3.1). Also, breaches in the berm were observed near sand sites S4, S7, and S8, where the beach slope is very mild, making these sites prone to wave run up and standing water (Fig. 3.3A). In addition, topographical surveys showed the dual effect of both the big watersheds (e.g. large breach coinciding with the pathway of stormwater runoff coming out from outfall O2) and wave action following a large summer storm. Erosion was more intense following a summer storm ranging from 3 cm to 61 cm and broad (including the rain gardens region) when compared to the erosion in the winter time. In the latter case, erosion ranged from 3 cm to 30 cm and was the result of wave action therefore more predominant in the shoreline region (Fig. 3.3B).

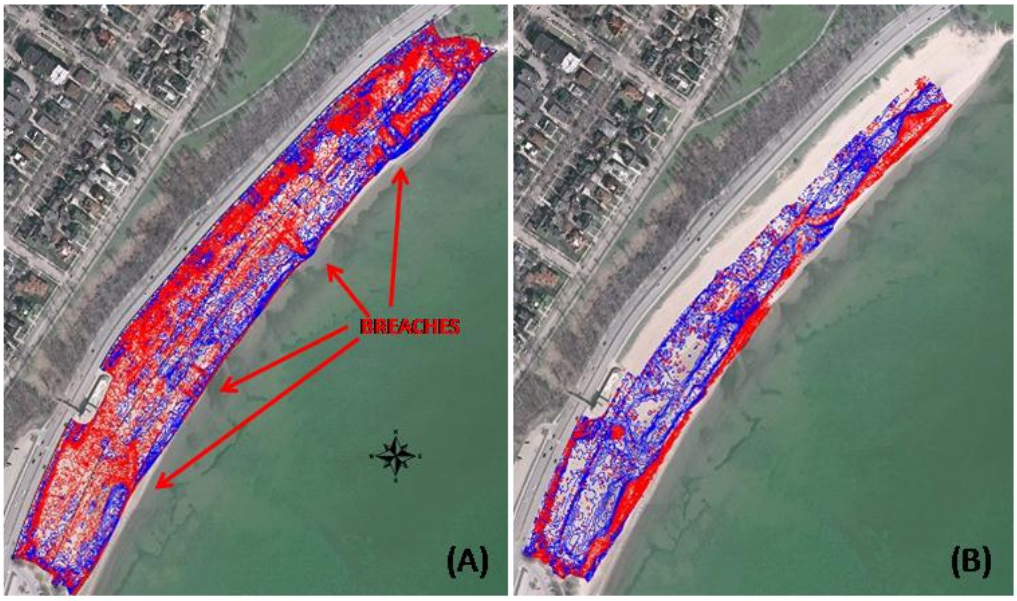

Figure 3. 3 "Differential" topographic map: (A) April 2010 and Post 7/22/10 storm. (B) November 2009 and April 2010. Red lines show erosion and blue lines show accretion.

Grain size distribution and hydraulic conductivity (K)

Standing water on the beach may also be aggravated by poor drainage caused by an accumulation of fine sands. Therefore we examined grain size at different sites on the beach. Comparison of sand d_{50} for 2007, 2009, and 2010 as a combined dataset indicated there was a significant difference between southern and northern side of the beach ($p<0.001$), with finer sand located on the northern part. The overall d_{50} was 0.253 mm (n=46) on the northern part and 0.326 mm (n= 25) on the southern part of the beach and was consistent for the three sampling seasons (Table S3.1 in the supplemental material). We also assessed K to evaluate drainage characteristics. Measurements of K in 2009 had an average of $3x10^{-3}$ cm/s (n=16) in the southern part of the beach and $3x10^{-3}$ cm/s (n=12) for the northern part. Although not statistically significant, measurements in the swales on the northern and southern portions of the beach had

slightly lower K values at K = $1x10^{-3}$ cm/s, which could contribute to the presence of standing water in the swales.

Geophysical surveys

Geophysical surveys characterized the material below the beach. From the sounding surveys, Bradford Beach was modeled as a three layer system consisting of a southward thickening sand body of about 3.35 m. The sand is underlain by a resistive (probably impervious to vertical flow of water) layer of Wisconsian age glacial till. The beach exhibits very little natural sedimentary history as evidenced by the lack of depositional structures in the sand (data not shown). This could be expected because it is an artificial beach and any natural sand was either removed, altered through reconstruction processes, or never existed in the survey areas. The electrical profile shows more resistive surface material toward the south part of the study area, suggesting coarser sand (Fig. S3.2 in the supplemental material). All the geophysical surveys suggest a fairly uniform depth between 3 and 4 m thick. Although there is evidence of some lateral variations, changes at this depth are unlikely to be affecting the surface sands, or causing the standing water.

Groundwater hydrology

We examined the overall groundwater dynamics at Bradford Beach to assess how the groundwater levels were influenced by environmental factors (rainfall, wind, lake level and wave height) and how any changes in these levels either facilitate or cause the standing water. Groundwater levels were obtained 1-2 days per week at least for two years, including the winter

season. These extended measurements compare to previous studies which relied on limited measurements per season.

Shallow groundwater depth can create chronically moist areas, minimize the infiltration process and facilitate standing water zones. The groundwater level was higher on the southern part of the beach and lower on the northern part of the beach, with a full range of 1.943 m difference in levels for all measurements performed at all sites (Table 3.1). Piezometers on the southern part of the beach presented the highest variability (Eq.1) in groundwater level.

Profiles of the elevation of the beach surface and groundwater table across different transects are presented in Fig.3.4. The average range of groundwater level below the ground surface at Bradford Beach in the standing water zones was 0.233 m to 0.651 m; the minimum depth to the groundwater table for all measurements was recorded as 10 cm at PZ-3 and PZ-7. In the non-saturated zones it was 0.796 m to 1.268 m, with the exception of PZ-6, which was 0.365 m (Table 3.1). Although PZ-6 has shallow depth to groundwater, slope towards the lake is accentuated as shown in Fig. 3.4, facilitating runoff.

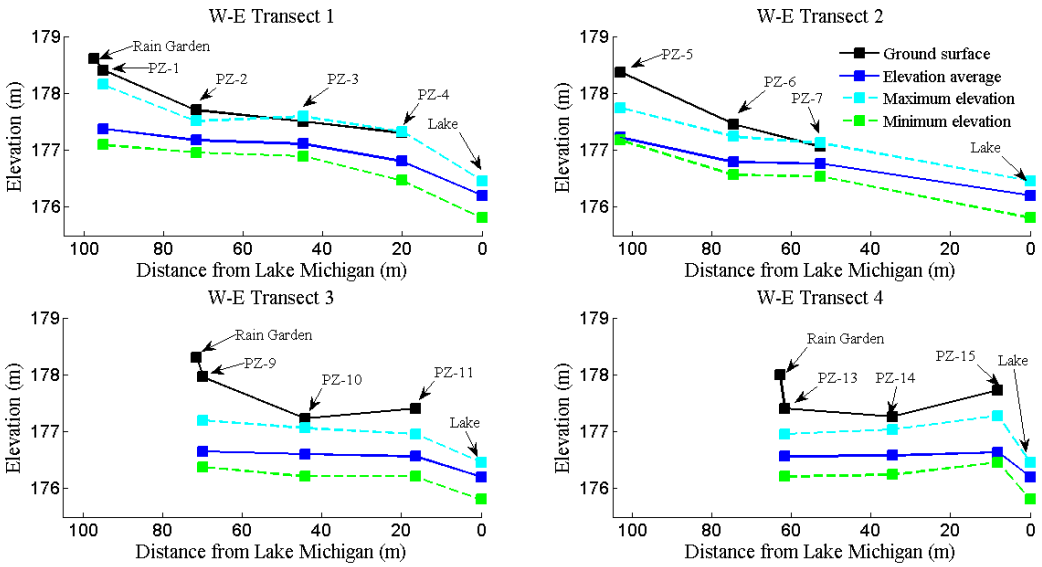

Figure 3. 4 Elevation of ground surface and groundwater table. Sample locations indicated by piezometer number. Topographical profiles are average of three surveys, except for PZ-2 (elevation estimated from contour maps) and groundwater elevations refer to the 2009-2010 measurements.

Groundwater levels measured in piezometers PZ-1, PZ-9 and PZ-13, the sites closest to the rain gardens, showed the greatest increase in groundwater elevation within 24 h following rainfall and the slowest recovery in the next 24 h (Table 3.2). Remaining piezometer sites also increased following rainfall, but to a lesser extent. Overall, groundwater elevations appear to be dependent on direct infiltration during rainfall events, infiltration from the rain gardens and overflow from rain gardens during heavy rainfall events. Groundwater level showed strong correlation with rainfall amount and lake level for the majority of the piezometers (Table S3.2 in the supplemental material).

Table 3. 2 Impact of rainfall in FIB concentration in groundwater (GW) and groundwater level.

	Piezometers (PZ) (average for June, July, and August 2010).		
	Next to the rain gardens[2] (PZ 1,9, and 13)	Middle of the beach (PZ 2,3,6,8,10,12, and 14)	Next to the lake (PZ 4,7,11, and 15)
(A) Impact of rainfall in GW level			
GW level increase within 24 hours of a rainfall event	0.302 m	0.196 m	0.119 m
GW level decrease 24 hours after a rainfall event	0.092 m	0.079 m	0.074 m
Decrease in GW level 24 hours after a rainfall event	31 %	40 %	62 %
(B) FIB concentration (CFU/100 ml)			
Baseline			
E. coli	1	2	13
Enterococci	1	0	0
Total coliforms	4,500	8,800	550
Day of rainfall event			
E. coli	3	640	18
Enterococci	47	1,800	65
Total coliforms	320	5,000	800
Day after rainfall event			
E. coli	16	1,500	360
Enterococci	31	2,000	340
Total coliforms	15,000	21,000	11,000

[2] PZ-5 was not listed because it was dry most of the time

Groundwater velocity was calculated to assess if groundwater movement from rain gardens could increase groundwater level in piezometers. Groundwater travels generally very slowly. Estimating porosity as 0.3, velocity of groundwater was computed by Eq. 2 as 173 m/day; assuming that the horizontal K is approximately two orders of magnitude higher than the measured vertical K (geometric mean 2×10^{-3} m/s) and the overall mean hydraulic gradient for all sites is 0.003 m/m. Thus it is expected to take 17 hours for groundwater to travel from the rain gardens to the lake. Our geophysical surveys show that groundwater beneath Bradford Beach occurs under unconfined conditions. An interpolation method was used to estimate groundwater levels at locations where no measurements were taken. Fig.3.5 shows that right after a rainfall event, groundwater table was higher on the SW corner of the contour, as expected, and on the NW corner due to a heavy rainfall event that day (6.96 cm), suggesting that during those events infiltration from nearby rain gardens contributed to an increased water table following rainfall, which could facilitate formation of standing water in the middle of the beach.

Negative gradients (sloping away from the lake) were observed in 23% of the readings, mainly around PZ-7 (Fig. S3.3 in the supplemental material), probably due to large waves washing over that portion of the beach (in which the beach face has milder slope) and recharging groundwater close to the shore. Average horizontal groundwater gradients were 0.008 m/m on the southern part of the beach and 0.004 m/m on the northern part of the beach, being typically eastward toward Lake Michigan, with a small component northward.

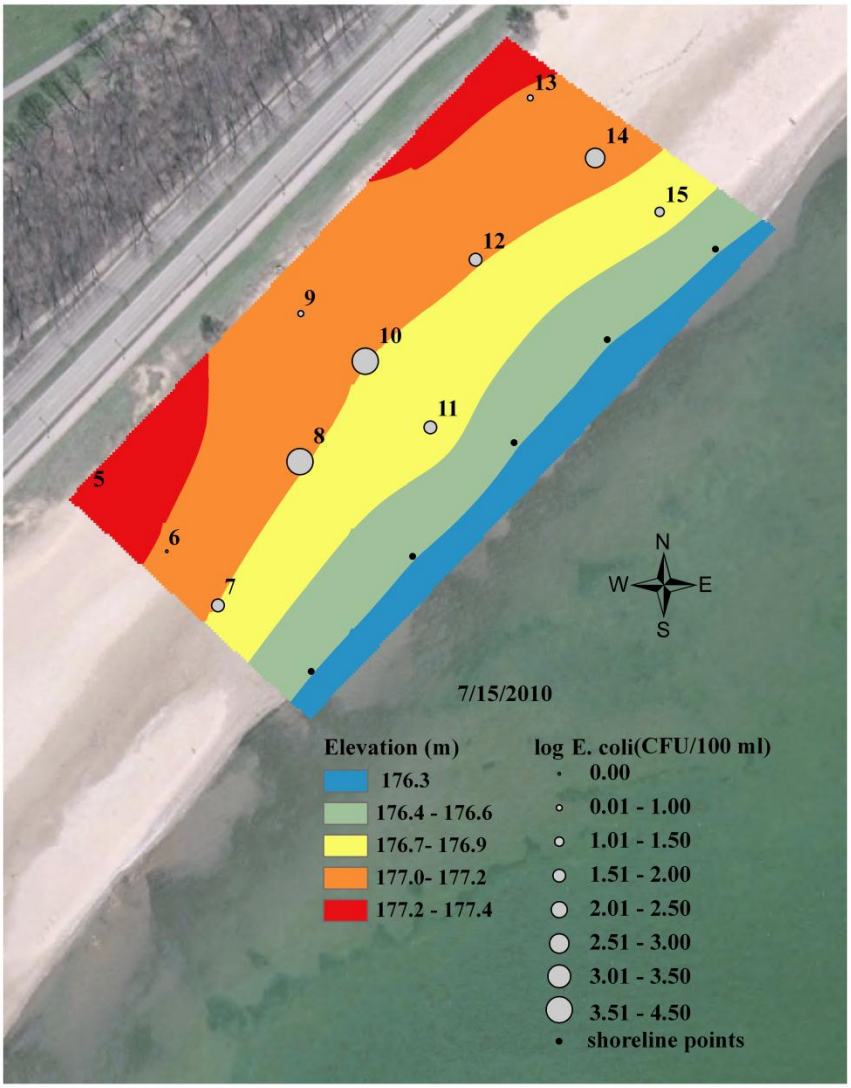

Figure 3. 5 Elevation contours for groundwater table on 7/15/10 show higher elevation on the SW corner of the contour (as expected) and on the NW corner probably due to infiltration from rain gardens on a rain event (6.96 cm). Higher concentration of bacteria was more predominant in the middle of the beach, where groundwater table was closer to the ground.

Formation of standing water

The formation of standing water at Bradford Beach involved several factors. Fig.3.6 shows the relationship between the presence of standing water, observed from an onsite camera over a two month period, and rainfall and wave action (here represented by wave height). Areas that showed

standing water were associated with lower depth to groundwater that brings the water table within a few centimeters of the sand surface (Table 3.1). There was a significant correlation between standing water and groundwater elevation (rho=0.853, p<0.01). Rainfall was strongly associated with the formation of standing water. A binary logistic regression model exhibited a good fit (goodness of fit, P value=0.009, where P<0.05 indicates a good model fit) and indicated that the odds of observing standing water at the beach increased by a factor of five for every one centimeter of increase in rainfall.

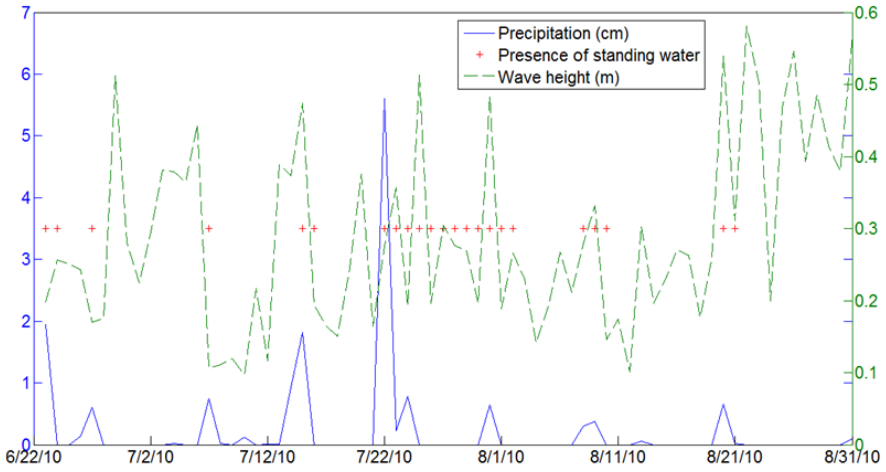

Figure 3. 6 Relationship of formation of standing water and wave height and rainfall. There is a stronger correlation between standing water and rainfall than standing water and wave height.

Standing water was also associated with wave runup that occurred where the beach slope was mild to flat, with waves reaching backshore sand during windy days with or without precipitation and water getting trapped in the swales in the middle of the beach. Binary logistic regression models shows that the odds of observing standing water at the beach increases by a factor of nine for every one meter of increase in wave height observed on the previous day, even though the

goodness-of-fit test p-value (p=0.279) was not significant. While there was no statistical evidence to suggest that wave height has a correlation with the presence of standing water, the phenomenon has been observed during fieldwork.

Relationship between FIB (*E. coli* and enterococci) and human *Bacteroides* 16S rRNA marker (HF183) at the beach environment

Detection of human *Bacteroides* in standing water was related to heavy rainfall events and/or days with high waves (Fig.3.7). The mean concentration of *Bacteroides* in standing water was 1,800 copies/100 mL (STDEV=300, n= 24). In contrast, concentration of human *Bacteroides* was 8 and 16 times greater in outfalls at the beach (O2 to O7) and north of the beach (O8 to O12), respectively, and 4-fold higher in lake samples (collected at the same time as when there was standing water at the beach) compared to standing water. The opposite pattern was seen with FIB, where levels were disproportionately high in standing water compared to potential sources, e.g. the outfalls. Concentration of *E. coli* found in outfalls at the beach and outfalls located north of the beach were 4 to 6-folds lower than the concentration found in standing water, respectively, with the concentration of enterococci was nearly the same (Table 3.3). In addition, the concentration of FIB in lake water (collected when there was standing water at the beach) was far lower (~ 100-fold for *E. coli* and 15-fold for enterococci) when compared to standing water.

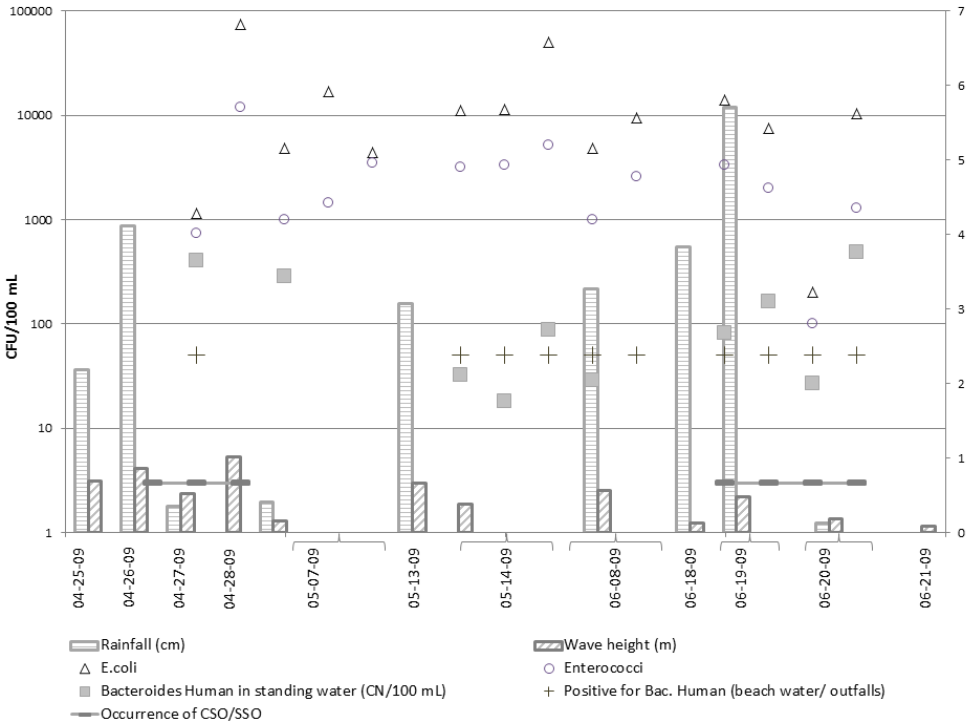

Figure 3. 7 Relationship between presence of sewage indicator in standing water and rainfall and wave height. *Bacteroides* human in standing water was frequently related to heavy rainfall events and/or wavy days, except on 5/9/2009.

Table 3. 3 Statistics of FIB in backshore sand and water at Bradford Beach during wet and dry days. [3]

		Wet days (CFU/100 mL)				Dry days (CFU/ 100 mL)			
		E. coli	**Enterococci**	**Total coliforms**	***Bacteroides***	***E. coli***	**Enterococci**	**Total coliforms**	***Bacteroides***
Backshore Surface sand (2009-2011)	Mean	4,900	11,000			1,300	2,000		
	Median	1,300	2,200			200	300		
	Standard deviation	8,400	19,000			4,200	7,500		
	N	33	22			44	34		
Stormwater outfalls (NORTH OF THE BEACH) (2009-2011)	Mean	2,500	12,000		29,952				329
	Median	750	3,000		1,498				
	Standard deviation	6,200	22,000		92,306				
	N	32	32		20				1
Stormwater outfalls (AT THE BEACH) (2009-2011)	Mean	3,500	10,000		12,315				BLD
	Median	740	2,500		2,463				
	Standard deviation	12,000	28,000		32,053				
	N	40	39		26				2
Groundwater beneath the beach (2009-2011)	Mean	720	2,500	50,000	1,296	2	4	105	
	Median	300	190	7,600	1,651	1	3	80	
	Standard deviation	1,000	7,900	145,000	1,296	2	3	113	
	N	190	188	165	13	56	56	26	
Runoff infiltrating through sand (2011)	Mean	4,300	4,000	440,000	1,347				
	Median	108	26	15,000	1,364				
	Standard deviation	10,000	9,600	1,010,000	331				
	N	6	6	6	10				
Lake water (2009-2011)	Mean	860	650		7,054	220	220		
	Median	148	40		1,332	45	12		
	Standard deviation	3,000	3,300		11,452	700	1,300		
	N	74	84		8	153	144		
Standing water (2009-2011)	Mean	14,100	9,200		1,771	4,800	4,100		BLD
	Median	10,500	2,600		289	4,800	4,100		
	Standard deviation	17,000	20,000		2,672				
	N	24	23		17	1	1		1

[3] Note: concentration of FIB in sand is expressed in CFU/100 g dry weight and concentration of *Bacteroides* in water samples is expressed in CN/100 mL; BLD – Below level of detection

Our study shows that high levels of human *Bacteroides* HF183 in outfalls correlate well with high levels of enterococci (rho=0.451, $p<0.05$) and *E. coli* (rho=0.354, $p<0.05$) in outfalls and high levels of enterococci (rho=0.769, $p<0.05$) and human *Bacteroides* (rho=1.000, $p<0.05$) in lake water, suggesting that HF183 is a good sewage indicator. Our study also shows that high levels of human *Bacteroides* in standing water correlates well with high levels of *E. coli* in standing water (rho=0.502, $p<0.05$), but not with enterococci (rho=0.472, $p<0.05$) in standing water and human *Bacteroides* (rho=0.429, $p<0.05$) in outfalls, showing that the sources of FIB and in standing water may be birds and gulls rather than sewage. High levels of enterococci in lake water correlate well with high levels of *E. coli* in lake water (rho=0.715, $p<0.05$) and outfalls (rho=0.502, $p<0.05$) and human *Bacteroides* in outfalls (rho=0.769, $p<0.05$) whereas high levels of *E. coli* in lake water did not present high correlation with high levels of FIB or human *Bacteroides* in outfalls. This raises the question of whether or not enterococci should also be used as an FIB in freshwater rather than only in marine waters.

FIB in piezometers samples

In piezometer samples, *E. coli* and enterococci concentrations were on average very low during baseline days whereas total coliforms, which are naturally occurring, were found to be 10^2-10^3 CFU/100 mL on average (Table 3.3). On the day of a rainfall event, *E. coli* and enterococci concentration increased significantly in the middle of the beach likely due to infiltration of contaminated stormwater runoff or wave runup, inversely total coliforms decreased significantly in all sites on these days, possibly due to dilution factor associated with rainfall. High levels of FIB were observed only in piezometers in the middle of the beach and closer to the lake (Fig. 3.5).

In order to track FIB transport in groundwater at the beach environment, we monitored FIB concentration at a 10- pan lysimeter array and at a 15- piezometer array. While there was no evidence of a horizontal gradient of concentration of FIB in piezometers, we were able to find a vertically decreasing gradient of FIB concentration moving from standing water, to lysimeter samples (which represent runoff infiltrating through sand), to piezometers samples. The ratio of average *E. coli* in standing water, lysimeter samples, piezometer samples was 20:6:1, respectively (Fig.3.8). This is evidence that the rain gardens were filtering FIB from stormwater outfalls. The ratio of average enterococci was 4:2:1, respectively. The ratio of average human *Bacteroides* was 1.4:1:1 (Table 3.3). This gradient could be due to the hydraulic path to the piezometers being larger than that to the lysimeters and the environmental sand (porous media) acting as a filter. Physical filtration is believed to be the primary process which limits bacteria mobility in soil (Gerba and Bitton 1984). Conversely this trend was not as evident with *Bacteroides* maybe due to differences in persistence since they are anaerobes. Our data suggest that FIB infiltrated into the piezometers vertically, representing localized overland runoff in these samples rather than widespread contaminated groundwater.

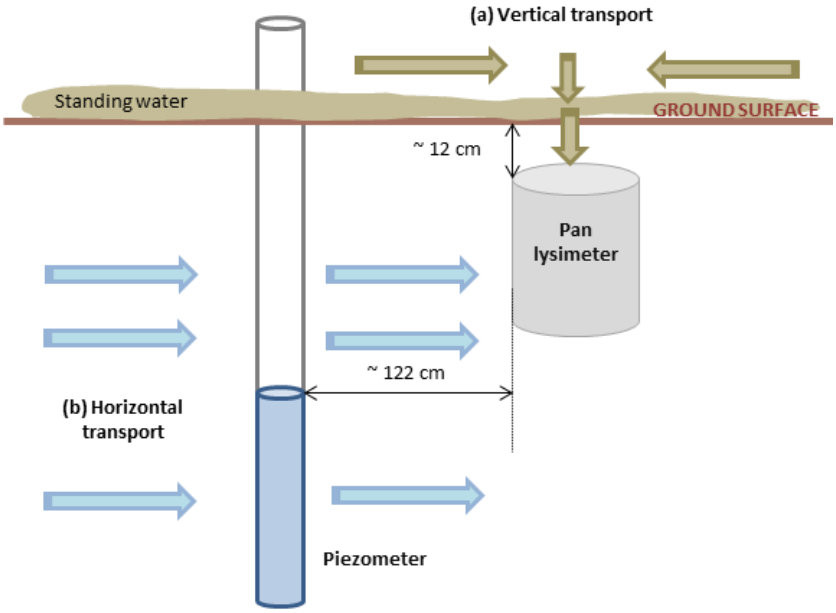

Figure 3. 8 Schematic illustration of transport of FIB at the beach environment. Vertical transport of bacteria infiltrating through the sand (sample collected at the pan lysimeter) and eventually reaching ground water (piezometer) was prevalent. No evidence of horizontal transport of bacteria through the groundwater was observed, suggesting this mechanism is not responsible for FIB movement through the beach.

3.5 DISCUSSION

In this study we examined hydrological and geophysical characteristics of the Bradford Beach and the linkage between standing water and persistence of contamination by FIB. Similar to previous studies (Beversdorf et al. 2007), *E. coli* densities and moisture content in sand were lower during dry days when compared to wet days. Our study showed that wet sand can act as a reservoir for FIB and indicated a significant, positive non-linear correlation between *E. coli* and moisture content. Low moisture has been associated with decreased cell survival or growth limiting conditions (Avery et al. 2003; Byappanahali et al. 2004). Also, certain sand sites were more subject to cycles of wetting and drying due to the action of waves through breaches in the berm, creating locations of higher FIB levels. These cycles have been associated with cell

number increase post-hydration due to *E. coli* outcompeting predators in relatively dry soil (Solo-Gabriele et al. 2000). Both the direct runoff washing fecal matter deposited by birds and contaminated runoff from stormwater outfalls being deposited in the sand sites are possible mechanisms that can facilitate introduction of FIB in to the sand. Availability of nutrients has been associated with growth of FIB, which can contribute creation of FIB reservoirs in the sand (He et al. 2007).

The physical condition of the beach had a profound effect on the FIB concentrations. Our research showed that the beach morphology results from the interaction of the beach surface and groundwater, and that a very shallow ground water table exasperates standing water or chronic conditions on the beach. The surface flows result from drainage of the watershed that extends west of the beach and up the bluff, and from lake varying levels and wave action. Rainwater infiltrates and flows as groundwater, governed by gravity, surface tension, varying lake levels and wave action. Large rainstorms can produce flooding, erosion and deposition of sand on the beach. Winds and wave action are stronger in winter, producing patterns of erosion and deposition on the beach. The interaction of stormwater flooding of the beach and a stable berm at the beach edge produced a swale parallel to the shoreline, that lead to standing water, with the water table at or above the beach surface. These swales correspond to the constant wet sand located in the backshore area, where the ground surface is closer to the groundwater table, thus helping to keep the sand constantly wet by capillary rise. High levels of FIB were not observed in piezometers that are closer to rain gardens, possibly because they are not in the pathway of contaminated water that overflow from them in an event of heavy rainfall (spillways are located on the side of the rain gardens).

Standing water pools were more frequently observed on the northern part of the beach, where there was lower variability in piezometers, and smaller sand d_{50}, suggesting slower infiltration in that region. Similarly to other studies (Portnoy et al. 2006; Skalbeck et al. 2010), *E. coli* appeared highest in relatively fine-grained sediments with high water content. These are evidence that physical beach conditions can be associated with wet conditions, fostering FIB reservoirs.

Evidence of potential health risks in the beach environment exists during heavy rainfall events, when standing water, lysimeters, and piezometers samples were positive for human *Bacteroides* marker. That evidence demonstrates that fecal contamination, possibly human sewage is at least partly responsible for the degradation of water quality at the beach, as reported elsewhere (Boehm et al. 2003; Yamahara et al. 2007). Rainfall-induced sanitary/stormwater discharge to water bodies in Milwaukee due to stormwater runoff/outfall discharge, leaking sanitary pipes, and illicit sanitary sewer connections are well documented (Salmore et al. 2006; Silva et al. 2010; Sauer et al. 2011). Potential sources of *Bacteroides* at Bradford Beach are outfalls at the top of the beach and immediately north of the beach. Human *Bacteroides* was found to be higher in potential sources than in standing water. Possible sources of sewage contamination, as indicated by detection of human *Bacteroides*, are the stormwater from the rain gardens that overflow and run across the beach or lake water contaminated by the northern outfalls that reach the swales in an event of high wave height. In agreement, higher levels of FIB were detected in piezometers sites in the middle of the beach and closer to the lake (Table 3.2). These sites are on the pathway of stormwater outfalls when rain gardens overflow. Sites closer to the rain gardens are not impacted by the overflows since the spillways are on the side of the rain gardens and do not reach these sites that are immediately in front of them.

Standing water was found to have high *E. coli* and enterococci levels in the absence of HF183 marker, which could indicate fecal pollution from birds (Haack et al. 2003; Bonilla et al. 2006) and shows some specificity of the marker for human fecal contamination. We also noted that FIB levels in standing water are higher than in the potential sources (stormwater outfalls and lake water) sampled on the same day, possibly as a result of residual FIB in the sand environment that accumulates or potentially grows. Standing water has been associated to higher levels of nutrients, lower dissolved oxygen, and more favorable temperature for bacteria growth than in flowing water (He et al. 2007).

Just recently a study suggested that the marker used in the study may not be completely specific to human fecal matter (Aslan et al. 2013). Authors reported a 71% specificity for HF 183, with dogs and gulls – animals frequently found on beaches, testing positive for this marker. Thus, HF 183, an indicator, may not be as specific to human fecal pollution as previously believed. Therefore, our study shows the benefits of the use of well-established, but non-specific fecal indicator bacteria, together with a marker more specific indicator of human fecal pollution (*Bacteroides* HF 183 by qPCR). In our study, human *Bacteroides* were found in stormwater outfalls, therefore cross-contamination with other animals is not believed.

While mechanisms of transport of FIB from sand to coastal waters were not the subject of investigation of this study, we can have some insight from field observations. Two mechanisms of transport have been documented: (1) 'overbeach transport', in which rising tide or wave runup reach FIB-laden sands and FIB is carried from the sands to coastal waters (Yamahara et al. 2007; Ge et al. 2010b) and 'through-beach transport', in which infiltrating sea water detaches FIB from beach sands and are transported to the groundwater table and are transported to coastal water by submarine groundwater discharge (SGD) (Russell et al. 2012). In our research, the first

mechanism is a possible route of FIB transport from sand to lake water, although not investigated further in this study. The second mechanism is as possible route at sites closer to the lake and very unlikely to happen in sites away from the lake due to the very low groundwater velocity.

Little is known about concentration of FIB in groundwater beneath beaches. Studies have shown a wide range of variability of concentration of bacteria, from none detected up to $>10^4$ MPN/100 mL (Table 3.4). Potential sources of contamination of groundwater are leaking sewer lines or storm drains (Weiskel et al. 1996; Boehm et al. 2003), surface runoff infiltration (Skalbeck et al. 2010), and upward hydraulic gradient (Haack et al. 2003). In our study there was evidence of linkage of low FIB levels with baseline conditions and high FIB levels with rainfall events. But the source of FIB was likely overland runoff (e.g. rain gardens overflowing or from wave runup). Our data indicate that concentration of FIB in groundwater was sporadic rather than a continuum. Our hypothesis is that measurements of FIB at the piezometers indicate local contamination at a particular location. Persistence of uneven concentration of bacteria in piezometers (data not shown) and inability of tracking a horizontal gradient of bacteria towards the lake support this hypothesis.

Table 3. 4 Variability of FIB in groundwater (GW) beneath the beach at different locations.

	FIB levels (MPN/100 ml)			
Beach location	***E. coli***	**Enterococci**	**Total coliforms**	**Reference**
Buttermilk Bay, MA			<11	Weiskel *et al*, 1996
Grand Transverse Bay, MI	30 – 320	16 – 182	210 – 650	Haack *et al*, 2003
Huntington Beach, CA	< 60 – 17,329	< 60 – 776	< 60 – >24,192	Bohem *et al*, 2004
Southern Lake Michigan beaches (IL and IN)	none (in GW discharging to the lake)			Whitman *et al*, 2006
Western Lake Michigan beaches (WI)	none – 579			Skalbeck *et al*, 2010

Based on our findings, we recommend some management techniques for beaches experiencing bacterial contamination associated with constant wetting conditions or standing water. First, beach grooming may improve conditions, but cannot compensate for lack of sand. Grooming aerates the top layer of sand, allowing it to dry out. Moisture content is strongly linked to *E. coli* survival; therefore, grooming can potentially reduce *E. coli* levels (Kinzelman et al. 2004b). In addition, grooming should not reduce the berm formation at the water line, as this serves as a barrier to wave run-up. Second, cross shore drainage channels could be built at locations that experienced significant breaches to the berm, such as the ones shown in Fig.3A, so wave runup could drain more freely. Finally, beach nourishment with larger grain sands would be useful for creating a drier beach environment, by steepening the grade of the beach to decrease ponding and by raising the grade of the beach above the water table to reduce the effects of capillary draw (Pittner et al. 2009; Skalbeck et al. 2010). Beach nourishment with smaller sands (<0.253 mm) is less likely to have a significant impact. In addition, the cost needs to be weighed against the estimated cost longevity of this solution as beach erosion would be expected to occur. Most importantly, beach slope alteration has been proven to result in an improvement of surface water quality (Kinzelman et al. 2009).

3.6 CONCLUSIONS

This study presents a systematic collection of water samples from storm outfalls at a beach, beach sand, groundwater, runoff infiltrating through sand collected in pan lysimeters and surface water. We used well-established, but non-specific fecal indicator bacteria (*E. coli* and enterococci) together with a marker more specific indicator of human fecal pollution (*Bacteroides* HF 183 by qPCR) to assess patterns of fecal pollution in the beach environment as well as presence of sewage. Our study shows the combined use of these tools is effective for

indication of sewage. In addition, our study showed that beach closings are frequently associated with bacterial contamination mainly linked to a number of point and nonpoint sources that can also be coupled to physical properties of the beach. The investigation of FIB in dry versus wet conditions and the relationship between sand size and FIB both point beach managers to practical approaches to reducing FIB concentration in sand. We have also provided some ideas about how to do beach nourishment and minimize erosion during large rainstorms. Identifying and mitigating sources of FIB and sewage contamination are a high priority for protecting recreational waters. This research contributes to a better understanding of the relationship of wetting sand conditions and standing water with persistent FIB contamination. Importantly, this study indicates that erosion/accretion patterns of the beach could bring groundwater table closer to the ground and mild to flat beach face slope could enhance wave action, facilitating persistent local spots of wet sand in the backshore area of the beach. This study also indicates that runoff infiltrating from rain gardens at a beach can help to raise groundwater table, which could slow infiltration process and facilitate standing water conditions. This is one of the first studies that indicate the health risks associated with potential sewage contamination in standing water at a beach environment.

3.7 ACKNOWLEDGEMENTS

This work was made possible through a grant from The Park People, a grant in support of the Blue Wave Award provided by MillerCoors, University of Wisconsin Sea Grant (grant No. NA10OAR4170070), and UWM Graduate School Dissertation Fellowship Award. Authors thank Bonnie Bills, Donald Szmania, Jessica VandeWalle, Jenny Ulbricht, Colin Peake, Jessica Sielick, Elizabeth Sauer, Patricia Bower, Melinda Bootsma, Rohan Jadhav, Ryan Newton, Robert Graziano, and Ryan English for assistance with fieldwork and with lab analyses. Daniel

Talarczyck performed comprehensive topographic surveys and Thomas Hansen provided digital images from Bradford Beach. We thank David Schwab and Gregory Lang from NOAA for providing wave data. We also thank Kim Weckerly for assisting with ArcGIS maps. Special thanks to Steve Keith, from Milwaukee County DTPW for helping us to choose the locations to install the piezometers.

3.8 REFERENCES

Abdelzaher, A. M., M. E. Wright, C. Ortega, H. M. Solo-Gabriele, G. Miller, S. Elmir, X. Newman, P. Shih, J. A. Bonilla, T. D. Bonilla, C. J. Palmer, T. Scott, J. Lukasik, V. J. Harwood, S. McQuaig, C. Sinigalliano, M. Gidley, L. R. W. Plano, X. F. Zhu, J. D. Wang, and L. E. Fleming. 2010. Presence of Pathogens and Indicator Microbes at a Non-Point Source Subtropical Recreational Marine Beach. Applied and Environmental Microbiology **76**:724-732.

Alm, E. W., J. Burke, and A. Spain. 2003. Fecal indicator bacteria are abundant in wet sand at freshwater beaches. Water Research **37**:3978-3982.

Aslan, A., and J. B. Rose. 2013. Evaluation of the host specificity of *Bacteroides thetaiotaomicron* alpha-1-6, mannanase gene as a sewage marker. Letters in Applied Microbiology **56**:51-56.

ASTM. 2006a. Standard test method for permeability of granular soils (constant head). Pages 5 p *in*. ASTM International, West Conshohocken, PA.

ASTM. 2006b. Standard test method for sieve analysis of fine and coarse aggregates. Pages 5 p *in*. ASTM International, West Conshohocken, PA.

Avery, S. M., and S. Buncic. 2003. *Escherichia coli* O157 diversity with respect to survival during drying on concrete. J Food Prot **66**:780-786.

Bernhard, A. E., and K. G. Field. 2000. A PCR assay to discriminate human and ruminant feces on the basis of host differences in *Bacteroides-Prevotella* genes encoding 16S rRNA. Applied and Environmental Microbiology **66**:4571-4574.

Beversdorf, L. J., S.M.Bornstein-Forst, and S.L.McLellan. 2007. The potential for beach sand to serve as a reservoir for *Escherichia coli* and the physical influences on cell die-off. Journal of Applied Microbiology **102**:1372-1381.

Boehm, A. B., J. A. Fuhrman, R. D. Mrse, and S. B. Grant. 2003. Tiered approach for identification of a human fecal pollution source at a recreational beach: case study at Avalon Bay, Catalina Island, California. Environ. Sci. Technol. **37**:673-680.

Boehm, A. B., G. G. Shellenbarger, and A. Paytan. 2004. Groundwater discharge: potential association with fecal indicator bacteria in the surf zone. Environ. Sci. Technol. **38**.

Boehm, A. B., and S. B. Weisberg. 2005. Tidal forcing of enterococci at marine recreational beaches at fortnightly and semidiurnal frequencies. Environ. Sci. Technol. **39**:5575-5583.

Bogosian, G., L. E. Morris, P. J. L. Morris, M. A. Heitkamp, and D. B. Weber. 1996. Death of the *Escherichia coli* K-12 strain W3110 in soil and water. Appl. Environm. Microbiol. **62**:4114-4120.

Bolton, F. J., S. B. Surman, K. Martin, D. R. A. Wareing, and T. J. Humphrey. 1999. Presence of campylobacter and salmonella in sand from bathing beaches. Epidemiol. Infect. **122**:7-13.

Bonilla, T. D., K. Nowosielski, N. Esiobu, D. S. McCorquodale, and A. Rogerson. 2006. Species Assemblages of Enterococcus indicate potential sources of fecal bacteria at a south Florida recreational beach. Mar. Pollut. Bull. **52**:807-810.

Brettar, I., and M. G. Hofle. 1992. Influence of ecosystematic factors on survival of *Escherichia coli* after large-scale release into lake water mesocosmos. Appl. Environm. Microbiol. **58**:2201-2210.

Byappanahali, M., and R. Fujioka. 2004. Indigenous soil bacteria and low moisture may limit but allow fecal bacteria to multiply and become a minor population in tropical soils. Water Sci Technol **50**:27-32.

Crowe, A. S., and G. A. Meek. 2009. Groundwater conditions beneath beaches of Lake Huron, Ontario, Canada. Aquatic ecosystem health & management **12**:444-455.

Edge, T. A., and S. Hill. 2007. Multiple lines of evidence to identify the sources of fecal pollution at a freshwater beach in Hamilton Harbour, Lake Ontario. Water Research **41**:3585-3594.

EPA, U. S. 2002. Method 1604: Total Coliforms and *Escherichia coli* in Water by Membrane Filtration Using a Simultaneous Detection Technique (MI Medium). EPA 821-R-02-024, U. S. Environmental Protection Agency, Washington DC.

Figueira, D., and M. Barata. 2007. Marine fungi from two sandy beaches in Portugal. Mycologia **99**:20-23.

Ge, Z., M. B. Nevers, D. J. Schwab, and R. L. Whitman. 2010. Coastal loading and transport of *Escherichia coli* at and embayed beach in Lake Michigan. Environ. Sci. Technol. **44**:6731-6737.

Haack, S. K., L. R. Fogarty, and C. Wright. 2003. *Escherichia coli* and enterococci at beaches in the Grand Transverse Bay, Lake Michigan: sources, characteristics, and environmental pathways. Environ. Sci. Technol. **37**:3275-3282.

Halliday, E., and R. J. Gast. 2011. Bacteria in beach sands: an emerging challenge in protecting coastal water quality and bather health. Environ. Sci. Technol. **45**:370-379.

He, L.-M., J. Lu, and W. Shi. 2007. Variability of fecal indicator bacteria in flowing and ponded waters in southern California: implications for bacterial TMDL development and implmentation. Water Research **41**:3132-3140.

Heaney, C. D., E. Sams, A. P. Dufour, K. P. Brenner, R. A. Haugland, E. Chern, S. Wing, S. Marshall, D. C. Love, M. Serre, R. Noble, and T. J. Wade. 2012. Fecal indicators in sand, sand contact, and risk of enteric illness among beachgoers. Epidemiology **23**:95-106.

Heaney, C. D., E. Sams, S. Wing, S. Marshall, K. Brenner, A. P. Dufour, and T. J. Wade. 2009. Contact with beach sand among beachgoers and risk of illness. American Journal of Epidemiology **170**:164-172.

IJC. 2010. Groundwater in the Great Lakes Basin. IJC, Windsor, Ontario, Canada.

Ishii, S., D. L. Hansen, R. E. Hicks, and M. J. Sadowsky. 2007. Beach Sand and Sediments are Temporal Sinks and Sources of *Escherichia coli* in Lake Superior. Environ. Sci. Technol. **41**:2203-2209.

Kinzelman, J., and S. L. McLellan. 2009. Sources of science-based management practices in reducing swimming bans - a case study from Racine, WI, USA. Aquatic ecosystem health & management **12**:187-196.

Kinzelman, J., S. L. McLellan, A. D. Daniels, S. Cashin, A. Singh, S. Gradus, and R. Bagley. 2004a. Non-point source pollution: determination of replication versus persistence of *Escherichia coli* in surface water and sediments with correlation of levels to readily measurable environmental parameters. J Water Health **2**:103-114.

Kinzelman, J., K. R. Pond, K. D. Longmaid, and R. C. Bagley. 2004b. The effect of two mechanical beach grooming strategies on *Escherichia coli* density in beach sand at a southwestern Lake Michigan Beach. Aquatic ecosystem health & management **7**:425-432.

Kishimoto, R. A., and G. E. Baker. 1969. Pathogenic and potentially pathogenic fungi isolated from beach sands and selected soils of Oahy, Hawaii. Mycologia **61**:537-548.

Lavender, J. S., and J. L. Kinzelman. 2009. A cross comparison of qPCR to agar-based or defined substrate test methods for the determination of *Escherichia coli* and enterococci in municipal water quality monitoring programs. Water Research **43**:4967-4979.

Mallman, W. L., and W. Litsky. 1951. Survival of selected enteric organisms in various types of soils. Amer. Pub. Health **41**:38-44.

Phillips, M. C., H. M. Solo-Gabrielle, A. M. Piggot, J. S. Klaus, and Y. Zhang. 2011. Relationships between sand and water quality at recreational beaches. Water Research **45**:6763-6769.

Pittner, P. G., and G. T. Kleinheinz. 2009. Bringing back our beaches: A naturalized approach to *E. coli* reduction. Pages 44-47 *in* Land and Water.

Portnoy, J. W., and J. R. Allen. 2006. Effects of tidal restrictions and potential benefits of tidal restoration on fecal coliform and shellfish-water quality. Journal of Shellfish Research **25**:609-617.

Russell, T. L., K. M. Yamahara, and A. B. Boehm. 2012. Mobilization and transport of naturally occurring enterocci in beach sands subject to transient infiltration of seawater. Environ. Sci. Technol. **46**:5988-5996.

Salmore, A. K., E. T. Jensen, and S. L. McLellan. 2006. Delineation of a chemical and biological signature for stormwater pollution in urban rivers. Journal of Water & Health **4**:247-262.

Sampson, R. W., S. A. Swiatnicki, V. L. Osinga, J. L. Supita, C. M. McDermott, and G. T. Kleinheinz. 2006. Effects of temperature and sand on *E. coli* survival in a northern lake water microcosm. Journal of Water and Health **4**.

Sauer, E., J. L. VandeWalle, M. J. Bootsma, and S. L. McLellan. 2011. Detection of the human specific *Bacteroides* genetic marker provides evidence of widespread sewage contamination of stormwater in the urban environment. Water Research **45**:4081-4091.

Silva, M. R., and S. L. McLellan. 2010. Environmental and social impact of stormwater outfalls at Lake Michigan beaches. International Journal of Social Ecology and Sustainable Development **1**:34-48.

Silva, P. F., I. M. Cavalcanti, J. I. Irmao, and F. J. Rocha. 2009. Commom beach sand contamination due to enteroparasites on the southern coast of Pernambuco State, Brazil. Rev. Inst. Med. Trop. Sao Paulo **51**:217-218.

Skalbeck, J. D., J. L. Kinzelman, and G. C. Mayer. 2010. Fecal indicator organism density in beach sands: impact of sediment grain size, uniformity, and hydrologic factors on surface water loading. Journal of the Great Lakes Research **36**:707-714.

Solo-Gabriele, H. M., M. A. Wolfert, T. R. Desmarais, and C. J. Palmer. 2000. Sources of *Escherichia coli* in a coastal subtropical environment. Applied Environmental Microbiology **66**:230-237.

Spina, N. E. 2011. Beach hydrology: implications for beach quality along southern Georgian Bay, Canada. Master's. McMaster University, Hamilton.

Tate, R. L. 1978. Cultual and environmental factors affecting the longevity of Escherichia coli in Hestisols. Appl. Environm. Microbiol. **35**:9325.

U.S.EPA. 1983. Health effects criteria for marine recreational waters.

U.S.EPA. 1984. Health effects criteria for fresh recreational waters.

U.S.EPA. 2002a. Method 1103.1: *Escherichia coli (E. coli)* in Water by Membrane Filtration Using membrane-Thermotolerant *Escherichia coli* Agar (mTEC). EPA 821-R-02-020, U. S. Environmental Protection Agency, Washington D. C.

U.S.EPA. 2002b. Method 1600: Enterococci in Water by Membrane Filtration Using membrane-Enterococcus Indoxyl-b-D-Glucoside Agar (mEI). EPA 821-R-02-022, U. S. Environmental Protection Agency, Washington D. C.

U.S.EPA. 2002c. Method 1604: Total Coliforms and *Escherichia coli* in Water by Membrane Filtration Using a Simultaneous Detection Technique (MI Medium). EPA 821-R-02-024, U. S. Environmental Protection Agency, Washington DC.

Visocky, A. P. 1977. Hydrologic study of Illinois Beach State Park. Illinois State Water Survey, Urbana.

Watanabe, T., Y. Watanabe, and K. Nakamura. 2003. *Myrothecium dimorphum*, sp. nov., a soil fungus from beach sand in the Bonin (Ogasawara) Islands, Japan. Mycoscience **44**:283-286.

Weiskel, P. K., B. L. Howes, and G. R. Heufelder. 1996. Coliform contamination of a coastal embayment: sources and transport pathways. Environ. Sci. Technol. **30**:1872-1881.

Whitman, R. L., and M. B. Nevers. 2003. Foreshore sand as a source of *Escherichia coli* in nearshore water of a Lake Michigan beach. Applied Environmental Microbiology **69**:5555-5562.

Whitman, R. L., M. B. Nevers, and M. N. Byappanahalli. 2006. Examination of the watershed-wide distribution of Escherichia coli along southern Lake Michigan: an integrated approach. Applied and Environmental Microbiology **72**:7301-7310.

WHO. 2003. Guidelines for safe recreational water environments - Coastal and freshwaters.

Yamahara, K. M., B. A. Layton, A. E. Santoro, and A. B. Boehm. 2007. Beach sands along the California Coast are diffuse sources of fecal bacteria to coastal water. Environ. Sci. Technol. **41**:4515-4521.

Yamahara, K. M., L. M. Sassoubre, K. D. Goodwin, and A. B. Boehm. 2012. Occurrence and persistence of bacterial pathogens and indicator organisms in beach sand along the California Coast. Applied Environmental Microbiology **78**:1733-1745.

Supplemental Material

Table S3. 1. Statistics of mean grain diameter (d_{50}) (mm) of sand on the northern and southern part of Bradford Beach.

Beach Region	d_{50} (mm)			
		2007	**2009**	**2010**
Northern part	Mean	0.248	0.249	0.254
	Standard deviation	0	0	0.031
	Median	0.248	0.249	0.248
	N	9	5	32
Southern part	Mean	0.363	0.314	0.306
	Standard deviation	0.086	0.084	0.087
	Median	0.42	0.249	0.248
	N	9	7	9

Table S3. 2 Spearman's rank correlation (rho) of groundwater levels and environmental variables. Significant correlations at $p \leq 0.05$ are flagged. PZ-5 is not listed because it was dry most of the time.

	RAINFALL AMOUNT	LAKE LEVEL
PZ1 (n=115)	0.250*	0.480*
PZ2 (n=79)	0.119	0.564*
PZ3 (n=121)	0.148	0.293*
PZ4 (n=122)	0.243*	0.404*
PZ6 (n=122)	0.359*	0.739*
PZ7 (n=97)	0.288*	0.190
PZ8 (n=120)	0.258*	0.571*
PZ9 (n=91)	0.350*	0.674*
PZ10 (n=122)	0.389*	0.657*
PZ11 (n=120)	0.443*	0.866*
PZ12 (n=122)	0.456*	0.844*
PZ13 (n=117)	0.345*	0.655*
PZ15 (n=47)	0.272	0.869*

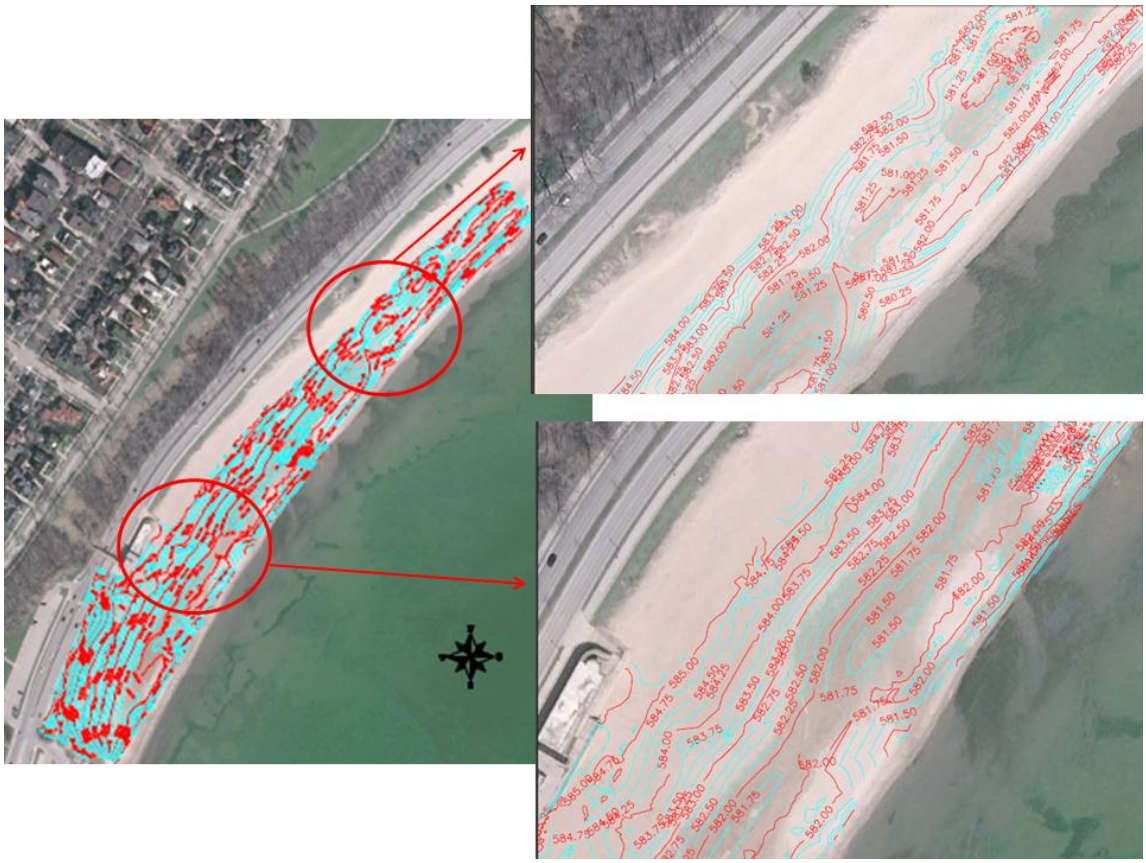

Figure S3. 1 Topographical survey performed on November 2009. Larger and deeper depressions are mostly located on the northern part of the beach around sand site S7 and S8 (581.25 ft = 177.17 m), but also on the southern part of the beach around sand site S4 (581.50 ft = 177.24 m).

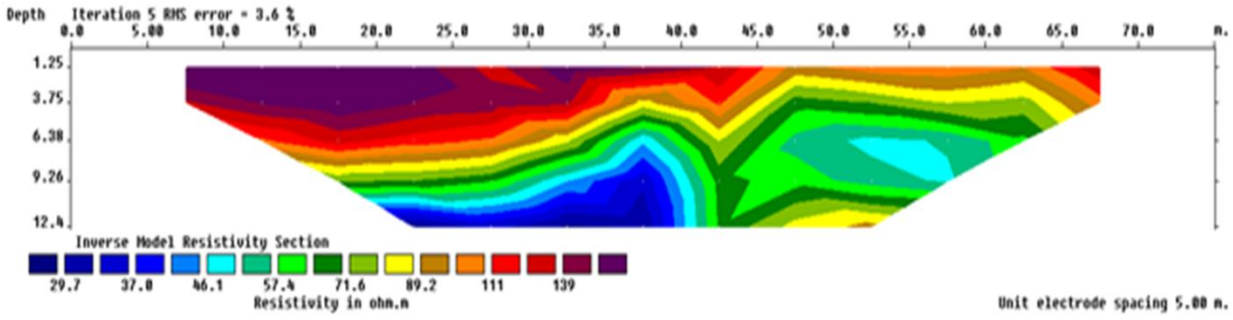

Figure S3. 2 Geophysical surveys characterized the material below the beach. Resistivity profile (pseudosection) with 5 meter spacing. It shows higher resistivity to the south (left-hand side of the figure) and lower resistivity at depth, indicating coarser sand to the south.

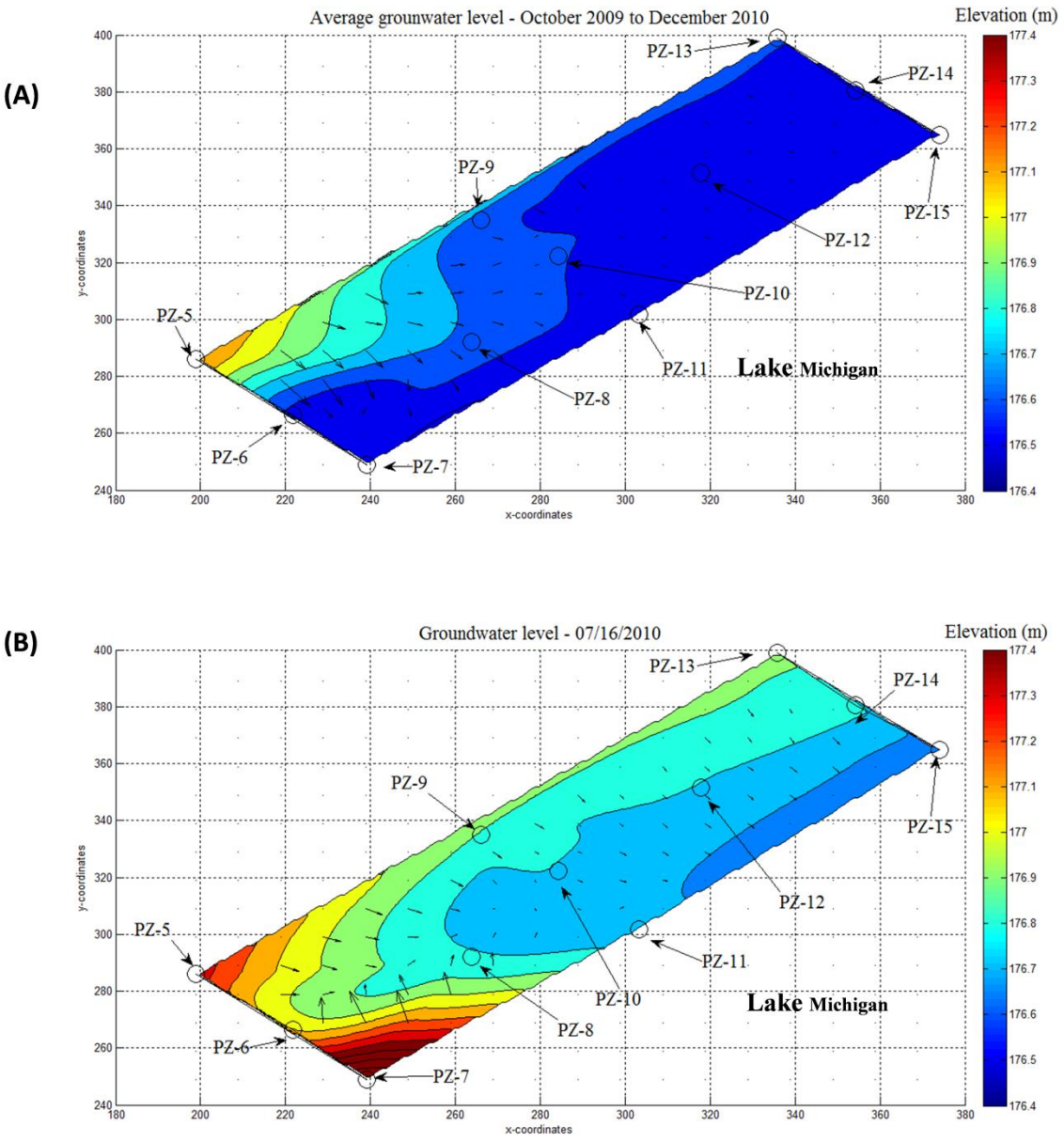

Figure S3. 3 Visualization of groundwater elevation contours on the northern part of the beach: (A) average level from October 2009 to December 2010 and (B) on July 16, 2010, after a rainfall event. It is possible to observe flow away from the lake in PZ-7 possibly due to wave wash at that location, which coincides with one of the breaches on Fig. 3.3A. Direction of water movement is indicated by arrows and their sizes indicate the relative magnitude of flow.

CHAPTER 4

DIRECT OPTICAL METHOD FOR ASSESSMENT OF GREEN FLUORESCENT PROTEIN (GFPuv)-LABELED *ESCHERICHIA COLI* IN BENCH-SCALE MODELED AQUEOUS SYSTEMS

4.1 ABSTRACT

This research presents a simple optical system for real-time laboratory bench-scale analysis of green fluorescent protein (GFPuv)-labeled *Escherichia coli* (*E. coli)* in aqueous systems. The optical system was able to visualize and measure the concentration of GFPuv- labeled *E. coli*

directly in clear water. A telescopic camera lens is applied to image the distribution of bacteria cells from a distance, making it an ideal device for non-intrusive measurements in a laboratory facility that models mixing processes in natural surface aquatic systems. Detection was also possible in tap water, lake water and lake water with added sand particles. This optical system can be sensitive enough to detect from 2.4 $x10^4$ colony forming unit (CFU) per 100 mL to 2.4 x 10^7 CFU/100 mL when 1.24 fluorescent particles (FP) to 1,191 FP per field of view (FOV) are detected on average, respectively. Laboratory flume experiment was performed and visualization and quantification of fluorescent bacteria were successful under a low flow condition. Although the presented system is not able to track bacteria flowing with a higher speed, it is conceptually possible with higher excitation energy and more sensitive image sensors. This research represents a very important step toward nondestructive monitoring systems of bacterial behavior and transport in laboratory scale systems.

4.2 INTRODUCTION

Assessment of the behavior of bacteria in aqueous systems and how they interact with the surroundings in aqueous systems is essential for the understanding of fate and transport of microbial pollutants in the environment. There are several methods that have been used for detecting the existence of bacteria and their concentration in laboratory and field assessments and the techniques have been reported elsewhere (Prosser et al. 1996; Connelly et al. 2012).They are either plate count methods or methods based on molecular biology techniques. These methods are usually invasive, deal with limited representative samples, and generate the results in a delayed time. Direct observation of bacteria in micro-channels and porous media has been used to study their swimming behaviors, cell-cell interactions and chemotaxis (McLaine et al. 2002; Liao et al. 2007; Wang et al. 2008; Asadishad et al. 2011). However, direct observation of

bacteria in a larger volume of moving fluid has not been reported previously. Questions remain about how hydrodynamic forcing would affect the transport of microbial pollutants in natural surface water flows, and how mixing and dispersion affects the association between bacteria and biotic and abiotic particles, and so on. Answers to these questions may significantly improve our understanding on the fate and transport of bacteria in streams, lakes and coastal oceans. To address this issue, experimental studies of bacteria behavior in laboratory scale that mimic the small scale hydrodynamics can reduce the complexity of a natural aquatic environment by eliminating a variety of variables that coexist on the field. Also, the application of a non-invasive method is critical to avoid disturbance to the flow, while assessing the interaction between cells and the flow field.

In order to be able to assess bacteria behavior and transport in laboratory scale there is a need of continuous development of two main fields: non-invasive techniques for the study of fluid flows and suspended sediments and development of biosensors for detecting the distribution of bacteria concentration.

Quantitative imaging (QI) techniques, particularly Particle Image Velocimetry (PIV) (Adrian 1991) or Particle Tracking Velocimetry (PTV) (Cowen et al. 1997) are non-invasive methods and are rapidly becoming standard laboratory measurement techniques for the study of fluid flows (Cowen et al. 2003). Several QI techniques are summarized elsewhere. (Sveen et al. 2004) Some advantages are its whole-field (2-D or 3-D) nature and great range in spatial resolution that often allows accurate experimental measurements to be made within traditionally difficult flow environments. Applications of PIV on microscale flow fields, namely the MicroPIV, are becoming an important diagnostic tool in the field of biomedical engineering. It is known that a good portion of pollutants are attached to sediment particles, therefore transported with them.

Non-invasive techniques for tracking sediments appear to be well-developed. There are several field techniques that have been used for suspended sediment measurement in the study of sediment transport and deposition. Operational principles, advantages, and disadvantages are well documented (Wren et al. 2000). The techniques used in the field are acoustic, bottle, pump, focused beam reflectance, laser diffraction, nuclear, optical backscatter, optical transmission, spectral reflectance (Wren et al. 2000), and particle image velocimetry (Liao et al. 2009). However, non-invasive techniques applied to the transport of microbial pollutants in turbulent surface water flows are yet to be developed.

Microbe-based sensors (MBS) consist of a transducer in conjunction with microbial cells to generate a measurable signal proportional to the concentration of the analytes. In the past decade, several review papers have been published to address the development of microbial biosensors (D'Souza 2001; Tecon et al. 2008; Su et al. 2011) In recent years a variety of MBS have been developed for public health, environmental monitoring, food safety, homeland security (Gooding 2006), and biomedical applications (Morrison et al. 2008), taking advantage of their specificity, small size, ease of handling, high precision, ability for real-time and on-spot analysis (Arya et al. 2006). Biosensors can be classified according to their method of signal transduction, such as electrochemical, optical, acoustic, mechanical, calorimetric, and electronic. Biosensors can also be classified according to their method of biological signaling mechanisms. They include antibody/antigen, enzymes, nucleic acids, cells and viruses, and biomnetic materials based methods (Morrison et al. 2008). The current imaging technologies utilizing fluorescence proteins include fluorescence resonance energy transfer, fluorescence lifetime imaging microscopy, imaging techniques for measuring molecular mobility, and chromophore-activated light inactivation (Wang et al. 2008).

Most bacteria imaging tracking systems in use are 2-D tracking systems. Usually a video camera connected to a microscope records pictures of moving organisms (Liao et al. 2007). Other researchers have used a video-based 3-D tracking system for microorganisms with a diameter of >10 μm, with the capability of tracking many cells simultaneously (Thar et al. 2000). These studies are still limited to exposing the sample to the apparatus and not the apparatus to the microorganism on a bench scale or laboratory flume evaluation. There are a few researchers that have presented the concept of *in situ* analysis for real-time assessment of bacteria (Hewitt et al. 2012) or a dye tracer (Treadaway et al. 1999) in the environment using fiber optical sensors. It should be noted that some significant advances have been made in the study of aerosol transport in air (To et al. 2009; Spitzer et al. 2010) and compounds transport in porous media (Rashidi et al. 1996; Lachhab et al. 2008; Monica et al. 2009) with optical techniques.

In this study we present the development of a simple optical system that can visualize and quantify GFPuv-labeled *E. coli* in a bench-scale environment that simulate mixing processes in natural surface aquatic systems. A telescopic camera lens is applied to image the distribution of bacteria cells from a distance, making it an ideal device for non-intrusive measurements. Limits of detection of the system were evaluated with the intention of assessing its future applications. Experiments were also performed in a hydraulic flume, although further research is necessary before it can be employed for tracking particles in this larger scale system. This simple optical technique is capable of directly observing bacteria in a volume of fluid larger than those used in other methods. The direct benefit of this technique is to facilitate and improve the study of the behavior of *E. coli* in aqueous systems with a non-invasive method capable of assessing bacteria in an experimental setting that closely resembles the natural environment.

This method was not designed to assess natural bacteria in the environment. This method was designed to assess a model organism, in this case GFPuv *E. coli* in laboratory scale to investigate questions related to bacteria behavior and transport that would be difficult to assess in the environment otherwise. Environmental Protection Agency (EPA) recommends a statistical threshold value for culturable *E. coli* measured in single samples of recreational waters of 235 CFU/100 mL for posting beach warning signs and 1000 CFU/100 mL for closing signs. Therefore, the understanding of the sources and mechanisms of transport of bacteria to the beaches is crucial for a better management on public health.

4.3 EXPERIMENTAL CONFIGURATION

Bacterial strain and culture preparation

E. coli strain JM 109 (Promega, Madison, WI) was used as the host strain. The pGFPuv vector (BD Bioscience, San Jose, CA) containing green fluorescent protein (GFP) and ampicillin resistance gene was transformed into chemically competent *E. coli* JM 109 cells, according to manufacture instructions (Promega, Madison, WI). Transformed colonies were selected on streaked lysogeny broth (LB) agar plates added with 100 μg/mL ampicillin and 100 μM isopropyl β-D-1-thiogalactopyranoside (IPTG) and grown at 37°C for 24 h. IPTG is required to turn on the lac promoter that controls GFP expression (Gather et al. 2011). *E. coli* cells containing the GFP plasmid cells were cultivated in 100 μg/mL ampicillin and 100 μM IPTG LB broth at 37ºC, shaking at 160 rpm for 16 h. Increased IPTG increases GFP production, which affects cell counts. Therefore the same amount of IPTG was used at all times as well as fresh

LB/AMP/IPTG plates (no older than a week) and fresh cells were used to generate standard curves.

Detection of GFPuv *E. coli* with the optical system

The optical system, illustrated in Figure 4.1, includes a 300 mW diode pumped solid state laser (DPSS) at 473 nm (LRS-473-TM-300-10, Laserglow Technologies, Toronto, CA) used to excite GFPuv-labeled *E. coli* which are contained in a beaker; and a monochrome charge-coupled device (CCD) camera (Point Grey FL2-08S2M) to capture the fluorescent image of bacteria. Individual bacteria can be identified through image processing; therefore their concentration can be determined by counting the number of cells in the field of view (FOV) of the camera. The laser and camera were mounted on a motorized two-axis translating stage system (Velmex Unislide® A4021W1-S6). The point of observation can be controlled in the y and z directions with resolution of 12.5 μm. The sample under observation was set up on an optical bench and the camera and the laser were positioned orthogonally to the observed volume.

The CCD camera has a 4.65 μm x 4.65 μm pixel size and a maximum resolution of 1024 x 768 pixels. It is connected to a telecentric lens, which magnification is 2.0X (NT58-431, Edmund Optics Inc., Barrington, NJ). A 500 nm long-pass filter (NT62-972, Edmund Optics Inc., Barrington, NJ) was placed directly in front of the CCD detector in order to exclude or minimize the scattering light of the laser beam and to capture fluorescent light emitted by the GFPuv cells. In order to account for the possible non-uniform distribution of cells, the CCD camera acquired images at five different sample volumes equally spaced vertically in the beaker. The observed volume is dependent on the FOV and the depth of field (DOF) of the camera, as well as the thickness of the laser beam. FOV was calibrated by positioning a ruler in front of the camera

without the optical filter and it was measured as 2.38 mm x 1.79 mm. The laser beam is parallel to the longer side of the CCD imager and the beam width is narrower than the height of the FOV (1.79 mm). Also the light intensity distribution of the laser beam is not uniform. Acquired images of cells are brighter near the centerline of the beam and the brightness decreases towards the edge. Because the width of the laser beam covers about ~70% of height of the FOV, the effective FOV is estimated to be 2.38 mm ×1.41 mm. The DOF was estimated to be 1.5 mm by positioning one object in front of the camera and moving it away until object became out of focus. The measured displacement of the object is the DOF. The observed volume is approximated as the DOF times the area of the FOV. Therefore, the sample volume is estimated to be 5.0 mm^3 or 5.0 μL. After image processing, total number of identified cells from the image divided by the sample volume is considered as the estimated cell concentration. The cell concentration is eventually converted to a unit of [fluorescent particles (FP)/100 mL] as equivalent to [CFU/100 mL].

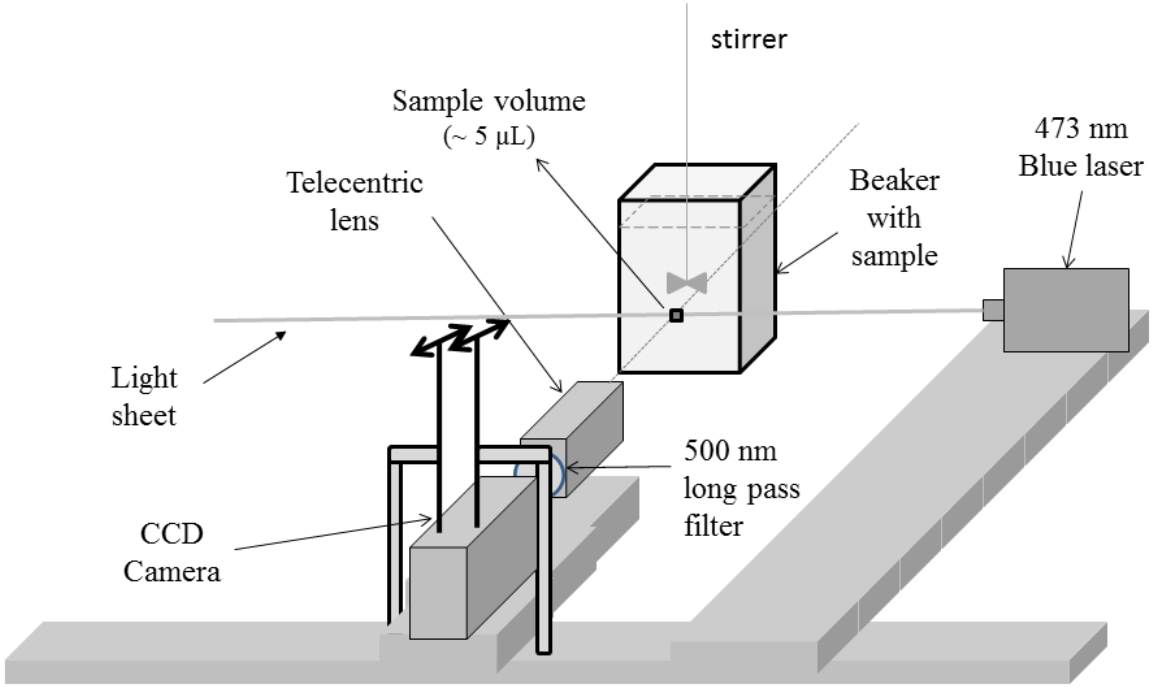

Figure 4. 1A schematic illustration of the experimental set up of the bench scale optical system; drawing not to scale.

The exposure time of a fluorescent cell was effectively controlled by the duration of the laser pulse. For most data presented in this paper, the exposure time or laser pulse was set to 40.93 ms and the camera gain was set at maximum (24 dB). The laser timing and duration was set via Point Grey FlyCap Software. The laser was synchronized with the camera shutter via General Purpose Input/ Output (GPIO) output signal. A custom computer acquisition program was designed in Matlab to control the hardware and present data in graphical format for user analysis. The set up of the beaker containing the sample was built on an optical bench. The system was set to acquire images at a rate of 0.5 frames per second (fps).

Standard cell count protocol

The standard cell count method is a plate culture method. One hundred microliters aliquot of the sample was obtained mid-height from the beaker after measurements with the optical system to avoid any disturbance of the sample volumes. This aliquot was diluted 1/100 with sterile water in a Falcon tube. One hundred microliters of this dilution was filtered through a 0.45 μm pore size 47 mm nitrocellulose filter and placed on LB/amp/IPTG plates and taken to a 37°C incubator for 24 h. Samples were filtered in duplicate. Plates were placed under the UV light source and fluorescent colonies were counted.

Optical method trial protocol

The first step is identification of the background of the aqueous sample without bacteria. Source water (Milli-Q water, tap water, lake water) is added into the beaker (199 mL). Samples were stirred with a digital mixer (50006-00, Cole-Parmer, IL) for 10 min at 300 rpm to ensure well mixing of particles and then rested for 10 min before acquisition of 100 images at five vertically equally spaced coordinates in the beaker. The second step was to determine the initial concentration of bacteria. One milliliter of GFPuv *E. coli* cells was added onto 199 mL of the source water in the beaker. Samples were stirred for 10 min at 300 rpm and then rested for 10 min before acquisition of images, to avoid image motion blur caused by the residual motion of the stirred water.

Quantification of GFPuv *E. coli* with the optical system

Matlab routine was developed and validated for quantification of GFPuv *E. coli* cells from acquired images. After acquisition of raw images using the optical system, images had to be treated, as shown in Figure 4.2. First, the image background was corrected for brightness variations, appearing in the background because of uneven illumination and for background auto fluorescence. Then a morphological opening operation was used for noise removal with a disk-shaped structuring element. The open image was then filtered using a Gaussian filter to eliminate sharp edges that may result from the opening operation. The background (non uniform illumination) was subtracted from the image. Image pixels of cells that appeared as bright "spots" were separated from background pixels by global thresholding, which is determined according to the overall background noise level, producing a binarized image with white cells on a black background. Then, the binary image was labeled according to the connectivity of "white" pixels to identify the fluorescent particles (FP). After that, centroids of the detected FPs were found as well as points that fall within a specified range of area which represents the size of a cell image. Similarly to procedure used on quantification of labeled bacteria from digital microscope images (Selinummi et al. 2005), the distance transform was then computed and the complement of the distance transform was obtained to force non-object pixels to infinity; finally the watershed transform was computed to separate clustered cells from each other by marker controlled water segmentation.

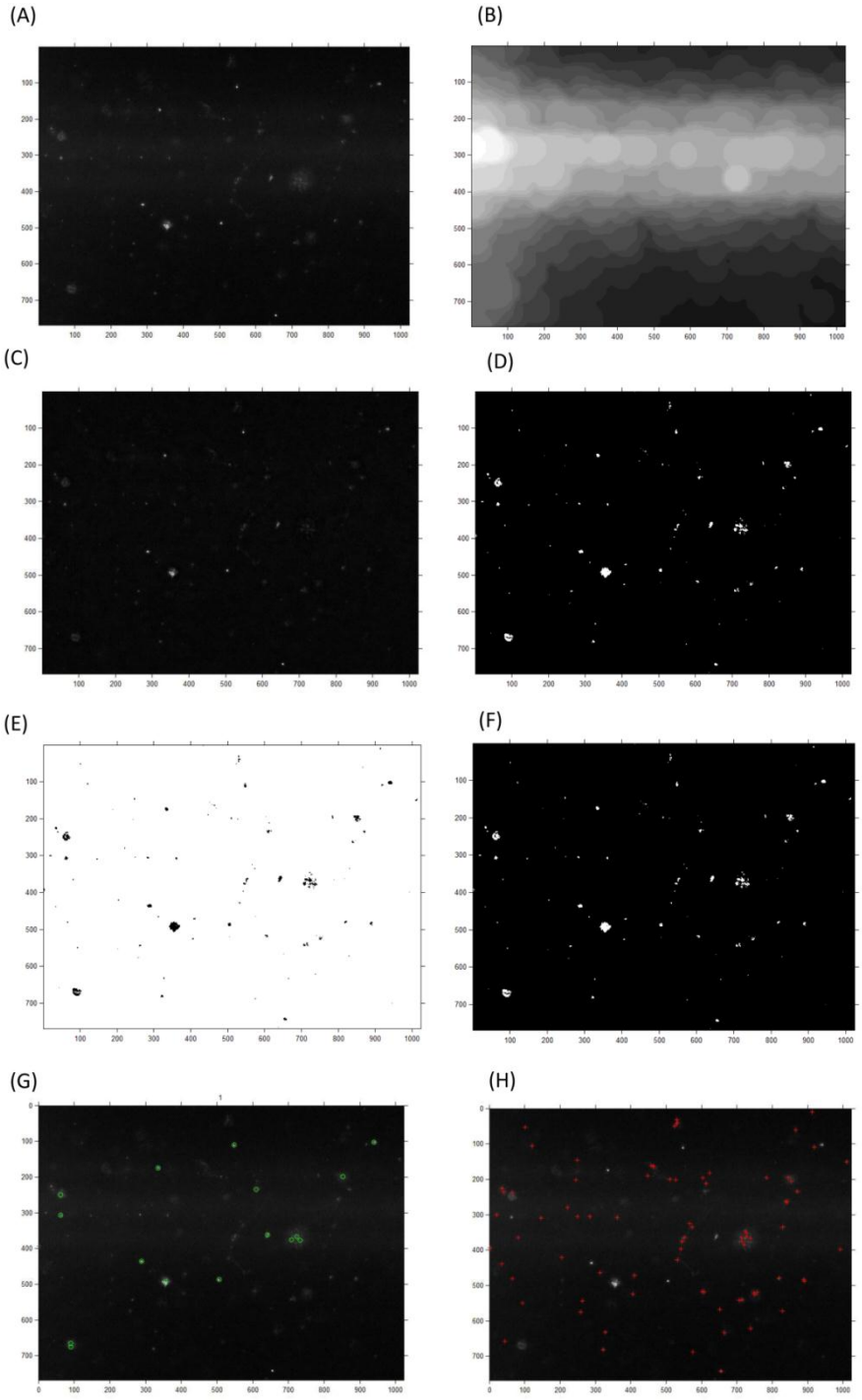

Figure 4. 2 Steps of image processing to count fluorescent particles: (A) Acquisition of raw images with image system; (B) Characterization of background level; (C) Subtraction of the background; (D) Separation of FP pixels from background pixels; (E) Computation of watershed transform; (F) Separation of clustered cells from each other by marker controlled watershed segmentation; (G) Removal of artifacts (particles < 2 pixels and > 50 pixels); (H) Quantification of fluorescent particles.

Even though the resolution of the imaging system is about 2.33 μm per pixel, the size of one typical GFPuv *E. coli* image was between 2 to 4 pixels along the longer axis of the cell image, which is larger than its actual size. This is possibly due to the optical aberration effect and other imperfection factors of the camera lens. Particles that occupied 5 to 50 pixels were treated as cells clustered together and were separated into single cells according to the procedure described previously. Objects smaller than 2 pixels or larger than 50 pixels were treated as either noise or particles naturally present in the water. They could be captured by the camera either because they were naturally fluorescent, such as phytoplankton, or due to scattering of fluorescent light.

With the intent of generating a standard curve between the optical method and the standard method, a known concentration of cells (determined by the standard cell count method) was used to prepare dilution series to be tested with the optical method. Dilution series of *E. coli* cells containing the GFP plasmid were prepared with sterile water (1/200, 1/400, 1/800, 1/2000, 1/4000, 1/20000, and 1/200000), corresponding to an average concentration of $2.4x10^7$, $1.3x10^7$, $6.4x10^6$, $2.4x10^6$, $1.3x10^6$, $2.4x10^5$, and $2.4x10^4$ CFU/100mL, respectively. Samples were stirred for 10 minutes at 300 rpm and then rested for 10 min before acquisition of images. Samples were carefully vortexed before any dilution step. A total of 600 images were taken for each sample at different vertical locations in the beaker

Limit of detection of an individual GFPuv- labeled cell

The limit of detection of an individual cell from one acquired image can be defined as the signal to noise ratio (SNR) of an identified cell image, i.e., the average brightness of the cell image vs. the standard deviation of the background noise, usually determined by the dark current of the CCD and the ambient light.

To calculate the background noise, identified cell images are excluded. Binary mask obtained from the particle image processing can be directly used to facilitate this operation. Even with an ideal configuration, the brightness of a cell image represented by the digital output of image pixels is determined by many factors, including the wavelength, energy and beam shape of the excitation laser beam, the efficiency of the quantum yield of the GFP molecule, the emission spectrum of the GFP, the optical configuration, the quantum efficiency of the CCD and the A/D conversion of the camera.

To determine the irradiance of the fluorescent light emitted from a GFPuv *E. coli* cell, we assume the cell and its image are small enough which can be approximated as point source and image. Assuming a simplified optical imaging system (SI Figure S4.3) we can estimate the intensity (or "brightness") of the image of a FP. Denoting E_c as the light energy emitted by an excited fluorescent cell, the current generated by one CCD sensor as it receives the irradiance of the fluorescent cell, I_{CCD}, can be approximated as

$$\mathrm{I_{CCD}} = \int_{\lambda_{LP}}^{\lambda_{IR}} \mathrm{R_\lambda \rho_E d\lambda} = \frac{\mathrm{m^2 E_c}}{16(1+\mathrm{m})^2(\mathrm{f/\#})^2} \frac{\mathrm{e}}{\mathrm{hc}} \int_{\lambda_{LP}}^{\lambda_{IR}} \mathrm{\lambda Q_E \rho_E d\lambda} \qquad \text{Equation 4. 1}$$

where m is the magnification ratio of the camera lens; $f/\#$ is the f-stop number of the lens; R_λ is the spectral responsivity of the CCD, which is related the quantum efficient of the CCD Q_E (a function of light wavelength, λ); e is the elementary charge, h is the Planck's constant and c is the speed of light in a vacuum space; λ_{LP} is the cutoff wavelength of the long-pass optical filter employed for the fluorescence imaging, and λ_{IR} is the cutoff wavelength of the infrared filter built in the CCD camera. ρ_E is the emission spectrum of GFPuv at a certain excitation state,

which has been determined with a Hitachi F-4500 Fluorescence Spectrophotometer with different excitation wavelengths. Emission spectra curve is available in the SI (Fig. S4.2).

Denoting the exposure time (the integration time of CCD) as t_E, the digital output of the CCD reading, which represents the "brightness" of the image, B_{CCD}, can be approximated as

$$B_{CCD} = CI_{CCD}t_E = E_c t_E \frac{\mathrm{m}^2}{16(1+\mathrm{m})^2(\mathrm{f}/\#)^2}\frac{\mathrm{e}}{\mathrm{hc}} C \int_{\lambda_{\mathrm{LP}}}^{\lambda_{\mathrm{IR}}} \lambda \mathrm{Q_E} \rho_{\mathrm{E}} \mathrm{d}\lambda \qquad \text{Equation 4. 2}$$

where the proportionality *C* combines effects of the capacitance of the CCD and the camera's A/D conversion electronics, i.e., the conversion of the electrical charge to a digital reading. The derivation of equations (4.1) and (4.2) is available in the SI (Derivation of equations S1).

Equation 4.2 provides an estimate of the digital reading of a cell image's brightness. In the presented study, however, we are not able to directly evaluate it due to the lack of knowledge on the conversion factor C, and the light emitted by the fluorescent cell E_C. In principle, E_C should be linearly proportional to the laser power, the amount of fluorescent proteins in the cell and their quantum yields, which has to be determined experimentally. We are, however, able to examine the effects of the optical configuration through varying the $f/\#$ and the integration time.

In order to evaluate the effect of photo bleach on fluorescent proteins and to operate with the optimum settings of the system, we have conducted a series of calibration tests, by taking cell images with varying exposure time (i.e., the duration of the laser pulse) and the lens aperture. One hundred images were taken at a rate of 0.5 Hz for each case. Average cell image intensity (brightness) over all identified cell images and the number of cell images per FOV were calculated for each set. Additional experiments were performed for investigation of fluorophore

photobleach by exposing the cells to the laser for a total of 3 hours and monitoring concentration of cells hourly. In this study, laser was set to pulse every 2 s for an extent of 40.93 ms (SI Figure S4.4).

Laboratory flume experiment

Experiments were carried out in a 30.5-cm-wide and 4.9-m-long and 0.5 m deep glass walled recirculating flume. A sediment bed was composed of pool filter sand, with mean grain diameter (d_{50}) of 387 μm. Tap water was filled to a depth of approximately 15 cm on the top of sand, so that the total depth of the sand bed and overlying water was approximately 20 cm. The camera was positioned perpendicular to the wall of the flume and the laser was sitting on a frame on the top of the flume, pointing down. The working distance of the lens is 7.5 cm. Therefore, the lens was positioned as close as possible to the wall of the flume so the sample volume could be situated the furthest possible away from the wall (~ 5 cm). Fifteen milliliters of GFPuv *E. coli* cells were injected with a sterile syringe into the domain of observation, with a total injection of 7.2 x10^{10} CFU. System was sanitized with 10% bleach concentration by recirculating the system overnight and then the water was released to the sanitary sewer system. Experimental apparatus of the optical system for laboratory flume and a video recording the cells travelling in the flume due to the background flow (85 μm s^{-1}) are available in the Supporting Information, SI (Video S4.1, Figure S4.1). Exposure time used for the experiment was 4 ms.

4.4 RESULTS AND DISCUSSION

Calibration of the optical cell counting method

Comparison between the bacterial concentration measured by image analysis and the bacterial counts obtained by the standard cell count method is shown in Figure 4.3. The error bar indicates the 95% confidence interval based on the standard error over 600 images. The validation of the imaging method is excellent as a linear trend could be observed between the image-measurement and the cell-count concentration. Linear regression with the intercept forced to be zero indicated that $y = 1.03\ x$ with the coefficient of determination $R^2 = 91\%$, where x is cell-count concentration of cells measured in CFU/100 mL and y is the image-concentration of FP/100 mL. The good linear relation and the nearly 1.0 slope suggest that the image counting method is very accurate and robust. Calibration curve for seven different dilutions of GFPuv *E. coli* in Milli-Q water was done using at least six trials per dilution. Concentration of cells was determined in duplicate from the fresh GFPuv *E.coli* cells culture via standard cell count and final concentration was calculated for each dilution.

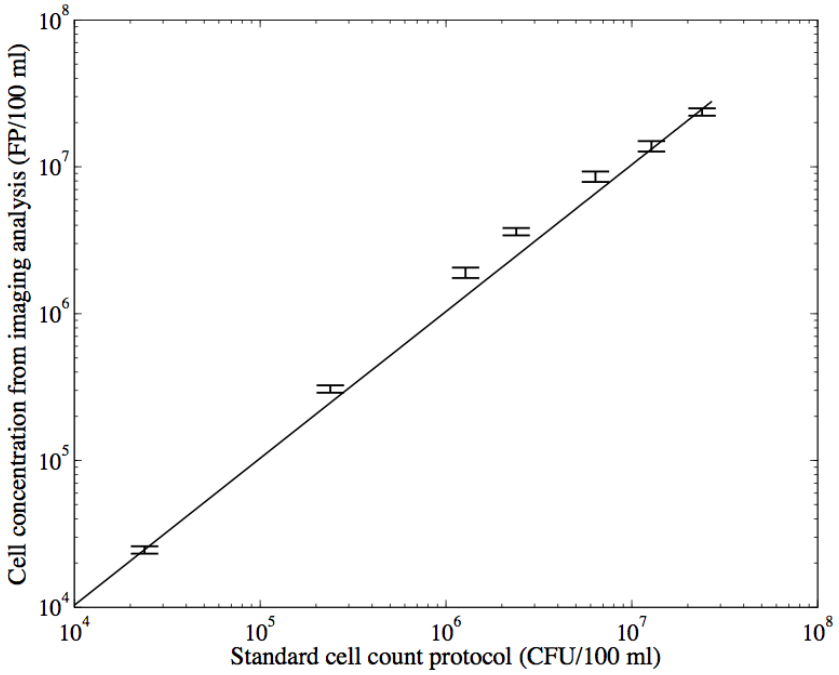

Figure 4. 3 Calibration curve for seven different dilutions of GFPuv-labeled *E. coli* in Milli-Q water comprised of at least six trials per dilution. R^2= 91%.

Calibration tests of the optical method

Following Eq. 4.2, it is expected that the brightness of a cell image increases linearly with the exposure time t_E and the inverse of $(f/\#)^2$, or the area of the lens aperture, D^2, as shown by equation (4.3) in the supplemental material. In agreement, as a result of the calibration tests, the mean brightness and cell number concentration vs t_E and the area of aperture representing as the % of the full openness are presented in Figure 4.4.

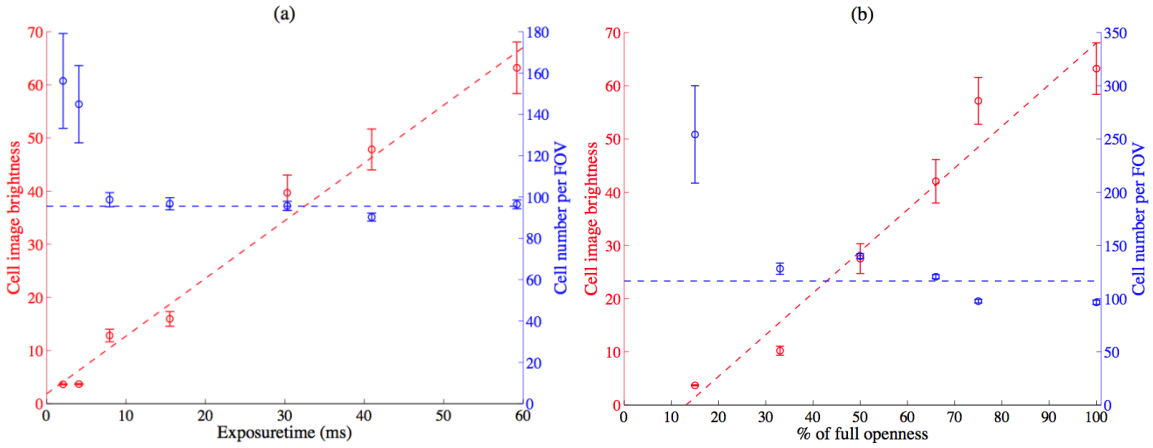

Figure 4. 4 Effects of (a) exposure time and (b) lens aperture on the mean cell image brightness and the measurements of cell concentration

As shown in Figure 4.4 (a), the mean cell image intensity increases linearly with the exposure time. Also, the cell number per FOV in Figures 4.4 (a) and 4.4 (b) showed no signs of photobleach at the highest exposure time of 60 ms. The extent of photobleaching of fluorescent proteins in a sample is a function of laser power and duration of excitation (Hewitt et al. 2012). Additional experiments were performed and fluorophore photobleach was below level detection for the extent of 3 hours (SI Figure S4.4).

As the exposure time reduced from 60 ms to 2 ms, the SNR reduces from 16 to 3, approximately. As a result, the measured cell number concentration increased rapidly as the exposure time became < 5 ms, approximately. With a low SNR, many falsely identified "cell" were actually background noise. The results in Figure 4.4 show that the measured cell concentration is rather independent of the exposure time as long as the SNR is high enough. Practically, we have considered exposure time = 5 ms as the threshold of the limit of detection for the current imaging system. Since the power of laser employed in this study is 300 mW, the minimal energy required is equivalent to 1.5 mJ.

Figure 4.4 (b) indicates that the mean cell image intensity is approximately linearly proportional to the lens aperture area, or the inverse of $(f/\#)^2$, as suggested by equation (S4.2) , and equation (S4.3) in the supplemental material. Similarly, the measured cell concentration is rather insensitive to the aperture except when the aperture area dropped to below 20% of the full openness, approximately.

Our ultimate goal is to apply this method to observe the transport of bacteria in moving fluids. In order to identify fluorescent cells in such an environment, the exposure time needs to be short enough so cell images will appear as bright "spots" instead of "streaks". Most cell images taken with the current system are about 2~4 pixels in diameter, corresponding to a physical dimension of about 6~12 μm. In order to avoid any significant "motion blur", it may require that the displacement of cell images be smaller than their sizes, e.g., about 10 μm. If the flow speed is about 0.1 m s^{-1}, the exposure time needs to be shorter than 0.1 ms, which is about 50 times shorter than the lower limit of detection for the present imaging system. To solve this problem, the power of the CW laser needs to be about 15 W. A better alternative is a Q-Switched laser with pulse energy greater than 1.5 mJ. Other improvements can be made to alleviate the

requirement on laser energy, including a better telecentric lens with larger aperture, a more sensitive imager sensor with lower SNR, or a laser with wavelength closer to the absorption peak of GFPuv.

Effects of water source on the sensitivity of the novel optical method

Sensitivity of the optical system was evaluated with different water sources in order to validate its potential for visualizing and quantifying bacteria in laboratory experiments. Concentration of bacteria used in all experiments was on average 100 FP/ FOV. The same particle identification method was applied to measure "bright particles" in water without GFPuv-labeled bacteria, hereafter called the "background particles" (denoted as BCK).

Table 4.1 shows ratio of FP to FP plus BCK, ratio of FP/FOV to derived CFU/FOV, and the SNR. There were essentially zero background particles in the Milli-Q water and the tap water, but many background particles in the lake water with and without sand particles. Nevertheless, by subtracting the background particle from the measured total number of particles as bacteria were added, the estimated concentration of bacteria agreed well with the known concentration from plate counting. The SNR increases as the turbidity increased for lake water, because of many identified particles are background particles and they are brighter than the GFPuv- labeled cells. Even though the relationship between the optical method and the standard method is close to 1, overall, the optical approach tends to overestimates due to the presence of background particles, when working with natural waters.

Table 4. 1 Sensitivity data of the GFPuv *E. coli* used in this research. FP denotes fluorescent particles and BCK denotes background particles.

Water source	Ratio: $\frac{FP}{(FP+BCK)}$	Ratio: $\frac{FP/FOV}{CFU/FOV}$	signal to noise ratio (SNR)	Turbidity (NTU)	Conductivity (mS/cm)
Milli-Q water	1.00	0.95	7.63	0.00	0.009
Tap water	1.00	1.02	7.12	2.03	0.052
Lake Michigan water	0.65	0.93	13.37	29.20	0.379
Lake Michigan water added with 150 mg/mL of environmental sand particles, stirred and settled.	0.59	1.00	18.81	38.17	0.385

Therefore, care should be taken when using the optical method to quantify bacteria in natural waters. Lake water has particles naturally present in the water that fluoresces at wavelengths close to GFP, such as chlorophyll and phycoerythrin. In addition, phytoplankton can be as small as bacteria, on the order of 1 micron. Therefore, the first step is to adjust the threshold in such way that the amount of cells per FOV corresponds on average to the amount of cells measured by the standard method. In practice, the threshold adjustment will depend on the magnitude of background present in the water source. In principle, the technique can be applied not only for freshwater, but for brackish water or salty water, with turbidity < 50 NTU, as indicated by our preliminary study.

Limitations of the system

The detection limit obtained in our study was 2.4 x 10^4 CFU/100 mL (Figure 4.3) which corresponds to an average of 1.24 FP per FOV. However, in theory the optical system can measure a much lower concentration when sampling more images. For example, it can measure even up to an average of 1 fluorescent cell every 10,000 images which correspond to 1 CFU/100 mL. On the other hand, when FP concentration is too high, the FOV is too "crowded" and the imaging algorithm is unable to count correctly. In the present system the upper limit was about 2.4 x 10^7 CFU/100 mL or average of 1,191 FP per FOV.

4.5 CONCLUSIONS

A simple optical system is presented for real-time laboratory visualization and measurement of concentration of green fluorescent protein (GFPuv)-labeled *Escherichia coli* (*E. coli)* in clean water. Detection was also possible in tap water, lake water and lake water with added sand particles. This optical system is sensitive enough to detect from 2.4 x10^4 colony forming unit (CFU) per 100 mL to 2.4 x 10^7 CFU/100 mL when 1.24 fluorescent particles (FP) to 1,191 FP per field of view (FOV) are detected on average, respectively. Laboratory flume experiment was performed and visualization and quantification of fluorescent bacteria were successful under a low flow condition. Although the presented system is not able to track bacteria flowing with a higher speed, it is conceptually possible with higher excitation energy and more sensitive image sensors. This research represents a very important step toward nondestructive monitoring systems of bacterial behavior and transport in laboratory scale systems.

As this technique identifies and quantifies cells based on their minimal fluorescence intensity that can be detected and considered as a cell it will not function with native bacterial populations lacking this property or with weak fluorescence; rather, its intended use is for obtaining an understanding of *in loco* system dynamics through the use of fluorescent model organisms, such as GFPuv *E. coli*. In principle the technique can be extended to any substance that emits measurable fluorescence and potential applications may include the use of fluorescent dyes or fluorophore-tagged chemicals or pharmaceuticals to assess their behavior and transport in water. Even though, there are some challenges yet to be solved in order to apply this technique to moving fluids, the technique works fine in motionless water and can therefore be utilized to answer scientific questions under this condition. This technique can potentially give light to a deeper understanding of environmental processes such as assessment of attachment of bacteria to particles, settling velocity of bacteria, diffusion of bacteria from sand, and intrusion of bacteria in sand.

4.6 ACKNOWLEDGMENTS

This work was made possible through a UWM Graduate School Dissertation Fellowship Award. We thank Jessica VandeWalle and William Hutchins for assistance with lab arrangements and Drew Nowakowski for assistance with the fluorescence spectrophotomer. We also thank Zeyun Yu for helpful insight on image processing and Thomas Hansen for his thoughtful review of our manuscript.

4.7 REFERENCES

Connelly, J. T.; Baeumner, A. J., Biosensors for the detection of waterborne pathogens. Anal Bioanal Chem 2012, 402, 117-127.

Prosser, J. I.; Kilham, K.; Glover, L. A.; Rattray, E. A. S., Luminescense- based systems for detection of bacteria in the environment. Critical Reviews in Biotechnology 1996, 16, (2), 157-183.

Asadishad, B.; Ghoshal, S.; Tufenkji, N., Method for the direct observation and quantification of survival of bacteria attached to negatively or positively charged surfaces in an aqueous medium. Enviornmental Science and Technology 2011, 45, 8345-8351.

Liao, Q.; Subramanian, G.; DeLisa, M. P.; Koch, D. L.; Wu, M. M., Pair velocity correlations among swimming Escherichia coli bacteria are determined by force-quadrupole hydrodynamic interactions. Physics of Fluids 2007, 19, (6).

McLaine, J. W.; Ford, R. M., Reversal of fagellar rotation is important in initial attachment of Escherichia coli to glass in a dynamic system with high-and low-ionic-strength buffers. Applied Environmental Microbiology 2002, 68, (3), 1280-1289.

Wang, Y.; Shyy, J. Y.-J.; Chien, S., Fluorescence proteins, live-cell imagig, and mechanobiology: seeing is believing. Annu. Rev. Biomed. Eng. 2008, 10, 1-38.

Adrian, R. J., Particle-imaging techniques for experimental fluid mechanics. Annu. Rev. Fluid Mech. 1991, 23, 261-304.

Cowen, E. A.; Monismith, S. G., A hybrid digital particle tracking velocimetry technique. Experiments in Fluids 1997, 22, 199-211.

Cowen, E. A.; Sou, I. M.; Liu, P. L.-F.; Raubenheimer, B., Particle image velocimetry measurements within a laboratory-generated swash zone. J. Eng. Mech. 2003, 129, 1119-1129.

Sveen, J. K.; Cowen, E. A., Quantitative imaging techniques and their application to wavy flows. In PIV and Water Waves, ed.; Grue, J.; Liu, P. L.-F.; Pedersen, G. K., World Scientific Pub. Co.: Singapore, 2004.

Wren, D. G.; Barkdoll, B. D.; Kuhnle, R. A.; Derrow, R. W., Field techniques for suspended-sediment measurement. Journal of Hydraulic Engineering-Asce 2000, 126, (2), 97-104.

Liao, Q.; Bootsma, H. A.; Xiao, J.; Klump, J. V.; Hume, A.; Long, M. H.; Berg, P., Development of an in situ underwater particle image velocimetry (UWPIV) system. Limnol. Oceanogr.: Methods 2009, 7, 169-184.

Thar, R.; Backburn, N.; Kuhl, M., A new system for three-dimensional tracking of motile microorganisms. Applied Environmental Microbiology 2000, 66, (5), 2238-2242.

Hewitt, B. M.; Singhal, N.; Elliot, R. G., Novel fiber optic detection method for in situ analysis of fluorescently labeled biosensor organisms. Enviornmental Science and Technology 2012, 46, 5414-5421.

Treadaway, A. C. J.; Lynch, R. J.; Bolton, M. D., Pollution transport studies using an in-situ fibre optic photometric sensor. Engineering geology 1999, 53, 195-204.

Spitzer, I. M.; Marr, D. R.; Glauser, M. N., Impact of manikin motion on particle transport in the breathing zone. Journal of Aerosol Science 2010, 41, (4), 373-383.

To, G. N. S.; Wan, M. P.; Chao, C. Y. H.; Fang, L.; Melikov, A., Experimental study of dispersion and deposition of expiratory aerosols in aircraft cabins and impact on infectious disease transmission. Aerosol Science and Technology 2009, 43, (5), 466-485.

Lachhab, A.; Zhang, Y. K.; Muste, M. V. I., Particle tracking experiments in match-index-refraction porous media. Ground Water 2008, 46, (6), 865-872.

Monica, M.; Cushman, J. H.; Cenedese, A., Application of photogrammetric 3D-PTV technique to track particles in porous media. Transport in Porous Media 2009, 79, (1), 43-65.

Rashidi, M.; Thompson, A.; Kulp, T.; Peurrung, L., 3-D microscopic measurement and analysis of chemical flow and transport in porous media. Journal of fluids engineering-transactions of the Asme 1996, 118, (3), 470-480.

D'Souza, S. F., Microbial biosensors. Biosensors & bioelectronics 2001, 16, 337-353.

Su, L.; Jia, W.; How, C.; Lei, Y., Microbial biosensors: a review. Biosensors & bioelectronics 2011, 26, 1788-1799.

Tecon, R.; Meer, J. R. v. d., Bacterial biosensors for measuring availability of environmental pollutants. Sensors 2008, 8, 4062-4080.

Gooding, J. J., Biosensor technology for detecting biological warfare agents: recent progress and future trends. Analytica Chimica Acta 2006, 559, 137-151.

Morrison, D. W. G.; Dokmeci, M. R.; Demirci, U.; Khademhosseini, A., Clinical Applications of micro- and nanoscale biosensors. In Biomedical Nanostructures, ed.; Gonsalves, K. E.; Laurencin, C. L.; Halberstadt, C. R.; Nair, L. S., John Wiley & Sons, Inc.: 2008.

Arya, S. K.; Chaubey, A.; Malhotra, B. D., Fundamentals and applications of biosensors. Proc. Indian Natn. Sci. Acad. 2006, 4, 249-266.

Gather, M. C.; Yun, S. H., Lasing from Escherichia coli bacteria genetically programmed to express green fluorescent protein. Optics Letters 2011, 36, (16), 3299-3301.

Selinummi, J.; Seppälä, J.; Yli-Harja, O.; Puhakka, J. A., Software for quantification of labeled bacteria from digital microscope images by automated image analysis. BioTechniques 2005, 39, 859-863.

Supplemental Material

Video S4. 1 Video recording the fluorescent cells travelling in the flume due to the background flow (85 µm s^{-1})

fluorescent_cells_flume_experiment.avi

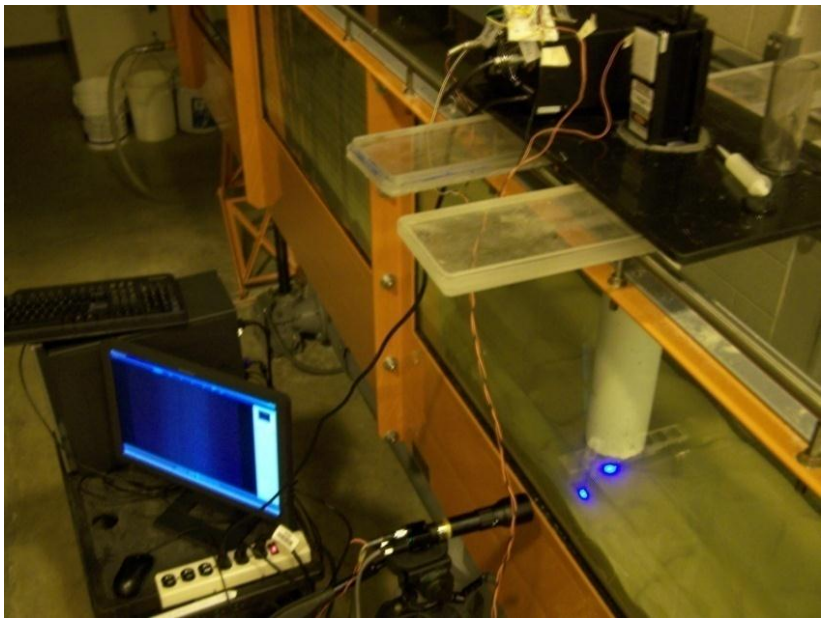

Figure S4. 1 Experimental set up of the optical system for laboratory flume experiment

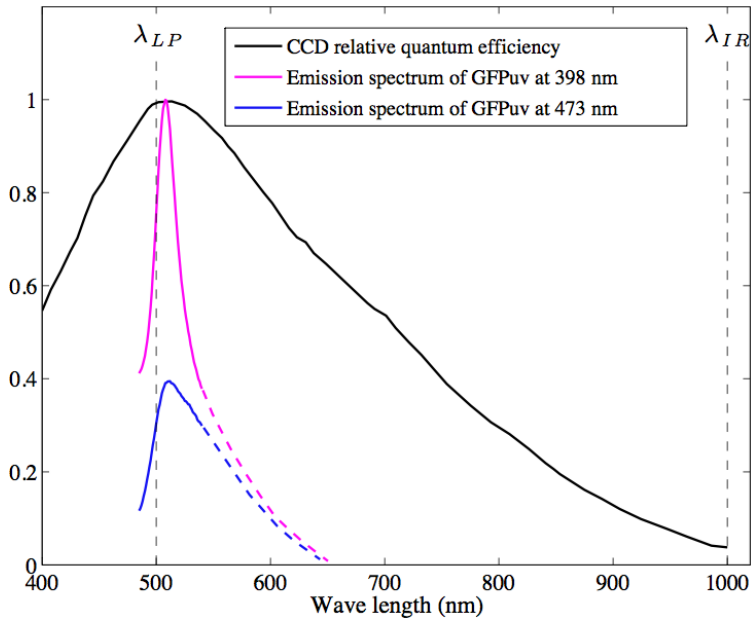

Figure S4. 2 Normalized quantum efficiency of the CCD sensor (SONY ICX204AL) and the emission spectra of GFPuv with excitation wavelength of 399 nm (peak absorption) and 473 nm (laser used in current study). Note: emission spectra are measured with scanning fluorescence with the emission wavelength between 485 and 540 nm. Dashed lines on the emission spectra are not real data but extrapolations from measurements.

Derivation of equations S1:

To determine the irradiance of the fluorescent light emitted from a GFPuv *E. coli* cell, we assume the cell and its image are small enough which can be approximated as point source and image. We consider a simplified optical imaging system as shown in the following figure, where A_c is the projected area of the cell; A_i is the area of the cell image on the CCD array; Ω_c and Ω_i are solid angles of the camera lens with respect to the cell and its image, respectively; d_c and d_i are the object and image distances from the lens; and D is the diameter of the lens aperture.

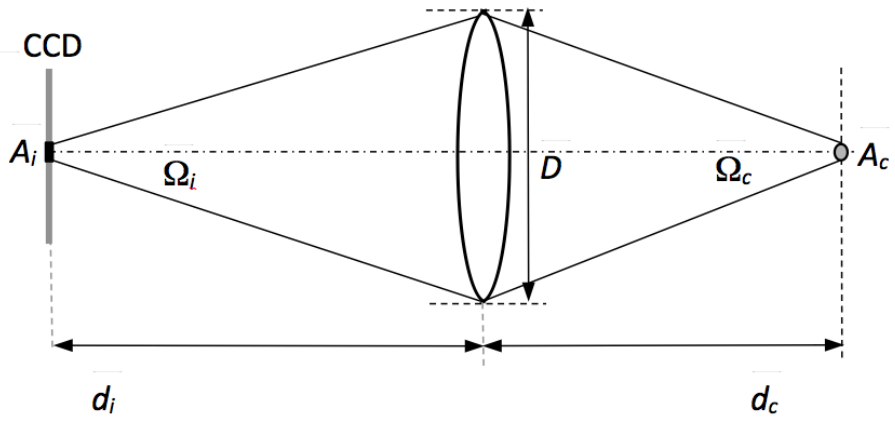

Figure S4. 3 Simplified optical configuration of the cell imaging system

Also we denote the focal length as f, the f-stop number of the lens as f/#, and the image magnification as m. For the simplified lens configuration, we have

$$m^2 = \left(\frac{d_i}{d_c}\right)^2 = \frac{A_i}{A_c}. \qquad \text{Equation S.4. 1}$$

$$\frac{1}{f} = \frac{1}{d_c} + \frac{1}{d_i} \qquad \text{Equation S.4. 2}$$

$$f/\# = \frac{f}{D} \qquad \text{Equation S.4. 3}$$

Denoting the power emitting by a cell as E_c (watt), then the radiance from the "point" source per solid angle is

$$L_c = \frac{E_c}{4\pi A_c} \qquad \text{Equation S.4. 4}$$

with a unit of (W m^{-2} sr^{-1}), where 4π is the solid angle of a unit sphere. In the air, the radiance and the product of $A\Omega$ (or the throughput) is conserved, so we have

$$L_i = L_c \quad \text{and} \quad A_c\Omega_c = A_i\Omega_i \qquad \text{Equation S.4. 5}$$

Therefore, the total radiation flux per unit area to the CCD image plane is

$$L_i\Omega_i = \frac{L_c\Omega_c A_c}{A_i} = \frac{L_c\Omega_c}{m^2} \qquad \text{Equation S.4. 6}$$

also we have

$$\Omega_c \approx \frac{\pi D^2}{4d_c^2} \qquad \text{Equation S.4. 7}$$

Substituting equations (2), (3), (4) and (7) into (6), and removing D, $L_c$and f, we have

$$L_i\Omega_i = \frac{\pi L_c}{4(1+m)^2(f/\#)^2} = \frac{E_c}{16(1+m)^2(f/\#)^2 A_c^2} \qquad \text{Equation S.4. 8}$$

Then the total irradiance energy that is received by the CCD can be derived from (1)~(5), that is,

$$E_i = A_i L_i \Omega_i = \frac{m^2}{16(1+m)^2(f/\#)^2} E_c \qquad \text{Equation S.4. 9}$$

With the estimation of the total irradiance to the CCD, the brightness of the cell image can be evaluated given the emission spectrum of the GFP and the quantum efficiency (Q_E) and A/D conversion relation of the CCD. The image brightness is largely determined by the electrical current resulting from the photoelectric conversion, it can be conveniently calculated by the spectral responsivity (R_λ) of the CCD, which is related to the quantum efficiency as

$$R_\lambda = \frac{e}{hc}\lambda Q_E \qquad \text{Equation S.4. 10}$$

where λ is the wavelength, e is the elementary charge, h is the Planck's constant and c is the speed of light in a vacuum space. The spectral distribution of Q_E can usually be obtained from the CCD's manufacturer.

Define the emission spectrum of the GFP at a certain excitation state as ρ_E, and it is normalized such that

$$\int \rho_E d\lambda = 1.0 \qquad \text{Equation S.4. 11}$$

The emission spectrum of GFPuv *E. coli* used in this study has been determined with a Hitachi F-4500 Fluorescence Spectrophotometer with different excitation wavelengths. We also found the peak absorption of GFPuv is 399 nm, and the total emission is several times higher than that under 473 nm (the laser used in the presented system).

Therefore the current generated by the CCD can be given as

$$\boxed{I_{CCD} = \int_{\lambda_{LP}}^{\lambda_{IR}} R_\lambda \rho_E d\lambda = \frac{m^2 E_c}{16(1+m)^2(f/\#)^2}\frac{e}{hc}\int_{\lambda_{LP}}^{\lambda_{IR}} \lambda Q_E \rho_E d\lambda} \qquad \text{Equation S.4. 12}$$

where λ_{LP} is the cutoff wavelength of the long-pass optical filter employed for the fluorescence imaging, and λ_{IR} is the cutoff wavelength of the infrared filter built in the CCD camera. Denoting the exposure time (the integration time of CCD) as t_E, the digital output of the CCD reading, which represents the "brightness" of the image, can be approximated as

$$B_{CCD} = CI_{CCD}t_E = E_c t_E \frac{\mathrm{m}^2}{16(1+\mathrm{m})^2(\mathrm{f}/\#)^2} \frac{\mathrm{e}}{\mathrm{hc}} C \int_{\lambda_{LP}}^{\lambda_{IR}} \lambda \mathrm{Q_E} \rho_E \mathrm{d}\lambda \qquad \text{Equation S.4. 13}$$

where the proportionality *C* combines effects of the capacitance of the CCD and the camera's A/D conversion electronics, i.e., the conversion of the electrical charge to a digital reading.

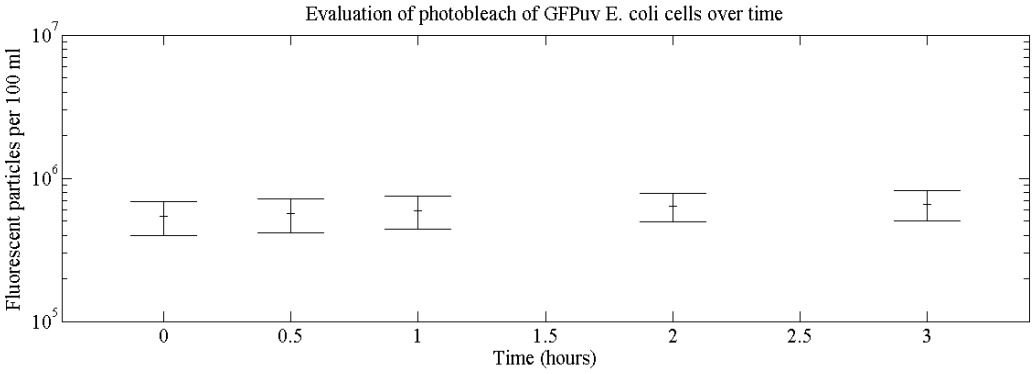

Figure S4. 4 Fluorophore photobleach assessment. Five hundred images were acquired at every time interval (*t* = 0, 0.5, 1, 2, and 3 hours) and concentration of FP was assessed. A t-test ($p<0.001$) showed that concentration of FP did not present statistically significant change over time, suggesting that fluorophore photobleach was below level detection for the extent of 3 hours. The source of water is Lake Michigan. Each data point corresponds to 500 measurements.

CHAPTER 5

QUANTITATIVE ANALYSIS OF THE ATTACHMENT OF FECAL INDICATOR BACTERIA TO SEDIMENT PARTICLES IN A SHEARED FLUID

5.1 ABSTRACT

Attachment of a model organism (green fluorescent protein (GFPuv)-labeled *Escherichia coli)* to environmental sand particles was investigated in a laboratory model simulating mixing processes in natural surface waters. Percent of bacterial attachment to sand particles was determined by the reduction in cell concentration in the water column measured experimentally at a given time.

This study shows that percent attachment of bacteria to sand particles increases with increasing mixing time and decreases with decreasing absolute value of Δ zeta potential between bacteria and sand particles. Attachment also increases with concentration of sand particles and increased ionic strength. We found attachment of bacteria to particles increases with increasing shear rate up to 31 s^{-1}, at which point attachment decreases with increasing shear rate due to decreasing collision efficiency (α). An indirect measurement of rate of aggregation (k_a) was performed following Smoluchowski's rectilinear model. The rate of aggregation of bacteria to sand particles in this study was overestimated by 1 order of magnitude by O'Melia and Tiller's model (which is a derived rectilinear model) and underestimated by 8 orders of magnitude by the curvilinear model. Collision efficiency (α) determined in this study was found to be comparable to α found in a lake containing low calcium content. This study is expected to provide insight into attachment of bacteria to particles under conditions found in the swash zone of a Lake Michigan beach.

5.2 INTRODUCTION

When moving particles in the water column come into contact with each other and attach to each other, this process is designated aggregation or coagulation. Aggregates are believed to be the main vehicles for vertical material transport in the marine environment (Kiorboe 1997; Kiorboe 2001; Zimmermann-Timm 2002; Gardes et al. 2011). This becomes extremely relevant especially at the beach environment where potentially infectious bacteria may attach to sediment particles in the swash zone and/or surf zone under certain environmental conditions. These bacteria can also detach from these particles under other conditions, with particles becoming intermittently a source or a sink. Although some research has been published on attachment of

bacteria to particles (Griffith et al. 1990; Fries et al. 2006) or detachment of bacteria from particles(Jamieson et al. 2005; Cho et al. 2010; Russo et al. 2011), conditions in which fecal indicator bacteria (FIB) attach or detach from particles in a beach environment are not fully understood. Aggregation processes and collision mechanisms can be quantified by collision efficiency (α) and collision frequency (β) which have been studied by scientists from different fields in laboratory experiments (Johnson et al. 1196; Camp et al. 1943; Swift et al. 1964; Ven et al. 1977; Han et al. 1992; O'Melia et al. 1993; Logan et al. 1995; Jiang et al. 1996; Veerapaneni et al. 1996; Li et al. 1997; Serra et al. 1997; Serra et al. 1999; Thomas et al. 1999; Li et al. 2002), marine environments (Eisma et al. 1991; Kiorboe 1997; Atteia 1998; Kiorboe 2001; Jahmlich et al. 2002; Sterling et al. 2005), rivers (Zimmermann-Timm 2002) and lakes (Ali et al. 1985; Weilenmann et al. 1989). Collision efficiency and collision frequencies have not been studied between bacteria and environmental sand under conditions representative of a freshwater beach environment.

Collision mechanisms responsible for aggregation comprise perikinetic aggregation (Brownian motion), differential settling (sedimentation) and orthokinetic aggregation (turbulent fluid shear) (Elimelech et al. 1995). Aggregation can be partitioned into three main processes: 1) particles must come in close contact (encounter); 2) they must collide (contact); and 3) they must stick together (stickiness) (Hill et al. 1990). The processes of physicochemical aggregation and deposition comprise two separate and sequential steps, a transport step followed by attachment step. Particle transport depends on physical processes such as hydrodynamics and external forces (e.g., gravity) (Adler 1981; O'Melia et al. 1993) and chemical processes such as chemistry of the aqueous phase and by the surface chemical properties of the two solids involved (McEldowney et al. 1986; O'Melia et al. 1993; Ong et al. 1999). Aggregation models are derived from the

classic Smoluchowski model (Smoluchowski 1917). In the Smoluchowski model, the collision efficiency (α) is considered to be unity for all collisions. This assumption ignores the effects of all short-range forces between approaching particles, such as electrostatic repulsion, van der Waals attraction, or hydrodynamic interactions, on collision efficiency (O'Melia et al. 1993; Sterling et al. 2005). Reviews of this and other aggregation models have been reported elsewhere (Atteia 1998; Thomas et al. 1999). Rectilinear models, such as the Smoluchowski model, ignore hydrodynamic retardation effects on α and curvilinear models account for these effects through correction factors.

In this study we present the assessment of attachment of bacteria to environmental sand particles added to Lake Michigan water. Experiments were performed in a laboratory model that simulates mixing processes in natural surface aquatic systems. Assessment of percent attachment was performed by measuring concentration of a modeled organism (GFPuv-labeled *Escherichia coli*) in the water column in different stages of the experiment with both the standard method protocol and with an optical system developed in our lab (Silva et al.__). The percent attachment of bacteria to particles was investigated varying several variables, such as turbulent kinetic energy (TKE) dissipation rate, concentration of sand particles, mean diameter and zeta potential of environmental sand, time of mixing, and ionic strength. Measured rates of aggregation under certain experimental condition were estimated by the Smoluchowski model and compared to predicted results obtained by a derived rectilinear model (O'Melia et al. 1993) and a curvilinear model (Han et al. 1992).

5.3 EXPERIMENTAL SECTION

GFPuv *E. coli* culture preparation and detection and quantification of the cells with standard cell count protocol and the optical system

Host cells of *E. coli* strain JM 109 (Promega, Madison, WI) were transformed with the pGFPuv vector (BD Bioscience, San Jose, CA) containing green fluorescent protein (GFP) and ampicillin resistance gene as described elsewhere (Silva et al.__). *E. coli* cells containing the GFP plasmid were cultivated in LB broth supplemented with 100 μg/mL ampicillin and 100 μM IPTG at 37ºC, shaking at 160 rpm for 16 h. Detection and quantification of GFPuv *E. coli* was performed with the standard cell count protocol. The standard cell count method consists of a plate culture method. Aliquot of sample collected from the beaker was properly diluted with sterile water and filtered through a 0.45 μm pore size 47 mm nitrocellulose filter and placed on LB/amp/IPTG plates and taken to a 37°C incubator for 24 h. Plates were placed under the UV light source and fluorescent colonies were counted. It was also performed with the optical system developed in our lab (Silva et al. __).

Attachment of bacteria to particles experimental protocol

These experiments were performed to determine bacterial attachment to particles under different conditions. The water sample (199 mL) was stirred with a digital mixer (50006-00, Cole-Parmer, IL) for 10 min at the rpm in which transport experiments would be conducted, varying from 300 rpm to 1100 rpm. Samples were then rested for 10 min before acquisition of 100 images at five equally vertically spaced coordinates in the beaker. This step was performed to ensure thorough mixing of sand particles. The concentration of bacteria measured at this step was considered the initial concentration ($n_b(0)$). One mL of the appropriate dilution of GFPuv *E. coli* cells was then

added to the source water in the beaker. Samples were stirred for 1h to 3h, according to each experiment, at the same rpm applied in step 1 and then rested for 10 min before acquisition of images, to avoid image motion blur caused by the residual motion of the stirred water. The concentration of bacteria measured at this step was considered the concentration at a given time ($n_b(t)$). Concentration of bacteria was also verified with the standard method protocol. Sample was collected only after measurements with the optical method to avoid disturbance of the fluid.

Estimation of GFPuv *E. coli* cell radii

GFPuv *E. coli* cells were prepared as described previously and a drop of the culture was observed with a Nikon TiE inverted microscope, equipped with a Roper Scientific Coolsnap FX monochrome digital camera and the Nikon EZC1 software. Total magnification was 400X. The length (L) and width (W) of the cells were determined using the Nikon EZC1 software. The equivalent cell radii (R) was determined as shown in Equation 5.1 (Haznedaroglu et al. 2008) :

$$R = \sqrt{\frac{LxW}{\pi}} \qquad \text{Equation 5. 1}$$

Environmental sands characterization

Grain size distribution was determined by placing the environmental sand samples in aluminum bowls and oven dried for 24 h at 110 °C, the oven dried samples were place in a stack of sieves (75-µm, 106-µm, 150-µm, 250-µm, 425-µm, 850-µm, 2-mm, and 4.75-mm), and then the stack was placed in a mechanical shaker for 10 min and the fraction of sample retained on each sieve was weighed on an electronic scale to nearest 0.01 g. The median diameter (d_{50}) of the particle size distribution was determined for each sample of sand.

Sand was pulverized and then suspended in the water source utilized on each experiment. The electrophoretic mobility of the bacterial cells and the environmental sand samples was measured using a zetasizer analyzer (Malvern Instruments). The Smoluchowski equation was selected to convert electrophoretic mobility values into zeta potentials.

Measurement of turbulent kinetic energy (TKE) dissipation in the modeled system

The particle image velocimetry (PIV) system used to measure TKE consisted of green laser (Solo 200XT PIV, New Wave Research), which provided frequency-doubled (k=532 nm) pulsed emissions of up to 20 mJ/pulse, and a pulse duration of approximately 5 ns. The time delay Dt between the two successive pulses was chosen to be 4 ms. A cylindrical lens collimated the laser light to a sheet of approximately 1-mm thickness at the measurement regions. The laser sheet was perpendicular to the axes of the helices, and images were taken from below, via a mirror inclined at 45°. A CCD camera (Imperx IPX-4M15-L) was used for recording the particle images. The CCD chip has an image plane measuring 15.15 mm (horizontal·vertical), and each pixel is square with side length 7.4 μm. The field-of-view of PIV images was set as 165·130.7 mm (lx·ly) for the flow measurement. A Nikon 105-mm manual lens with f#=2.8 was attached to the CCD camera with a bandpass filter at 522 ± 5 nm. Custom MATLAB code was used for the image recording; time synchronization control between the laser, and the CCD camera; and subsequent data processing. The velocity vectors were calculated using a 32·32- pixel interrogation window with adjacent windows overlapping by 50%. Velocity profiles were obtained from PIV analysis. Turbulent kinetic energy dissipation rate was calculated as published elsewhere (Liao et al. 2009).

Characterization of particle associated GFPuv *E. coli* by filtration

Subset of experiments was performed to determine both the percentage of bacteria attached to particles that remain most of the time on the bottom of the beaker and percentage of bacteria attached to particles that settle within 30 min after stopping transport experiments. A Laser In-Situ Scattering and Transmissometry (LISST-100X, Sequoia Scientific, Bellevue, WA) was used to asses particle size-distribution (PSD) of the particles present in the water column. LISST has the capability of determining volume concentration of particles sizes between 1.25 to 250 µm, totaling 32 class sizes. Therefore, number concentration of suspended particles was determined before and after stopping the stirrer following 3 hours of mixing time between bacteria and sand particles (d_{50}=366 µm) at G=31s^{-1} (conditions in which larger percentage of bacteria attached to particles was determined) and (b) percentage of GFPuv *E. coli* cells associated with particles in both cases. Transport experiments were prepared in as similar fashion as described previously. Just before stopping the mixer, water samples were collected from the water column in the beaker by introducing a pipette at or above mid height, trying to avoid the walls and the paddle, while the mixer was turned on, since root mean square (RMS) of the vertical velocity component are higher closer to these regions (data not shown). Samples were also collected from the water column while the mixer was turned off and rested for 10 min. Samples collected from the beaker were transferred to the horizontal chamber of the LISST. A stirrer plate was placed underneath of the chamber and a magnetic stirrer was placed inside. This way, most of the particles were kept suspended in water during the measurements of particle size. Duplicate samples were each filtered through 47- mm-diameter 0.45 µm mixed esters of cellulose filters (Millipore, Billerica, MA) for determination of bacteria concentration by using the standard method. The particle analyses were conducted on 50 mL samples collected before and after stopping the mixer. The

LISST-100X was set with full path mixing chamber for bench work and a minimum of 20 readings were averaged per water sample.

Visualization of GFPuv *E. coli* coating the surface of the sand

GFPuv *E. coli* culture was prepared as described in a previous section. Experiments were performed as described previously. When transport experiments were finished, water was removed very carefully from the beaker by positioning a pipette on the internal wall of the beaker and pipetting the liquid out very slowly. Sand grains were collected with a bulb pipette from the inner layer of sand and transferred to microscope slides, which were observed with the microscope as described in a previous section. Images were acquired using GFP filter and bright field (BF) of the same field of view (FOV).

Calculation of % attachment of bacteria to sand particles (% Attachment bs)

The percentage of attachment of bacteria to sand particles was calculated as shown in Equation 5.2. Results obtained by both the standard method and the optical method were compared.

$$\%\ Attachment_{bs} = \left(1 - \frac{n_{b(t)}}{n_b(0)}\right) * 100 \qquad \text{Equation 5. 2}$$

Calculation of collision efficiency (α) and collision frequency function (β)

The classical aggregation theory was first proposed by Smoluchowski in 1917(Smoluchowski 1917) and assumes that particles were in laminar shear field. Because experiments are carried under turbulent conditions, Smoluchowski derived values of β for different transport mechanisms: perikinetic aggregation (due to Brownian motion), differential sedimentation

(differences in settling velocities of individual particles), and orthokinetic aggregation (due to shear flow). In this study we will focus only on orthokinetic aggregation, which was the predominant mechanism under the experimental conditions.

Aggregation is primarily a kinetic phenomenon. The rate of aggregation for a monodisperse suspension can be determined as (O'Melia et al. 1993):

$$\frac{dn}{dt} = -k_a n^2 \qquad \text{Equation 5. 3}$$

where

n is the number concentration of particles in suspension at time t

k_a is a second order rate constant with dimensions [L^3/T] that is a function of physical and chemical properties of the system

For aggregation k_a can be written as (O'Melia et al. 1993):

$$k_a = \alpha\beta \qquad \text{Equation 5. 4}$$

where

β is a mass transport coefficient with dimensions [L^3/T]

α is a dimensionless sticking coefficient. It is called collision efficiency and represents the fraction of successful collisions

Our system is a heterodisperse solution (bacteria and sand particles). Therefore, Equation 1 becomes:

$$\frac{dn_b}{dt} = -k_a n_b n_s \qquad \text{Equation 5. 5}$$

Where dn_b/dt is the ratio of attachment of bacteria to particles, n_b is the number concentration of bacteria and n_s is the number concentration of sand particles, assuming uniform sand particles of the mean size diameter (d_{50}). This equation also assumes that coalescence of bacteria is negligible; therefore there is no formation of bacterial aggregates.

Combining Equation 2 and 3, it leads to Equation 5. 6:

$$\frac{dn_b}{dt} = -\alpha\beta n_b n_s \qquad \text{Equation 5. 6}$$

Rearranging Equation 5.6 leads to:

$$\frac{dn_b}{n_b} = -\alpha\beta n_s dt \qquad \text{Equation 5. 7}$$

Integrating Equation 5.7 and taking the inverse of the logarithm leads to:

$$n_b(t) = n_0 e^{-\propto\beta n_s t} \text{ Equation 5. 8}$$

Replacing Equation 5.8 into Equation 5.6 and multiplying by (-1), it becomes:

$$ln\frac{n_0}{n_b(t)} = \alpha\beta n_s t \qquad \text{Equation 5. 9}$$

With the intent of comparing results obtained experimentally with values predicted by three other selected models, namely rectilinear model, curvilinear model and O'Melia and Tiller model, a series of points were therefore matched for different values of $ln\frac{n_0}{n_b(t)}$ and *t*. Using Equation 5.9, the slope (m) of $ln\frac{n_0}{n_b(t)}$ vs. *t* was determined as:

$$m = \alpha\beta n_s \qquad \text{Equation 5. 10}$$

The calculation of α was performed by using Equation 5. 11, which is for aggregation for a heterodisperse suspension (suspension containing particles of more than one size), Smoluchowski's description of the kinetics aggregation can be written as follows:

$$\frac{dn_k}{dt} = \frac{1}{2}\sum_{i+j=k} \alpha(i,j)\beta(i,j)n_i\, n_j - n_k \sum_{all\ i} \alpha(i,j)\beta(i,k)n_i \quad \text{Equation 5. 11}$$

Where the subscripts i, j, and k refer to number concentration of particles i, j, and k, respectively, β(i,j) and β(i,k) are collision frequency functions between particles of the size classes indicated, and α(i,j) and α(i,k) are corresponding collision efficiencies.

Assuming no aggregation between bacteria and no aggregation between sand particles, the first term on the right hand side of Equation 5.11 can be dropped, which leads to Equation 5.12:

$$\frac{dn_b}{dt} = -n_b(0)\alpha(b,s)\sum_{all\ s} \beta(b,s)n_s \quad \text{Equation 5. 12}$$

Where:

$\beta(b,s)$ is the summation of the collision frequencies between bacteria and particles of mean particles diameter of all size classes of sand

d_b is the mean equivalent diameter of bacteria

d_s is the mean diameter d_{50} of sand particles in a given size class

$n_b(0)$ are the number concentration of bacteria measured at the beginning of the transport experiments

t – mixing time (s)

G- average shear rate (s^{-1})

As proposed by Camp and Stein (Camp et al. 1943), averaged shear rate here $\overline{G}$ can be inserted in place of G, where $\overline{G}$ is the mean velocity gradient for the whole system and ϵ is the average energy dissipation for the whole system (Camp et al. 1943):

$$\overline{G}=\sqrt{\frac{\epsilon}{\nu}} \qquad \text{Equation 5. 13}$$

Where ν is the kinematic viscosity of the fluid ($=\mu/\rho$, where ρ is the density) and ϵ is the turbulent kinetic energy dissipation [L^3/T^2].

The collision frequency function (β) was calculated from β_{rec} (Table 5.1). The left hand side of Equation 5.11 was estimated experimentally by multiplying the slope in Equation 5.9 times n_b, according to Equation 5.6. Value of α was then selected such that the observed and the calculated results were in agreement.

Table 5.1 presents the summary of equations utilized to calculate collision efficiency (α) and collision frequency (β) following other models.

Table 5. 1 Equations used to calculate collision efficiency (α) and collision frequency (β)

Model	Collision efficiency (α)	Collision frequency (β)
Rectilinear(Serra et al. 1999)	$\alpha_{rec} = \frac{ln\left(\frac{n_0}{n_b}\right)}{\frac{1}{6}Gt\ \sum_{all\ s}(d_b + d_s)^3\ n_s}$	$\beta_{rec} = \frac{1}{6}G\sum_{all\ s}(d_b + d_s)^3$
Curvilinear(Serra et al. 1999)	Method proposed by Han and Lawler (Han et al. 1992) [b]	$\beta_{cur} = e_{cur}\beta_{rec}$ [a]
O'Melia and Tiller(O'Melia et al. 1993)	$\alpha_{O-T} = \frac{\pi}{4\varphi Gt} ln \frac{n_0}{n_t}$	$\beta_{O-T} = \frac{1}{6}G\sum_{all\ s}(d_b + d_s)^3$

[a] $e_{cur} = \frac{8}{(1+\lambda)^3} exp\left[4.5 + 3.5log(\gamma) - \lambda\left(20.7 + 11.5log(\gamma)\right)\right]\ (for\ \gamma < 1)$ where $\lambda = d_i/d_j$, $\gamma = A/\left[36\pi\mu G\left(a_i + a_j\right)^3\right]$, A is the Hamaker constant assumed to be 4x10^{-20} J, and μ=0.0095 g cm^{-1} s^{-1} is the fluid viscosity

[b] $\varphi = \sum_{all\ s}\frac{4\pi}{3}(a_b + a_s)^3 n_s$[volume fraction]

5.4 RESULTS AND DISCUSSION

Characterization of bacteria and sand particles

The length of the cells was measured as 2.7 ± 0.4 μm and the width as 0.29±0.03 μm. The average equivalent radii of *E. coli* cell is therefore 0.5 μm and the average equivalent diameter is 1 μm. Zeta potential of *E. coli* cells suspended in Lake Michigan was measured as δ= -13.73 ±1.84 mV. Characterization of sands utilized in this study is presented in Table 5.2.

Table 5. 2Characterization of sand particles used in this study

Sand	Mean sand diameter (d_{50}) [μm]	Zeta potential (δ) [mV]
Environmental sand 1	366	-24.10 ±0.26
Environmental sand 2	248	-4.71 ±0.37
Pool filter sand	357	-17.23±6.01

Initial number concentration of bacteria ($n_b(0)$) was 9.76 $x10^3$ ± 2.40 $x10^1$ CFU mL^{-1} and 1.10 $x10^4$ ± 2.47 $x10^1$ fluorescent particles (FP) per mL by optical method. Total number concentration of sand particles suspended in the water column was measured by LISST. Number concentration of the remaining particles >231μm was estimated as the same as that of 231μm. Particles <250 μm correspond to 70.4% (by weight, from sieve analysis) and 99.99% in terms of number concentration suspended in the water column (from LISST data), as can be seen in Figure 5.1. In this study, we are interested on the attachment of bacteria to sand particles that settle within 10-30 min after stopping the mixer. Contribution of particles naturally present in Lake Michigan were considered negligible as the water was settled previous to experiments. Attachment of bacteria to suspended particles that did not settle within 30 min after stopping the mixer was not subject of this study.

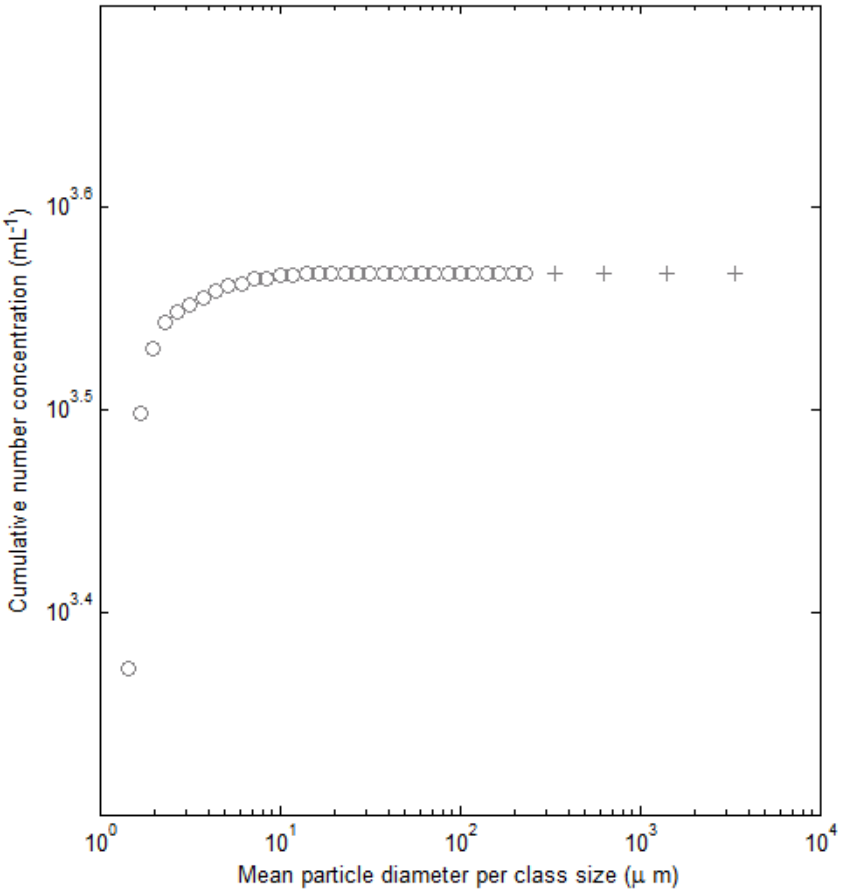

Figure 5. 1 Cumulative particle size distribution of environmental sand particles in the water column. Distribution of particles ≤ 231µm was measured by LISST (indicated by O). Number concentration was estimated for particles >231µm (indicated by +).

Percent of attachment of bacteria to sand particles

Findings from this research show attachment of bacteria to sand particles is driven by a combination of physical and chemical variables (Figure 5.2). The percent of attachment of bacteria to sand particles increased linearly with increasing shear rate up to $31s^{-1}$(Figure 5.2A). This corresponds to TKE dissipation measured in the swash zone. This suggests that increased TKE dissipation would favor attachment of bacteria to sand particles reducing the concentration of bacteria in the water column and favoring sand as a sink of bacteria. When exposed to higher

shear rates, sand starts acting as a source of bacteria as the collision efficiency (α) reduces and bacteria would be sheared off from the sand surface and being released back in the water column.

Percent of attachment of bacteria to particles increased linearly with increased concentration of sand particles (Figure 5.2B). Percent of attachment of bacteria to particles was essentially the same for environmental sand particles which mean sand diameter d_{50} is 248 μm and 366 μm (Figure 5.2C). Our experiments failed to prove the initial hypothesis that higher d_{50} would imply in significant higher bacterial attachment to particles. Percent of attachment of bacteria to particles increases linearly with increasing mixing time up to 3hr (Figure 5.2D).

Percent of attachment of bacteria to particles nearly doubled when ionic strength in terms of $CaCO_3$ M increases one order of magnitude (Figure 5.2E). In agreement with findings from other research, calcium ions act as destabilizing agents and enhance natural coagulation(Weilenmann et al. 1989). Percent of attachment of bacteria to particles decreases with decreasing absolute value of Δ zeta potential between bacteria and sand particles (Figure 5.2F). This is because repulsion forces increase when surface charges are similar.

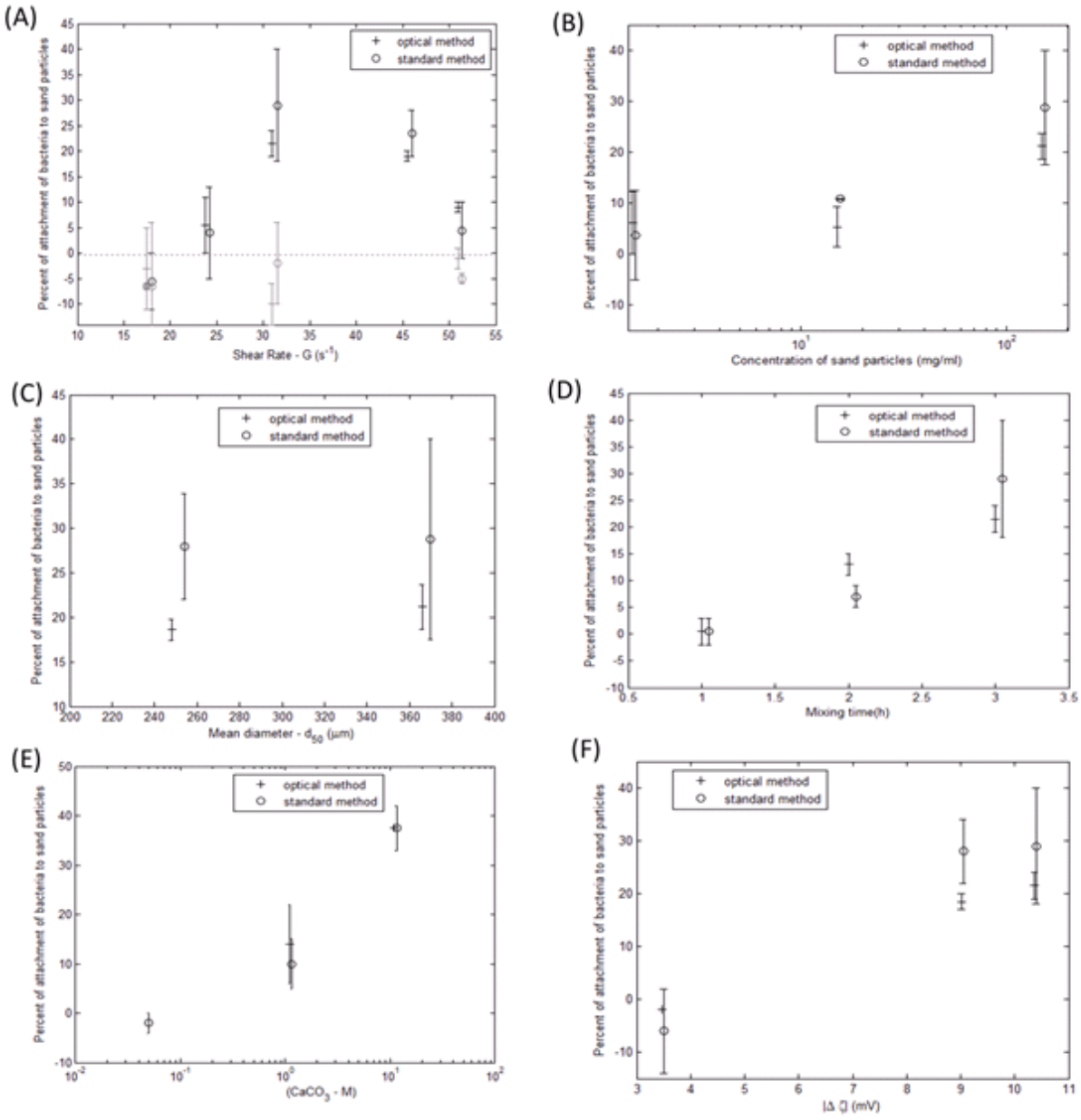

Figure 5. 2 Measurement of percent attachment of bacteria to sand particles: (A) shear rate (17, 23, 31, 42, and 51 s^{-1}); (B) concentration of sand particles (1.5, 15 and 150 mg/ml); (C) diameter of sand particles (248 µm and 366 µm); (D) mixing time (1, 2, and 3 hours); (E) ionic strength (0, 1.1 and 11 M $CaCO_3$); (F) absolute value of Δ zeta potential between bacteria and sand particles (3.47, 9.02, 10.37 mV). All experiments were submitted to shear rate of 31s^{-1} for 3hr and 150 mg/ml sand (d_{50} =366 µm), when not informed otherwise. Error bars in grey in (A) refer to control experiments (no addition of sand) performed at 17, 31, and 51 s^{-1}. Although results of standard method and optical method pertain to the same experimental conditions, there is a lag between respective error bars to facilitate reading.

Bacteria approaching a surface may show exploratory swimming behavior and decide to leave rather than attach, and some attached bacteria may detach again (Kiorboe 2001). Results of this study solely represent the scenario of percent of attachment of bacteria to particles within 10 to 30 min after stopping the transport experiments. Ten minutes after the transport experiments is when images start to be acquired and it takes 20 minutes to acquire 100 images on each of the five vertical coordinates in the beaker.

Determination of collision efficiency (α)

Collision efficiency (α) was determined as described in a previous section. Collision frequency (β) is 2.15×10^{-1} $cm^{-3}s^{-1}$ when considering both all particles suspended in the water column or only particles larger than 6.14 μm. In both cases, when considering the slope to have intercept non-zero, $\alpha\beta n_s$ is 3×10^{-5} s^{-1} and α=6 $\times 10^{-3}$. It may be possible to obtain more accurate value when forcing intercept to zero. By forcing intercept to zero, the term $\alpha\beta n_j$ equals to 2×10^{-5} s^{-1} (Figure 5.3). As the percent of attachment of bacteria to particles is below level detection at t=10, 20, and 30 min (data not shown), the assumption that the intercept is zero is reasonable. In that case, collision efficiency (α) is estimated to be 4×10^{-3}.

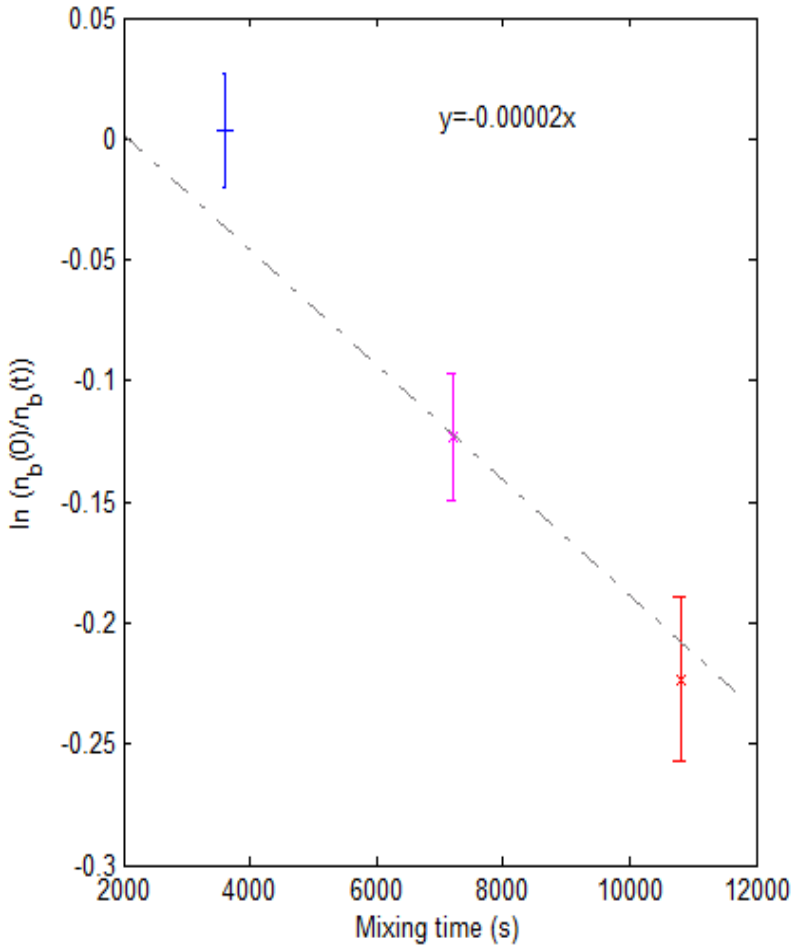

Figure 5. 3Measurements of the term $\alpha\beta n_j$ by determining the slope between ln (n_0/n_t) *vs* t.

The rate of aggregation (k_a) was obtained by diving the term $\alpha\beta n_j$ by the number concentration of sand particles (n_s). It was also calculated using curvilinear and O'Melia and Tiller coagulation models. Table 5.3 shows that k_a measured in this study is overestimated by 1 order of magnitude by the O'Melia and Tiller model and underestimated by 8 orders of magnitude by the curvilinear model.

Table 5. 3 Comparison of parameters obtained experimentally and by coagulation models for the same experimental conditions

Coagulation models	$\alpha\beta n_s$ [s^{-1}]	$\alpha\beta$ [$cm^{-3}s^{-1}$]
This study (rectilinear approach)	2.00E-05	3.69E-07
O'Melia and Tiller	1.84E-04	3.39E-6
Curvilinear	4.86E-11	8.97E-13

When compared to transport experiments performed in laboratory (Table 5.4), collision efficiency (α) is 1 to 2 orders of magnitude lower. Most of experiments listed had applied coagulants. On the other hand collision efficiency found in this study is comparable to α found in lakes comprising low calcium content (Lake Sempach) (Weilenmann et al. 1989) and inversely it is up to 1 order of magnitude lower when compared to lakes comprising high calcium content (Lake Zurich, Lake Luzern, and Lake Greifen) (Weilenmann et al. 1989).

Table 5. 4Measurements of collision efficiencies (α) in transport experiments or in the field

Coagulant	Colloid	Other particles	Collision efficiency (α)	Researcher
NaCl	polystyrene latex		0.364	Swift and Friedlander (1964)
NaCl	polystyrene latex		0.344-0.448	Birknen and Morgan (1968)
Al (III)	Silica		0.011	Hahn and Stumm (1968)
NaCl	clays		0.012-0.12	Edzwald , Upchurch, and O'Melia (1974)
Synthetic sea water	clays		0.02-0.15	Edzwald , Upchurch, and O'Melia (1974)
Synthetic sea water	estuarine sediments		0.05-0.22	Edzwald , Upchurch, and O'Melia (1974)
Ca^{+2}	Al_2O_3		0.01-0.063	Osman-Sigg (1982)
Filtered lake water	Al_2O_3		0.086	Osman-Sigg (1982)
polymer coagulant	Bacterial aggregates made from activated sludge supernatant from WWTP	latex microspheres (0.49μm)	$\alpha_{rec}=\alpha_{curv}=0.5$ (estimated)	Serra and Logan (1999)
NaCl	Red-dyed latex beads	latex microspheres (0.49μm)	α_{rec} = 0.769 and $\alpha_{curv}=0.719$	Serra and Logan (1999)
Lake Zurich[1]	natural particles		0.054-0.13	Weilenman, O'Melia and Stumm (1989)
Lake Sempach[1]	natural particles		0.005-0.019	Weilenman, O'Melia and Stumm (1989)
Lake Luzern[1]	natural particles		0.055	Weilenman, O'Melia and Stumm (1989)
Lake Greiffen[1]	natural particles		0.047	Weilenman, O'Melia and Stumm (1989)
Settled Lake Michigan water	planktonic *E. coli*	environmental sand	0.004	This study
Settled Lake Michigan water	planktonic *E. coli*	pool filter sand	<0.0001	This study

[1] Measurements of α were performed in samples collected in the field.

Evidence of bacteria coating the sand grains

The method applied in this study to measure rate of attachment of bacteria to sand particles assumes that the loss of concentration of cells in the water column implies that they attach to sand particles. Figure 5.4 shows images of sand grains observed with the microscope after completion of transport experiments. We can see that bacteria are coating the sand surface. These images are unable to provide information about adsorption or absorption of bacteria to sand surface.

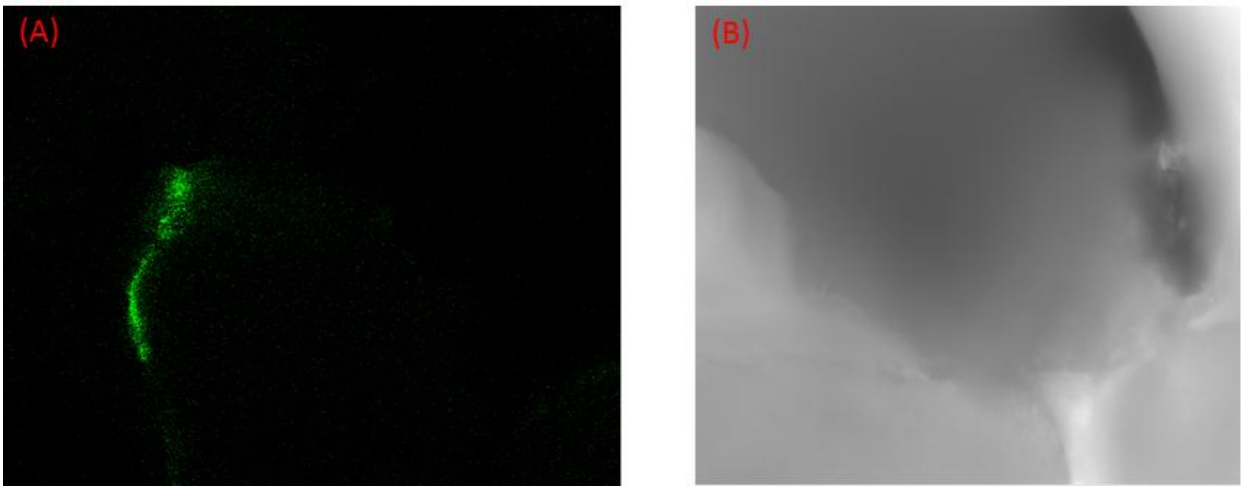

Figure 5. 4 Sand grains collected from the bottom of the beaker after transport experiments observed with the microscope with GPF filter (A) and BF (B).

GFPuv *E. coli* associated with particles that settle within 30 min after transport experiments

In order to determine the percentage of attachment of bacteria associated with finer particles (<231 μm) suspended in the water column and that get settled within 30 min after stopping the mixer, further investigation was performed. Transport experiments were performed under the following conditions: environmental sand (d_{50}: 366 μm), mixing time: 3 hours, lake water, G=

$31s^{-1}$, initial total mass concentration of sand of 150 mg/ml. The best attachment of bacteria to particles was obtained experimentally in this study under these conditions.

Concentration of bacteria in the water column was measured using the LISST instrument at the beginning of the experiment and before and after stopping the mixer. By the end of the 3 hours mixing time, and just before stopping the mixer, 12% of cells were missing in the water column; therefore they were associated with larger particles that were on the bottom of the beaker. After stopping the mixer and waiting for the 10 min of resting time, 23% more of the cells were missing in the water column and therefore associated with larger particles that were suspended in the water column and settled when the mixer was stopped. A total of 35% of cells were therefore associated with particles that were suspended in the water column and settled within 10 - 30 min after stopping the mixer. The remaining amount of cells persisted in the water column.

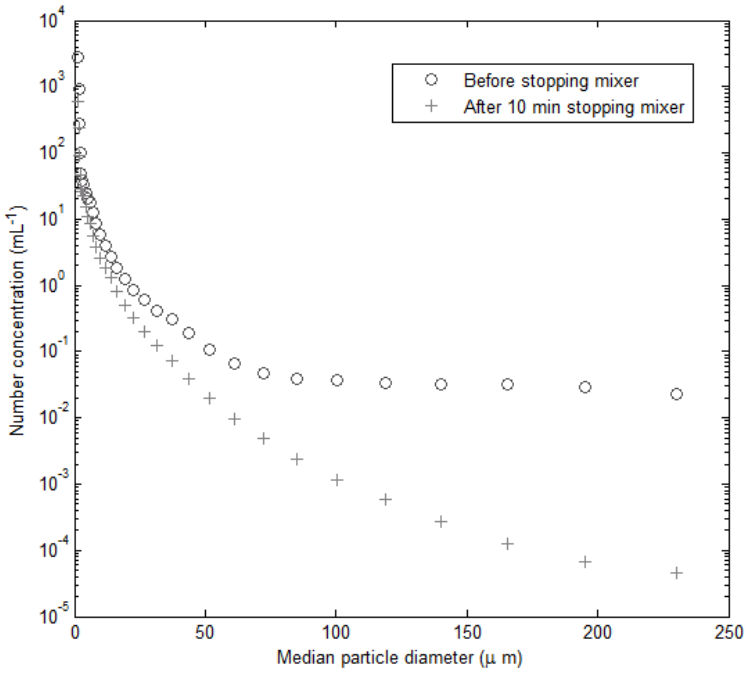

Figure 5. 5 Particle size distribution (PSD) of particles suspended in the water column after 3 hours mixing bacteria and sand particles (d_{50}=366 µm) at G=$31s^{-1}$ just before stopping the mixer and 10-30 min just after. Particles larger than >6.14 µm settle at least one order of magnitude in terms of number concentration.

Environmental implications

Findings from this research suggest that waters with higher concentration of finer sands that can get resuspended in the water column under shear flow are more likely to work as a sink of bacteria because they contribute to collisions that may result in orthokinetic aggregation. In addition, extended periods of high winds or waves increase the likelihood of bacteria transport due to shear. Our results also indicate waters with higher calcium content provide a more favorable environment for attachment of bacteria to sand particles. The percent attachment nearly doubles with an increase of one order of magnitude in molarity in terms of calcium content.

Our results also provide insight of one more mechanism of source and sink of bacteria in the swash zone. Our results indicate that attachment of bacteria to environmental sand particles increases with increasing turbulent kinetic energy dissipation up to 9.55×10^{-4} m^2/s^3. Beyond that point, collision efficiency (α) reduces with increasing collision frequency (β) and bacteria is sheared off from the sand surface returning back to the water column. That could explain why high levels of bacteria are found to increase in the swash zone with no clear point source of pollution, especially in windy or wavy days.

5.5 ACKNOWLEDGMENTS

This work was made possible through a UWM Graduate School Dissertation Fellowship Award. We thank Jessica VandeWalle and William Hutchins for assistance with lab arrangements. We thank Jianen Xiao for assistance with measurements of TKE dissipation rate. We acknowledge the support provided by the NIEH CEHSCCenter (Grant # ES004184-24) for use of microscope facility.

5.6 REFERENCES

Kiorboe, T., Formation and fate of marine snow: small-scale processes with large-scale implications. *Scientia Marina* **2001,** 65, (2), 57-71.
Kiorboe, T., Small-scale turbulence, marine snow formaiton, and planktivorous feeding. *Scientia Marina* **1997,** 61, (1), 141-158.
Gardes, A.; Iversen, M. H.; Grossart, H.-P.; Passow, U.; Ullrich, M. S., Diatom-associated bacteria are required for aggregation of *Thalassiosira weissflogii*. *International Society for Microbial Ecology* **2011,** 5, 436-445.
Zimmermann-Timm, H., Characteristics, dynamics and importance of aggregates in rivers - an invited review. *Internat. Rev. Hydrobiol.* **2002,** 87, (2-3), 197-240.
Griffith, P. C.; Fletcher, M., A model system derived from marine diatoms for investigating the activity of particle-associated bacteria. *Journal of Microbiological Methods* **1990,** 12, 65-74.
Fries, J. S.; Characklis, G. W.; Noble, R. T., Attachment of fecal indicator bacteria to particles in the Neuse River estuary, N.C. *Journal of environmental engineering* **2006,** 132, (10), 1338-1345.
Cho, K. H.; Pachepsky, Y. A.; Kim, J. H.; Guber, A. K.; Shelton, D. R.; Rowland, R., Release of Escherichia coli from the bottom sediment in a first-order creek: experiment and reach-specific modeling. *Journal of Hydrology* **2010,** 391, 322-332.
Russo, S. A.; Hunn, J.; Characklis, G. W., Considering bacteria-sediment associations in microbial fate and transport modeling. *Journal of environmental engineering ASCE* **2011,** 137, (8), 697-706.
Jamieson, R. C.; Joy, D. M.; Kostaschuk, R.; Gordon, R. J., Resuspension of sediment-associated *Escherichia coli* in a natural stream. *J. Environm. Qual.* **2005,** 34, 581-589.
O'Melia, C. R.; Tiller, C. L., Physicochemical aggregation and deposition in aquatic environments. In *Environmental Particles*, ed.; Leeuwen, J. B. a. H. p. v., 'Ed.'^'Eds.' Lewis: 1993; 'Vol.' 2, p^pp 353-386.
Serra, T.; Logan, B. E., Collision frequencies of fractal bacterial aggregrates with small particles in a sheared fluid. *Enviornmental Science and Technology* **1999,** 33, 2247-2251.
Li, X.; Logan, B., Collision frequencies of fractal aggregates with small particles by differential sedimentation. *Environmental Science and Technology* **1997,** 31, 1229-1236.
Li, X.-Y.; Yuan, Y., Collision frequencies of microbial aggregrates with small particles by differential sedimentation. *Environmental Science and Technology* **2002,** 36, 387-393.
Jiang, Q.; Logan, B. E., Fractal dimensions of aggregates produced in laminar and turbulent shear devices. *J. AWWA* **1996,** 88, (2), 100-113.
Han, M.; Lawler, D. F., The (relative) insignificance of G in flocculation. *J. Am. Water Works Assoc.* **1992,** 84, (10), 79-91.
Veerapaneni, S.; Wiesner, M. R., Hydrodynamics of fractal aggregates with radially varying permeability. *Journal of colloid and interface science* **1996,** 177, (1), 45-57.
Thomas, D. N.; Fawcett, S. J. J., Flocculation modeling: a review. *Water Research* **1999,** 33, (7), 1579-1592.
Ven, T. G. v. d.; Mason, S. G., The microrheology of colloidal dispersions VII. Orthokinetic doublet formation of spheres. *Colloid & Polymer Sci.* **1977,** 255, 468-479.
Camp, T. R.; Stein, P. C., Velocity gradients and internal work in fluid motion. *J. Boston Soc. Civ. Eng.* **1943,** 30, 219-237.

Johnson, C. P.; Li, X.; Logan, B., Settling velocities of fractal agregrates. *Environmental Science and Technology* **1196,** 30, 1911-1918.
Serra, T.; Colomer, J.; Casamitjana, X., *Aggregation and break up of particles in a shear flow* **1997,** 187, 466-473.
Logan, B. E.; Kilps, J. R., Fractal dimensions of aggregates formed in different fluid mechanical environments. *Wat. Res.* **1995,** 29, (2), 443-453.
Swift, D. L.; Friedlander, S. K., The coagulation of hydrosols by Brownian motion and laminar shear flow. *J. Colloid Sci.* **1964,** 19, 621-647.
Atteia, O., Evolution of size distributions of natural particles during aggregation: modeling versus field results. *Colloids and surfaces A: Physicochemical and Engineering Aspects* **1998,** 139, 171-188.
Sterling, M. C.; Bonner, J. S.; Ernest, A. N. S.; Page, C. A.; Autenrieth, R. L., Application of fractal flocculation and vertical transport model to aquatic sol-sediment systems. *Water Research* **2005,** 39, 1818-1830.
Eisma, D.; Bernhard, P.; Cadee, P.; Ittekkot, G. C.; Kalf, V.; Laane, R.; Martin, J. M.; Mook, W. G.; Put, V. A.; Schumacker, T., Suspended-matter particle size in some west- european estuaries. Part I. Particel size distribution. *Netherland Journal of Sea Research* **1991,** 28, 193-214.
Jahmlich, S.; Lund-Hansen, L. C.; Leipe, T., Enhanced settling velocities and vertical transport of particulate matter by aggregation in the benthic boundary layer. *Danish Journal of geography* **2002,** 102, 37-49.
Ali, W.; O'Melia, C. R.; Edzwald, J. K., Colloidal stability of particles in lakes: measurements and significance. *Water Sci. Technol.* **1985,** 17, 701-712.
Weilenmann, U.; O'Melia, C. R.; Stumm, W., Particle transport in lakes: models and measurements. *Limnol. Oceanogr.: Methods* **1989,** 34, 1-18.
Elimelech, M.; Gregory, J.; Jia, X.; Williams, R., *Particle deposition and aggregation. Measurement, modeling and simulation.* ed.; Butterworth Heinemman: Oxford, 1995; 'Vol.' p.
Hill, P. S.; Nowell, A. R. M.; McCave, I. N., The potential role of large, fast-sinking particles in clearing nepheloid layers. *Philosophical Transactions Royal Society of London* **1990,** 331(A), 103-117.
Adler, P. M., Interaction of unequal spheres I. Hydrodynamic interaction: colloidal forces. *Journal of colloid and interface science* **1981,** 84, 461-474.
McEldowney, S.; Fletcher, M., Variability of the influence of physicochemical facteros affecting bacterial adhesion to polystyrene substrata. *Applied Environmental Microbiology* **1986,** 52, (3), 460-465.
Ong, Y.-L.; Razatos, A.; Georgiou, G.; Sharma, M. M., Adhesion forces between *E. coli* bacteria and biomaterial surfaces. *Langmuir* **1999,** 15, 2719-2725.
Smoluchowski, M., Versuch einer mathematischen theorie der koagulationskinetik kolloider losungen. *Z. Phys. Chem.* **1917,** 92, 129-168.
Silva, M. R.; Liao, Q.; McLellan, S. L.; Bravo, H. R., 20__.Novel Optical-Based Method for Assessment of green fluorescent protein (GFPuv)-labeled *Escherichia coli* in modeled aqueous systems. In preparation.
Haznedaroglu, B. Z.; Bolster, C. H.; Walker, S. L., The role of starvation on *Escherichia coli* adhesion and transport in saturated porous media. *Water Research* **2008,** 42, (6-7), 1547-1554.
Liao, Q.; Bootsma, H. A.; Xiao, J.; Klump, J. V.; Hume, A.; Long, M. H.; Berg, P., Development of an in situ underwater particle image velocimetry (UWPIV) system. *Limnol. Oceanogr.: Methods* **2009,** 7, 169-184.

CHAPTER 6

CONCLUSIONS AND FUTURE WORK

Conclusions

The objective of this work was to apply an integrative approach to study the sources, fate and transport of bacteria in Milwaukee coastal beaches. This objective was completed by:

(I) Examining how stormwater outfalls, rainfall and river discharge impact the quality of the lake water at nine beaches in Milwaukee coastal area, by quantifying FIB and human *Bacteroides* in lake water and outfalls and establishing relationship with rainfall events and CSO/SSO events. (Chapter 2)

(II) Examining other possible sources of bacteria at a selected study site, including groundwater, runoff infiltrating through sand, sand matrix and standing water (Chapter 3)

(III) Examining the transport of bacteria by attachment to sediment particles at small scale (laboratory experiments) under different hydrodynamic conditions by using a non-invasive method (Chapter 4 and 5)

(IV) Examining bacteria loading and transport of bacteria in two selected study sites (Bradford Beach and Atwater Beach) at a large scale through statistical model and time series. Exploring other possible new hydrodynamic variables that could be impacting FIB concentration at the swash zone (Appendix)

The results of these investigations support the following conclusions:

(i) (1) The major source of sewage contamination at the beaches are stormwater outfalls, (2), and (2) CSOs or SSOs are not the main sources of sewage contamination in Milwaukee coastal area.

(ii) (1) The combined use of non-specific fecal indicator bacteria (*E. coli* and enterococci) together with a marker more specific indicator of human fecal pollution (*Bacteroides* HF 183 by qPCR) to assess fecal pollution in the beach environment as well as presence of sewage these tools is effective for indication of sewage. In addition, beach closings are frequently associated with bacterial contamination mainly linked to a number of point and nonpoint sources that can also be coupled to physical properties of the beach. (2) The investigation of FIB in dry versus wet conditions and the relationship between sand size and FIB both point beach managers to practical approaches to reducing FIB concentration in sand. (3) This research contributes to a better understanding of the relationship of wetting sand conditions and standing water with persistent FIB contamination. (4) This study indicates that erosion/accretion patterns of the beach could bring groundwater table closer to the ground and mild to flat beach face slope could enhance wave action, facilitating persistent local spots of wet sand in the backshore area of the

beach. (5) This study also indicates that runoff infiltrating from rain gardens at a beach can help to raise groundwater table, which could slow infiltration process and facilitate standing water conditions. (6) This is one of the first studies that indicate the health risks associated with standing water at a beach environment.

(iii) (1) The novel optical method was successful on visualization and quantification of GFPuv *E. coli* in different water sources. (2) This optical system can be sensitive enough to detect from 2.4 $x10^4$ colony forming unit (CFU) per 100 mL to 2.4 x 10^7 CFU/100 mL when 1.24 fluorescent particles (FP) to 1,191 FP per field of view (FOV) is detected on average, respectively. (3) Laboratory flume experiment was performed and visualization and quantification of fluorescent bacteria in hydraulic flume experiments have yet to be improved due to the inability of tracking fluorescent particles in turbulent flows with the limited laser power. (4) This research represents a very important step toward nondestructive monitoring systems of bacterial behavior and transport in laboratory scale systems.

(iv) Findings from this research suggest that waters with higher concentration of sands that can remain resuspended for a longer time in the water column under shear flow are more likely to work as a sink of bacteria due to increased collisions that may result in orthokinetic aggregation. In addition, extended periods of high winds or waves increase the likelihood of bacteria transport due to shear. This research indicates that waters with higher calcium content provide a more favorable environment for attachment of bacteria to sand particles. The percent attachment nearly doubles with an increase of one order of magnitude in molarity in terms of calcium content.

This study also provides insight of one more mechanism of source and sink of bacteria in the swash zone. Our results indicate that attachment of bacteria to environmental sand particles increases with increasing turbulent kinetic energy dissipation up to 9.55×10^{-4} m^2/s^3. Beyond that point, collision efficiency (α) reduces with increasing collision frequency (β) and bacteria is sheared off from the sand surface returning back to the water column. That could explain why high levels of bacteria are found to increase in the swash zone with no clear point source of pollution, especially in windy or wavy days.

(vi) Preliminary analysis of multiple linear regression models (MLR) correlating log *E. coli* and meteorological and physical variables without accounting for their transforms indicate that the main variables with higher correlation with *E. coli* concentrations in the swash zone at Bradford Beach are rainfall in the past 24 h, river discharge at Milwaukee River mouth, turbidity, and wave and wind direction. From time series this study suggests that higher concentration of *E. coli* is associated with higher concentration of suspended sediments. This study also validates in the field findings from laboratory experiments in which optimum attachment of bacteria to sediment particles were found to occur when turbulent kinetic energy dissipation is maintained nearly constant throughout the time.

Future work

The work presented in this thesis lays a foundation for a variety of multidisciplinary research. Here I will outline some ideas for future studies.

- Investigation of particle stability in Milwaukee harbor and nearshore and implications on fate and transport of particles and associated pollutants and nutrients

- Investigation of groundwater response to hydrological conditions at Bradford Beach at different locations (near the rain gardens, near the lake, in the middle of the beach)
- Spectral analysis of hydrologic process and FIB at Bradford Beach and Atwater Beach
- Bacteria transport in the sediment flume under different hydrodynamic conditions
- Entrainment of bacteria to sand under different hydrodynamic conditions
- Investigation of through beach transport at Bradford Beach at a site near the lake

APPENDIX:

COASTAL LOADING AND TRANSPORT OF FECAL INDICATOR BACTERIA AT TWO LAKE MICHIGAN BEACHES

INTRODUCTION

Fluctuation of FIB in the surf zone has been attributed to 1) sediment resuspension events (Ge et al. 2012b), which cause deposition–resuspension cycles of *E. coli*, 2) diel variability due to bacterial-dark-and-solar-related decay (Ge et al. 2012a), 3) foreshore processes and 4) submerged sand. Other studies have proposed new variables, such as bed shear stress and wave runup (Ge et al. 2010a). Characterization of sources of fecal indicator bacteria (FIB) and fluctuations of these sources in nearshore waters is of particular importance for development of water quality standards and design of monitoring programs for the protection of public health. Also, microbiological techniques recommended by EPA to measure levels of FIB in beach water usually take 18- 24 hours to generate the results. Therefore, development of a statistical model which accounts for particular physical beach features and sources of pollution may become a powerful way of anticipating conditions for beach closings.

A number of common variables have been frequently used in statistical beach models, such as *E. coli* concentration in foreshore sand and submerged sediment, bed shear stress, beach width, current, wave and wind components (Ge et al. 2010a). In this study, we assessed the main variables that have higher correlation with *E. coli* concentrations in the swash zone at Bradford Beach through multiple linear regressions. We then further explored through time series other hydrodynamic variables that could be impacting variability of FIB, such as grain size distribution of suspended sediments, turbulent kinetic energy (TKE) and turbulent kinetic energy dissipation (ϵ). Finally we assessed the net direction of FIB loading in the surf zone during dry and wet periods.

MATERIALS AND METHODS

Study sites

Bradford Beach and Atwater Beach are two urban Lake Michigan beaches located in Milwaukee, WI. Bradford Beach spans a total distance of approximately 700 m along shore and the cross shore extends 125 m from the water's edge to Lincoln Memorial Drive. Bradford Beach has seven subwatersheds that discharge through stormwater outfalls designated as O0 and O2 to O7 in Fig. A.1. These outfalls previously discharged directly onto the sand, but since June 2008 discharge to constructed rain gardens. The beach is also impacted by outfalls located north of the beach (O8 to O12), which discharge stormwater often contaminated with sewage, directly to the lake that can reach the beach through alongshore currents. Atwater Beach is located approximately 5 km north of Bradford Beach, in the Village of Shorewood. It spans a total distance of approximately 215 m along shore and the cross shore extends 45 m from the water's edge to the bluff. Atwater Beach has three groins built in early 1900s to retain sand. Because the groins are a physical obstacle, they can interfere with lake water circulation at the beach. Atwater Beach has a submerged stormwater outfall located ~ 200 m north of the beach which discharges intermittently into the lake, independent of rainfall events. From previous studies, outfalls at Bradford Beach and Atwater Beach have been found positive for human *Bacteroides*, which are sewage indicators (Silva et al. 2010).

Figure A. 1 Sampling sites at Bradford Beach (A) and Atwater Beach (B)

Collection and analysis of water samples

Lake water samples were collected at Bradford Beach 1-2 m from shore in knee-deep water (Fig.A.1-A). Samples were collected at Atwater Beach by using waders at a distance of about either 2 m or 7 m from the shoreline (Fig.A.1-B). Water samples were collected into Nalgene® polypropylene bottles, which were full-volume flushed three times with water from the sample site. All water samples were placed on ice and in darkness until filtering in the lab the same day for culture of FIB.

Each water sample was filtered through a 0.45-µm-pore-size 47 mm nitrocellulose filter and placed on modified m-TEC (Difco, Sparkes, MD) agar according to the EPA method for *E. coli* enumeration (U.S.EPA 2002a).

Hydrometeorological data collection

Daily lake water levels were obtained from station ID 9087057 operated by NOAA (http://tidesandcurrents.noaa.gov/data), located just south of Milwaukee Harbor. Daily precipitation data were obtained from the weather station operated by NOAA at the Milwaukee Mitchell Airport, located 16.7 km south of Bradford Beach. Although not as conveniently located, the station was sufficiently close to provide useful precipitation data for the study. Hourly incident wave and current parameters were provided by the NOAA Great Lakes Coastal Forecasting System (http://www.glerl.noaa.gov/res/glcfs) at the nearest model grid point, approximately 2 km from the beach. Flow discharge was obtained from USGS website (http://waterdata.usgs.gov/usa/nwis/nwis) for station ID 04087170 at the Milwaukee River mouth.

For Atwater Beach, current data was also obtained by deployment of an Acoustic Doppler Current Profiler (ADCP, Nortek Aquadopp current profiler, Nortek USA) close to the shoreline at 43°05.404' N 87°52.312' W (location indicated in Figure A.1-B; water depth approximately 1.5 m) from 7/31/09 to 08/07/09 to measure the general characteristics of the nearshore current flow. The ADCP, mounted upward looking on a bottom frame that placed the transducer 15 cm above the bed, profiled current velocity every 1 hour.

Statistical model to assess bacteria loading at Bradford Beach

Virtual Beach 2.3 (http://www.epa.gov/ceampubl/swater/vb2/) was used to build statistical models to establish relationships between *E. coli* concentration and other variables at Bradford Beach. A summary of variables used in the following statistical analyses are listed on Table A.1. It is important to note that linear regression models used here are not for prediction purposes but for identifying relationships among variables. Preliminary analysis was performed without transformation of the variables. Further investigation including the transforms of these variables may be performed.

The shoreline at Bradford Beach is oriented 37° E of north. Alongshore and onshore components of current, wind and wave data were determined based on this orientation. *E. coli* measurements were transformed for log *E. coli.* A model evaluation threshold of 235 CFU/100 ml was selected to evaluate the performance of the models. This is the EPA threshold for concentration of *E. coli* in freshwater for determination in posting advisories signs at the beaches. The best transformation in terms of the correlation (Pearson's coefficient) with the response to the variable log *E. coli* was determined. Variables or their transforms with Pearson coefficient > 0.2 were selected. Akaike Information Criteria (AIC) was used to measure the relative goodness of fit of a statistical model. To evaluate model performance, predicted vs. observed values were compared with the EPA threshold for *E. coli* and Type I (false positive) and II (false negative) errors, sensitivity, specificity, and accuracy of the models were determined.

Table A. 1 Variables used in statistical analysis performed in Virtual Beach.

Variable	Units
E. coli (average for sites BB1,BB2,BB3)	CFU/100 ml
Turbidity (average for sites BB1, BB2, BB3)	NTU
Current speed	m s^{-1}
Current direction	degrees
Wave height	m
Wave direction	degrees
Wave period	s
Lake level	m
Rainfall in the past 24h	cm
Rainfall in the past 48h	cm
Wind speed	m s^{-1}
Wind direction	degrees
River discharge	m^3 s^{-1}

Measurements of *E. coli* were performed during the summer seasons of 2008, 2009 and 2010. Samples were collected at the three sites as shown in Figure A.1-A. *E. coli* measurements were averaged per day (N=50) and used as an input parameter in the model (2008 (N=18), 2009 (N=15) and 2010 (N=17)). Turbidity at the same sample sites was measured in the lab and averaged daily for the three summer seasons (N=39). As turbidity is known as an important parameter on the impact of the water quality, the sample size used to generate the models was N=39.

Time series were performed to investigate bacteria loading and association with particle size distribution of suspended sediments, turbulent kinetic energy (TKE) and TKE dissipation (ϵ)

FIB concentration was measured hourly at Atwater Beach on 08/04/09 and 08/05/09 from 8 am to 5 pm at 10 different sampling sites as shown in Figure A.1-B. Time series were performed to evaluate the relationship between bacteria loading and grain size distribution of suspended sediments and TKE and TKE dissipation (ϵ) at the surf zone.

The occurrence of sediment resuspension is related to bed form, bed shear stress and sediment mobility. Sediment mobility can be estimated by the number concentration of suspended sediments obtained indirectly from a Laser In-Situ Scattering and Transmissometry (LISST-100X, Sequoia Scientific, Bellevue, WA). We used LISST to assess particle size-distribution (PSD) of the particles present in the water column and to estimate number concentration of suspended sediments. The particle analyses were conducted on 50 mL samples collected before and after stopping the mixer on a LISST-100X, which characterized particle sizes between 1.25 to 250 µm and calculated the total volume of each size class in the water sample. The LISST-100X was set with full path mixing chamber for bench work and a minimum of 20 readings were averaged per water sample. LISST provides results in volume concentration (VC) (µl/l). Number concentration is obtained by dividing the VC per class size by the volume of perfect spherical particles which diameter corresponds to the mean diameter of the corresponding class size.

Additional variables that are potentially important for explaining the bacteria loading are turbulent kinetic energy (TKE) and TKE dissipation (ϵ) in the surf zone. These variables can be estimated from velocity components obtained from the ADCP deployed at Atwater Beach as explained in a previous section. Equations applied to calculate these variables were:

$$TKE = \frac{1}{2}\overline{q^2} = \frac{1}{2}\int_0^T (u'^2 + v'^2 + w'^2)dt \quad \text{Equation A. 1}$$

$$\epsilon = (u'^2 + v'^2 + w'^2)^{3/2}/\mathrm{L} \qquad \text{Equation A. 2}$$

where:

u, v, w are velocity components

$\bar{u}$, $\bar{v}$, and $\bar{w}$ are mean velocity components and hence $u' = u - \bar{u}$, $v' = v - \bar{v}$, and $w' = w - \bar{w}$ are components of velocity fluctuations, respectively;

T denotes a time period that is sufficiently long to bear statistical meaning

L is the characteristic length; a typical water depth, 1.5 m, was used as this large-scale characteristic length;

ϵ – turbulent kinetic energy dissipation ($\epsilon \sim U^3/L$)

Aquadopp was set for sampling frequency of 2 Hz, which means that we lost high frequency of the velocity spectrum. The high frequency end of water turbulence, or the equilibrium range for estimating epsilon, would be 1KHZ. Therefore, in order to determine the time scale for turbulence averaging process for epsilon, we considered the length scale of 1.5 m and average current speed of 0.065 m/s; so the large time scale was determined as 0.03 s for ϵ. As we lost the high frequency part of the velocity spectrum, the large time scale for TKE is 0.03 s as well.

Sediment traps deployment and sample collection and analysis

Another way of assessing sediment resuspension and association with bacteria as well as net direction of bacteria loading and transport is through deployment of sediment traps. Sediment traps were deployed at 1 m and 2 m depths at Bradford Beach from 8/14/09 to 8/31/09 and from 8/31/09 to 19/11/09 and at Atwater Beach from 7/31/09 to 8/14/09 and from 11/15/09 to 11/30/09 at locations as indicated in Figure A.1. A six-replicate horizontal array of plastic tubes was mounted vertically on a 45 cm length of strut channel was employed. Each trap consisted of a 47 mm (I.D.) by 24 cm long piece of clear butyl styrene (1.5 mm wall thickness) core liner with a polyethylene end cap attached to the bottom of the tube, resulting in a 5:1 aspect ratio. Traps were affixed to the strut channel using a 2 inch Versa-Mount strut clamp and spaced 5 cm on center. The loaded array was then held in the water column with the open end (top) of the

traps at 0.5 m above the substrate by clamping the piece of strut to a 1m length of galvanized tubing (3 inch boat dock legs with auger-tipped foot) bored via scuba diver vertically into the sand. The tops of the traps remained open during the deployment period. Upon retrieval, a diver sealed the contents of each replicate trap by placing a poly end cap on the top of the tube before releasing it from the Versa-Mount clamp. At the same time, pre-labeled clean traps were clamped in place for the subsequent redeployment.

Twenty grams of sediment samples were diluted with 30 ml sterile water, shaked for 5 min and vortex mixed (30 s). Each water sample was filtered through a 0.45-µm-pore-size 47 mm nitrocellulose filter and placed on modified m-TEC (Difco, Sparkes, MD) agar according to the EPA method for *E. coli* enumeration (U.S.EPA 2002a), on mEI agar (Difco, Sparkes, MD) for enterococci enumeration (U.S.EPA 2002b), and on MI agar (Difco, Sparkes, MD) for total coliforms enumeration (EPA 2002; U.S.EPA 2002c). Sediment dry weights were determined by drying the sediment at 60°C for 48 hours. Bacterial counts associated with suspended sediment samples were expressed at CFU/100 g dry sediment.

RESULTS AND DISCUSSION

General results

Model A had the highest $R^2 = 0.275$ followed by Model C (0.258) and Model B and D had the same R^2 (0.256). Model C and D had the lowest Type II error (12 false negatives), followed by Model A (13 false negatives) and Model B (14 false negatives). All the models presented the same Type I error (1 false positive). More details on the models are shown on Table A.2.

All the top four models have very similar R^2. All of them consider flow at the Milwaukee River Mouth and turbidity as variables in the model. Models A and B include rainfall in the past 24 hours. B, C and D include wave direction and B and D include wind direction.

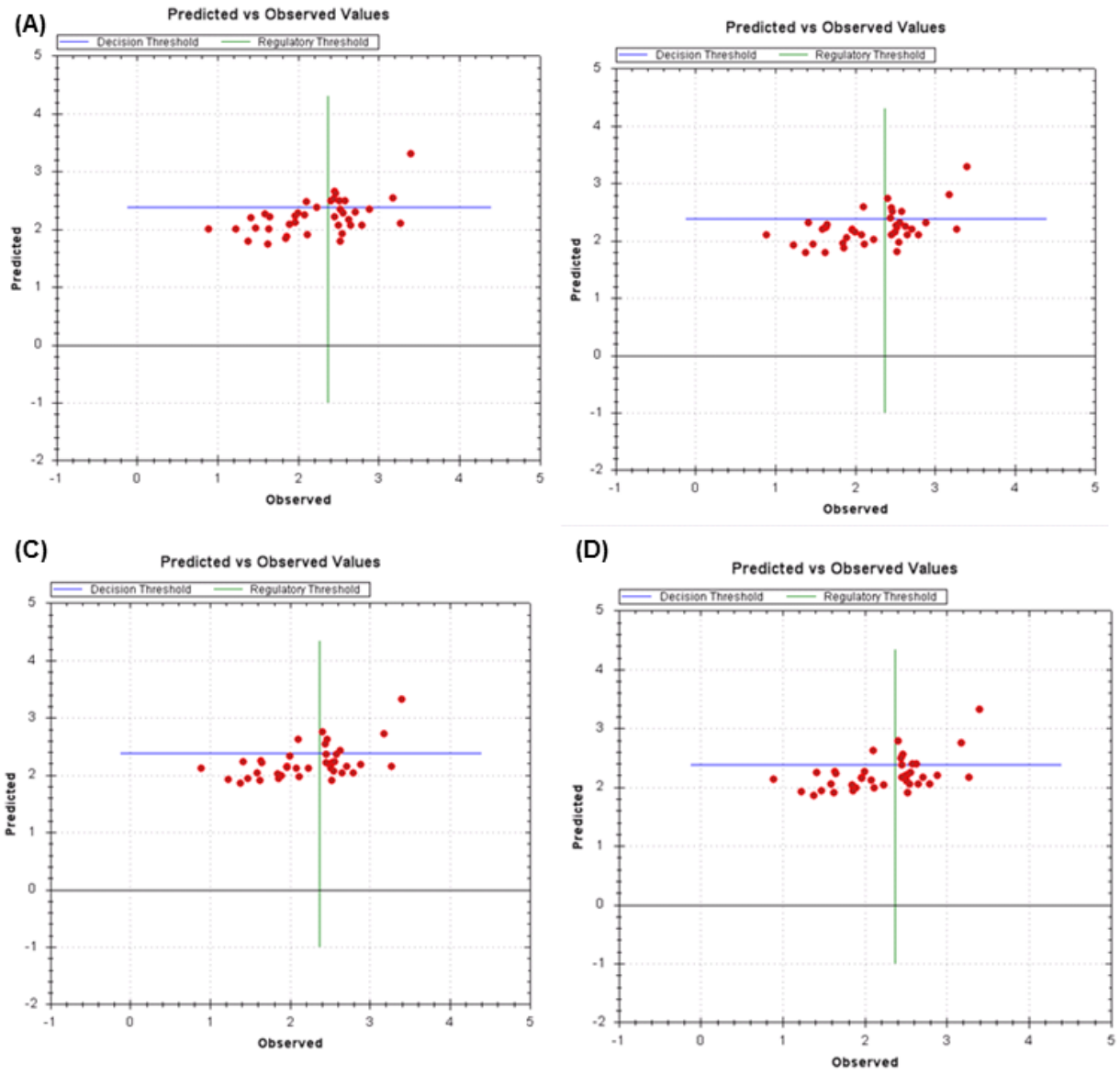

Figure A. 2 Scatter plot of observed versus predicted values for top four statistical models. On the plots, false positives (Type I error) represent data points in the upper left quadrant of the graph and false negatives (Type II error) represent points in the lower right quadrant. The blue and green lines represent EPA threshold for *E. coli*: log of 235 CFU/100 ml.

Table A. 2 Determination of Type I, Type II, specificity, sensitivity, accuracy, and R^2 of the best four models

Model	A	B	C	D
False positives	1	1	1	1
Specificity	0.94	0.94	0.94	0.94
False negatives	13	14	12	12
Sensitivity	0.5	0.3	0.4	0.4
Accuracy	0.35	0.61	0.66	0.66
R^2	0.275	0.256	0.258	0.256

Equations describing the multiple linear regression (MLR) predictions of models A, B, C, and D are listed in Table A.3.

Table A. 3 Multiple linear regressions predictions of the top four models

Model	Multiple Linear Regression (MLR) prediction
A	$\text{Log}\, E.coli = 2.276 + 0.075(\text{rain}_{24\text{hr}}) - 0.0017(wind_{dir}) + 0.0015(Q) + 0.002(Turb)$
B	$\text{Log}\, E.coli = 1.873 + 0.0014(\text{wave\_dir}) - 0.0009(wind_{dir}) + 0.0018(Q) + 0.003(Turb)$
C	$\text{Log}\, E.coli = 1.648 + 0.0016(\text{wave\_dir}) + 0.017(rain_{24hr}) + 0.0016(Q) + 0.003(Turb)$
D	$\text{Log}\, E.coli = 1.638 + 0.0016(\text{wave\_dir}) + 0.0017(Q) + 0.003(Turb)$

Net direction of bacteria loading and transport during resuspension events

Sediment traps were deployed both at Bradford Beach and Atwater Beach (Table A.4). At Bradford Beach average total load of *E. coli* during dry period was one order of magnitude lower than wet period. Possible sources of FIB during dry period are gulls dropping being washed from sand by wave effect. In both cases (wet and dry period) the average total load of *E. coli* was

higher at 1m when compared to 2 m depth. This suggests that the net direction of bacteria loading during both dry and resuspension events associated with rainfall events is lakeward. Mass of sediments collected at sediment traps at 1 m was nearly 3 times higher than mass collected at 2 m during both wet and dry period. This indicates that accumulation of sediments is higher closer to the coast and mainly in the surf zone. This is expected to impact on FIB variability in the surf zone with increasing turbulent shear caused by strong winds and waves which promote resuspension events. In addition, mass of sediments collected during wet period was nearly 3 times higher than collected at 2 m, illustrating that the sediment that is being transported lakeward is ~ 3 times higher during wet periods when compared to dry periods as erosion increases with storms.

At Atwater Beach, the mass of sediments at 1 m and 2 m depth was about the same and average total *E. coli* loading at 1 m and 2 m depth was nearly the same, suggesting that both sediments and FIB tend to get retained within the groins, making difficult to determine net direction of both sediments and FIB loading.

Table A. 4 FIB concentration and mass of sediments collected at two-week periods of deployment of sediment traps at different hydrologic scenarios at Bradford Beach and Atwater Beach. Results represent average (AVE) and standard deviation (STD) of FIB concentration and mass of sediment collected at six-replicate horizontal array.

	Cumulative rain	depth		CFU /100 g dry sediment			Sediments	Total load of *E. coli*
	(cm)	(m)		*E. coli*	Enterococcus	Total coliforms	(g dry weight)	CFU
Bradford Beach	0	1	AVE	1.43E+04	8.84E+02	1.11E+06	57.68	8.27E+03
			STD	2.43E+03	4.44E+02	4.13E+05	3.29	7.98E+01
		2	AVE	1.99E+03	4.76E+01	2.66E+05	14.1	2.81E+02
			STD	5.87E+02	8.02E+01	1.29E+05	2.09	1.23E+01
	4.72	1	AVE	9.05E+03	2.63E+03	5.10E+05	253.15	2.29E+04
			STD	3.48E+03	1.51E+03	2.21E+05	9.59	3.33E+02
		2	AVE	1.10E+04	5.49E+03	1.20E+06	82.77	9.12E+03
			STD	1.13E+03	4.31E+03	2.98E+05	2.02	2.29E+01
Atwater Beach	4.55	1	AVE	1.58E+03	0.00E+00	2.53E+05	63.03	9.97E+02
			STD	1.85E+03	0.00E+00	5.46E+04	8.91	1.65E+02
		2	AVE	4.75E+03	1.37E+02	5.97E+04	40.87	1.94E+03
			STD	3.72E+03	2.01E+02	3.44E+04	1.96	7.30E+01
	5.54	1	AVE	6.04E+04	1.36E+04	5.30E+05	361.51	2.18E+05
			STD	1.32E+04	6.61E+03	1.91E+05	9.17	1.21E+03
		2	AVE	1.32E+05	3.22E+04	4.74E+06	238.38	3.14E+05
			STD	1.93E+04	1.65E+04	9.62E+05	11.06	2.13E+03

Effect of grain size distribution of suspended sediments, TKE and TKE dissipation on FIB fluctuations

We further investigated other variables that could be affecting bacteria loading at Milwaukee beaches. We examined the association of higher concentration of bacteria in the water column to grain size distribution of suspended sediments at Atwater Beach. Variability of particles was evaluated at only one sampling site to eliminate other sources of interference. The site selected was ATW2 because we had a larger sample size (N=10). When comparing the concentration of

E. coli in the water column higher than 100 CFU/100 ml *vs*. less than 20 CFU/100 ml, this indicates that higher concentration of bacteria is associated with higher concentration of sediments (Figure A.3). It is important to note that the air temperature varied from 19.4 to 27.2 °C during sampling time throughout the two days of field work at Atwater Beach and there was no trace of rain.

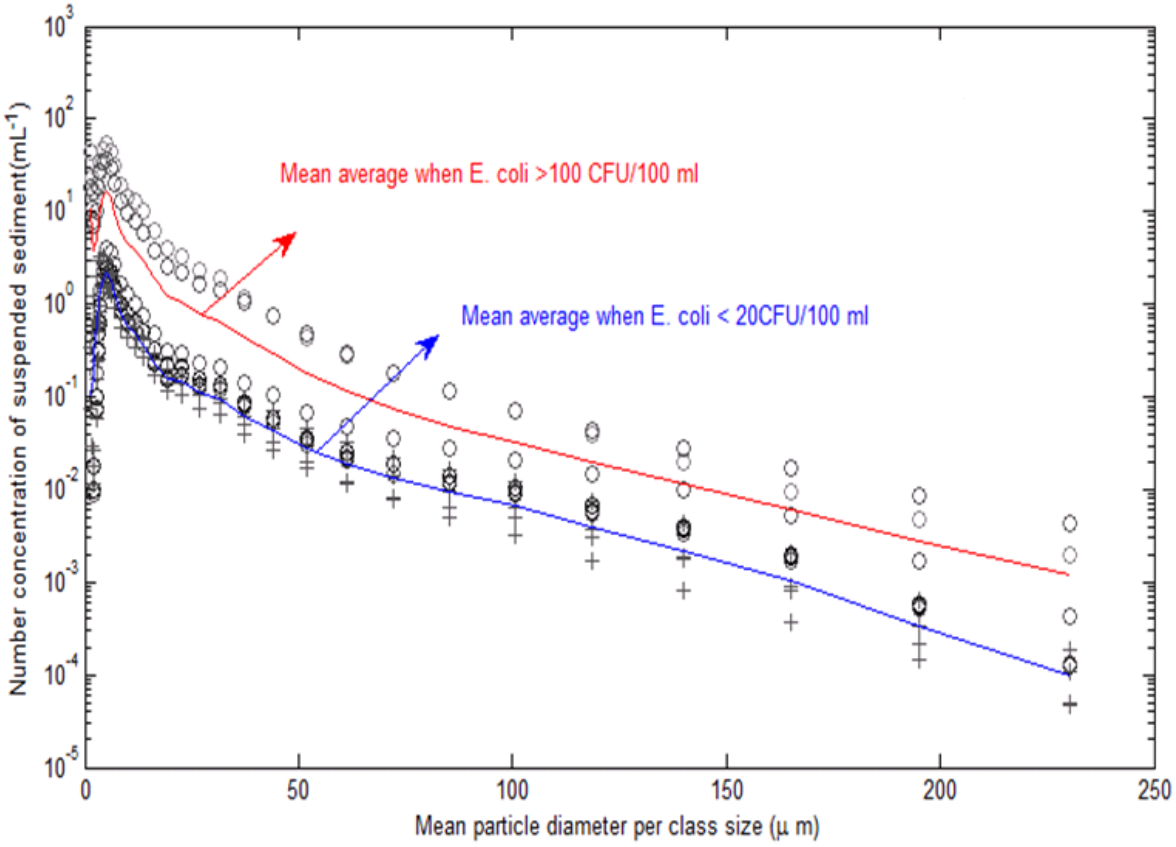

Figure A. 3 Cumulative number concentration of suspended sediments during 08/04/09 and 08/05/09.

There were two sampling times at which number concentration was two orders of magnitude higher than when low levels of *E. coli* were present corresponded to higher turbulent kinetic energy dissipation (>2.87 x10^{-4} m^2/s^3) (Figure A.4). It is known that ϵ is a function of shear rate.

As shear rate increases, it is expected to find a significant increase of sediment in the water column.

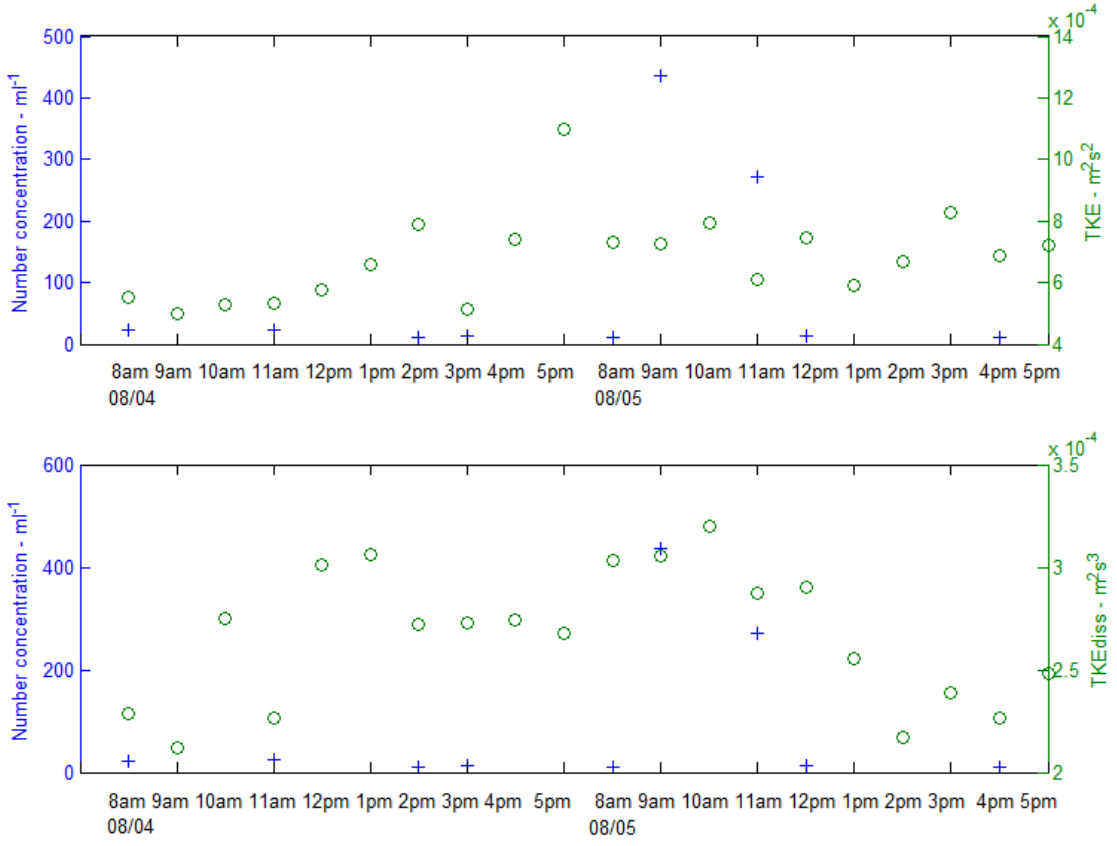

Figure A. 4 Cumulative number concentration of suspended sediment obtained from LISST. The date and time indicated with arrows show the only two data points in which suspended sediment increased coinciding with increased TKE dissipation.

Concentration of *E. coli*, enterococcus, and total coliforms was averaged hourly combining the 2 m and 7 m station. Time series of FIB and TKE and ϵ were examined. TKE ranged from 4.99 $x10^{-4}$ to $1.10x10^{-3}$ m^2s^2 on 08/04/09 and from $5.89x10^{-4}$ to $8.3x10^{-4}$ m^2s^2 on 08/05/09. TKE dissipation ranged from $2.12x10^{-4}$ to $3.06x10^{-4}$ m^2s^3 at 1pm on 08/04/09 and it ranged from $2.17x10^{-4}$ to $3.20x10^{-4}$ m^2s^3 on 08/05/09. No noticeable trend was observed between concentration of bacteria and TKE and ϵ, except on 08/04/09 (Figure A. 5). Initially, FIB

concentration followed the same trend as TKE dissipation. FIB concentration was decreasing when TKE dissipation were descending from 8 am to 9 am and FIB concentration increased when TKE dissipation had a net increase from 9 am to 1pm. TKE dissipation reached a peak of 3.06×10^{-4} m^2s^3 at 1 pm and stabilized at about 2.7×10^{-4} m^2s^3 for the following 4 hours. FIB concentration decreased after 1pm. This is in agreement with laboratory experiments (Silva et al.__), where higher attachment of bacteria to sediment particles is proportional to increase shear rate up to $\epsilon = 9.55 \times 10^{-4}$ m^2s^3 and proportional to increased mixing time at the same ϵ (here represented by a plateau at the same ϵ) when it is expected to have a decrease of bacteria in the water column.

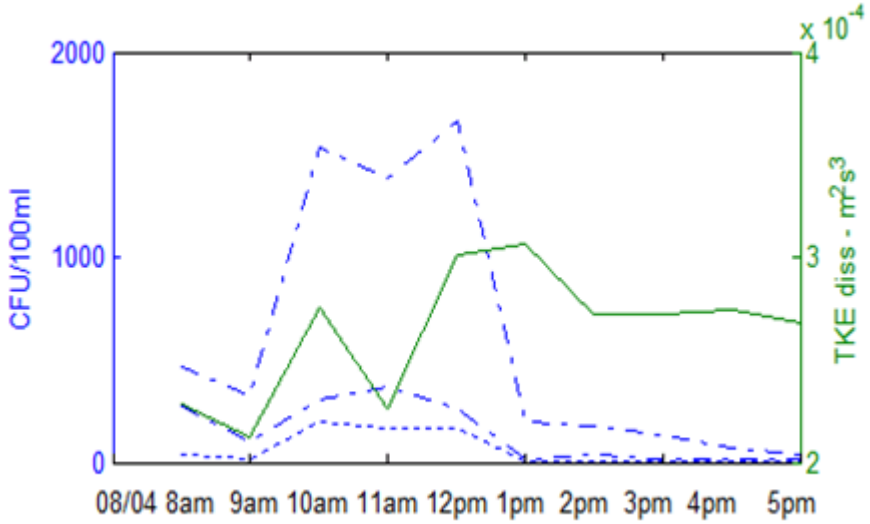

Figure A. 5 Time series of FIB and TKE dissipation (ϵ) during 08/04/09.

ACKNOWLEDGMENTS

This work was made possible through a UWM Graduate School Dissertation Fellowship Award. We acknowledge the help of the Osprey crew and Donald Szmania on the deployment of Aquadopp and sediment traps. We thank Kim Weckerly for assistance with ArcGIS maps.

REFERENCES

Ge, Z.; Whitman, R. L.; Nevers, M. B.; Phanikumar, M. S.; Byappanahali, M. N., Nearshore hydrodynamics as loading and forcing factors for *Escherichia coli* contamination at an embayed beach. *Limnol. Oceanogr.* **2012,** 57, (1), 362-381.

Ge, Z.; Whitman, R. L.; Nevers, M. B.; Phanikumar, M. S., Wave-induced mass transport affects daily *Escherichia coli* fluctuations in nearshore water. *Environmental Science and Technology* **2012,** 46, 2204-2211.

Ge, Z.; Nevers, M. B.; Schwab, D. J.; Whitman, R. L., Coastal loading and transport of Escherichia coli at an embayed beach in Lake Michigan. *Environmental Science and Technology* **2010,** 44, (17), 6731-6737.

Silva, M. R.; McLellan, S. L., Environmental and social impact of stormwater outfalls at Lake Michigan Beaches. *International Journal of Social Ecology and Sustainable Development* **2010,** 1, (3), 34-48.

U.S.EPA *Method 1103.1: Escherichia coli (E. coli) in Water by Membrane Filtration Using membrane-Thermotolerant Escherichia coli Agar (mTEC)*; EPA 821-R-02-020; U. S. Environmental Protection Agency: Washington D. C., 2002.

U.S.EPA *Method 1600: Enterococci in Water by Membrane Filtration Using membrane-Enterococcus Indoxyl-β-D-Glucoside Agar (mEI)*; EPA 821-R-02-022; U. S. Environmental Protection Agency: Washington D. C., 2002.

EPA, U. S. *Method 1604: Total Coliforms and Escherichia coli in Water by Membrane Filtration Using a Simultaneous Detection Technique (MI Medium)*; EPA 821-R-02-024; U. S. Environmental Protection Agency: Washington DC, 2002.

U.S.EPA *Method 1604: Total Coliforms and Escherichia coli in Water by Membrane Filtration Using a Simultaneous Detection Technique (MI Medium)*; EPA 821-R-02-024; U. S. Environmental Protection Agency: Washington DC, 2002.

Silva, M. R.; Liao, Q.; McLellan, S. L.; Bravo, H. R.,20__. Quantitative analysis of the attachment of fecal indicator bacteria to sediment particles in a sheared fluid. In preparation.

Supplemental Material

Table SA. 1 Raw data collected in 2008, 2009 and 2010 and utilized in MLR models

	current_ms	dir_deg	wave_height_m	wave_dir_deg	wave_per	lake_level_m	rainfall_24_cm	rainfall_48_cm	win_spd_ms	wind_dir	Q_m3s	Ecoli_av	Turb_avg
5/29/2008	0.09	56.71	0.09	230.92	1.21	176.08	0.03	0.03	9.83	160	8	92	44.3
5/30/2008	0.15	56.96	0.35	322.04	2.71	176.11	3.53	3.56	15.65	320	25	420	59.0
6/5/2008	0.09	223.75	0.21	274.50	2.14	176.18	4.70	4.75	16.99	140	55	2480	370.0
6/9/2008	0.12	66.42	0.28	330.54	2.43	176.18	0.23	5.94	12.96	150	300	1487	18.1
6/10/2008	0.09	22.63	0.17	35.79	1.63	176.17	0.23	0.46	14.75	250	265	510	6.1
6/11/2008	0.11	199.29	0.38	175.42	2.44	176.20	0.00	0.23	9.39	20	246	281	11.0
6/12/2008	0.13	156.38	0.34	287.46	2.62	176.27	2.39	2.39	13.86	240	220	127	43.5
6/13/2008	0.11	29.50	0.35	300.88	2.77	176.30	1.19	3.58	15.65	260	326	257	28.0
6/14/2008	0.10	24.08	0.26	22.83	1.95	176.21	0.64	1.83	16.54	270	289	333	14.6
6/15/2008	0.09	37.75	0.19	51.42	1.68	176.21	0.00	0.64	16.54	250	241	92	6.1
6/16/2008	0.09	216.33	0.18	141.67	1.66	176.23	0.00	0.00	12.52	290	184	316	2.9
6/24/2008	0.12	82.67	0.21	169.25	1.79	176.23	0.00	0.00	10.73	150	34	78	3.1
7/8/2008	0.06	71.83	0.20	53.50	1.72	176.26	1.30	4.57	10.73	240	40	120	101.7
7/23/2008	0.16	184.79	0.52	219.04	3.25	176.30	0.00	0.00	8.05	40	13	382	119.8
8/4/2008	0.10	136.21	0.25	194.29	2.01	176.30	1.73	1.73	16.09	10	26	323	29.2
8/28/2008	0.15	20.33	0.39	303.00	2.82	176.26	0.00	0.00	10.28	210	5	44	37.3
9/4/2008	0.21	192.29	1.38	231.29	4.96	176.25	4.98	5.11	11.18	320	36	100	57.7
9/8/2008	0.11	166.67	0.28	142.21	2.05	176.20	0.56	0.56	6.26	320	9	334	3.6
5/1/2009	0.10	209.29	0.14	104.96	1.43	176.33	0.00	0.56	13.41	300	79	129	12.0
5/14/2009	0.17	167.04	0.20	66.21	1.68	176.40	0.00	3.07	14.75	250	89	30	13.3
6/8/2009	0.17	8.50	0.42	196.33	2.66	176.53	3.28	3.28	10.73	280	52	287	37.3
6/19/2009	0.10	194.75	0.52	321.38	3.32	176.49	5.72	9.55	16.54	250	199	290	14.6
6/20/2009	0.13	141.21	0.12	99.42	1.30	176.52	0.13	5.84	10.73	310	56	73	13.8
6/25/2009	0.13	75.92	0.05	208.58	1.01	176.50	0.00	0.00	8.05	150	13	614	13.4
6/26/2009	0.13	23.08	0.22	209.71	1.97	176.49	0.00	0.00	8.94	40	11	38	14.7
6/29/2009	0.06	74.13	0.42	131.17	2.49	176.46	0.10	0.10	14.75	340	9	42	9.4
7/9/2009	0.06	84.25	0.28	240.25	2.41	176.50	0.00	0.00	10.73	120	6	44	58.3
7/15/2009	0.13	155.29	0.46	227.54	2.95	176.47	1.22	1.22	13.86	280	8	355	7.0
7/16/2009	0.14	21.46	0.21	101.88	1.73	176.44	0.00	1.22	13.86	310	6	24	13.6
7/20/2009	0.05	157.67	0.20	224.67	1.84	169.11	0.00	0.00	8.94	140	5	453	8.8
7/21/2009	0.09	91.33	0.18	269.50	1.93	176.49	0.00	0.00	8.05	130	5	1868	20.5
7/23/2009	0.28	191.38	0.26	199.75	2.29	176.48	0.05	0.05	8.05	60	6	763	69.3
8/27/2009	0.07	256.88	0.56	241.92	3.39	176.48	0.48	0.99	7.15	110	6	363	65.0
4/6/2010	0.17	197.17	0.65	233.79	3.41	176.16	3.20	3.99	19.22	320	48	7	
4/8/2010	0.35	179.88	1.67	215.92	6.16	176.28	0.08	0.86	13.86	330	69	8	
4/13/2010	0.04	254.29	0.51	289.17	3.35	176.24	0.00	0.03	13.86	110	37	26	21.3
4/15/2010	0.15	13.33	0.32	192.63	2.45	176.19	0.00	0.00	15.65	230	28	8	38.5

	current_ms	dir_deg	wave_height_m	wave_dir_deg	wave_per	lake_level_m	rainfall_24_cm	rainfall_48_cm	win_spd_ms	wind_dir	Q_m3s	Ecoli_av	Turb_avg
6/1/2010	0.14	160.17	0.25	216.83	2.00	176.18	0.00	0.03	9.39	140	10	28	
6/3/2010	0.11	195.50	0.32	239.25	2.44	176.21	0.00	1.63	8.05	20	15	1890	
6/9/2010	0.07	116.25	0.25	135.42	1.92	176.25	0.03	1.07	15.65	270	18	38	
6/16/2010	0.10	183.21	0.12	160.33	1.42	176.33	0.00	1.09	10.28	310	38	70	19.3
6/23/2010	0.08	98.54	0.21	116.88	1.81	176.26	4.95	4.95	16.54	260	89	169	18
7/8/2010	0.04	190.71	0.07	136.96	1.10	176.27	0.05	1.93	7.60	270	18	75	
7/15/2010	0.12	194.42	0.36	206.33	2.45	176.29	4.62	6.96	18.33	320	246	280	28
7/16/2010	0.07	110.71	0.22	55.58	1.80	176.25	0.00	4.62	13.41	260	105	17	6.2
7/23/2010	0.05	68.21	0.22	95.25	1.81	176.32	0.56	14.81	11.62	230	292	263	
7/26/2010	0.12	101.83	0.23	218.38	1.90	176.31	0.00	0.00	9.39	140	75	2603	
7/27/2010	0.09	26.00	0.35	332.04	2.69	176.31	0.00	0.00	10.28	140	59	1477	
7/29/2010	0.11	150.29	0.27	227.04	2.25	176.28	0.00	0.00	6.26	140	39	245	
9/8/2010	0.10	175.67	0.51	191.33	3.09	176.06	0.00	0.00	11.18	280	12	24	

CURRICULUM VITAE

Marcia Silva

Place of birth: Porto Alegre, Brazil

Education

University of the Sinos Valley, Brazil	Food Engineering	B.E.	2004
University of Wisconsin-Milwaukee	Environmental Engineering	M.S.	2006
University of Wisconsin-Milwaukee	Environmental Engineering	Ph.D.	2013

Dissertation tile: "An integrative investigation of sources, fate, and transport of bacteria in Milwaukee Coastal Beaches"

Appointments

2010-2011, 2013: Teaching Assistant for Engineering Principles of Water Resources Design, Civil Engineering, UWM

2011-2012: Dissertator Fellow, Civil Engineering, UWM

2004-2012: Research Assistant, Department of Civil Engineering and School of Freshwater Sciences, UWM

2004: Teaching Assistant for Water Quality Assessment, Civil Engineering, UWM

2002-2003: Instructor of engineering courses, Dom Feliciano Technical School, Brazil

Publications

Silva, M. R., McLellan S. L., and Li, J. 2006. The removal of green fluorescent labeled *Escherichia coli* by pilot scale drinking water biofilters, Recent Progress in Slow Sand and Alternative Biofiltration Processes. Edited by Rolf Gimbel et al., IWA Publishing. ISBN: 9781843391203.

Silva, M. R. Q. 2006. "Removal of green fluorescent labeled *Escherichia coli* using bench-scale drinking water biofilters: a comparison of biofilm developed under different conditions." Master's thesis, pp. 115. University of Wisconsin-Milwaukee.

Silva, M. R. and S.L. McLellan. 2010. "Environmental and social impact of stormwater outfalls at Lake Michigan beaches."International Journal of Social Ecology and Sustainable Development, 1(3), 34-48.

Silva, M. R., F. Schlenker, S. Bingham, J. Chepp, and D. Cox. 2009. "Application of an automatic event controlled sampler for biological analysis and monitoring: studies on plume tracking in Milwaukee Harbor, Milwaukee, Wisconsin." Proceedings of the MTS/IEEE Oceans 2009 Conference, Biloxi, MS, Oct. 26-29, 2009.ISBN: 978-1-4244-4960-6.

Silva, M. R., S. L. McLellan, H. R. Bravo, J. V. Klump, W. Kean. March 2012. "Bradford Beach Standing Water Investigation", Milwaukee, WI – School of Freshwater Sciences - UWM Great Lakes WATER Institute, UWM Department of Civil Engineering and UWM Department of Geosciences. Report prepared for Milwaukee County.

Silva, M. R., and S. L. McLellan. 2005. "MMSD high rate treatment pilot study – Ten day test unit for the Trojan UV pilot unit with secondary effluent – Coliphage and *bacteroides* analyses." Report No. MS2005-02, McLellan Lab, UWM Great Lakes WATER Institute. Report prepared for CH2M Hill.

Silva, M. R., and S. L. McLellan. 2005. "MMSD high rate treatment pilot study – Coliphage and *bacteroides* analyses." Report No. MS2005-01, McLellan Lab, UWM Great Lakes WATER Institute. Report prepared for CH2M Hill.

Silva, M.R. & T.R. Naik. 2010. "Sustainable use of resources – recycling of sewage treatment plant water in concrete." Second International Conference on Sustainable Construction Materials and Technologies (SCMT). Edited by J. Zachar, P. Claisse, T. R. Naik, and E. Ganjian, Ancona, Italy. ISBN: 978-1-4507-1490-7.

Silva, M. R. 2004. "Comparison of two male-specific (F+) / Somatic coliphage and evaluation of their usefulness for testing stormwater." Report No. MS2004-01, McLellan Lab, UWM Great Lakes WATER Institute.

Silva, M.R. & T.R. Naik. 2007. Review of composting and anaerobic digestion of municipal solid waste and a methodological proposal for a mid-size city, Sustainable Construction Materials and Technologies. Edited by Y. M. Chun, P. Claisse, T. R. Naik & Ganjian, Taylor & Francis, Coventry, U.K. ISBN:9780415446891.

Selected public talks

- Great Lakes WATER Institute, Milwaukee, WI. "An integrative approach of sources, fate and transport of bacteria in Milwaukee coastal beaches." May 2, 2013.
- College of Physical and Environmental Oceanography - Ocean University of China, Qingdao, China. "Application of a novel optical method for assessment of attachment of bacteria to particles at a sheared fluid simulating beach environment conditions", January 9, 2013.
- Department of Hydraulics Engineering-Zhejiang University, Hangzhou, China. "Application of a novel optical method for assessment of attachment of bacteria to particles at a sheared fluid simulating beach environment conditions", January 8, 2013.
- State Key Laboratory of Estuarine and Coastal Research - East China Normal University, Shanghai, China. Application of a novel optical method for assessment of attachment of bacteria to particles at a sheared fluid simulating beach environment conditions", January 7, 2013 (http://english.sklec.ecnu.edu.cn/s/71/t/180/8c/d9/info36057.htm)
- Beijing Normal University - School of Environment, Beijing, China. "Application of a novel optical method for assessment of attachment of bacteria to particles at a sheared fluid simulating beach environment conditions", January 4, 2013.
- UFRGS - Universidade Federal do Rio Grande do Sul, Porto Alegre, Brazil. "Engineering science at land – water interface"– August 26, 2011.
- Forschungszentrums Dresden-Rossendorf, Research Center FZD, Dresden, Germany. "An Integrative Investigation of Sources and Transport of Bacteria in Milwaukee Coastal Beaches." July 1, 2010.
- Oceanographic Institute - University of Sao Paulo, Sao Paulo, Brazil. "An Integrative Investigation of Sources and Transport of Bacteria in Milwaukee Coastal Beaches." December 18, 2009.

Honors and Awards

- 2004-2012 – UWM Chancellor's Graduate Student Award
- 2007, 2010, 2013 – UWM Travel Award
- 2011 – 2012 - UWM Graduate School Dissertator Fellowship Award
- 2010-2011 - George A. Boyer Scholarship
- 2009 - UWM Center for Latin American and Caribbean Studies Graduate Student Travel Grant

Professional Service

- Reviewer for: Journal of American Water Works Association (AWWA); Revista Igapo, Brazil
- Judge for the Building the Water Generation ROV Competition, UWM, Milwaukee, WI – March 18, 2012 and March 17, 2013.
- Judge for the ASCE Student Technical Paper Competition 2011, UWM, Milwaukee, WI, April 2, 2011.